

NASA/CR- 1998- 208267

1N-05
2252EB

ANALYSIS AND DESIGN OF FUSELAGE STRUCTURES
INCLUDING RESIDUAL STRENGTH PREDICTION METHODOLOGY

- FINAL REPORT -

for

NASA Grant NAG-1-1588

Submitted to:

Structural Mechanics Branch
Structures Division
NASA Langley Research Center
Hampton, Virginia 23681-0001
Dr. James H. Starnes, Jr., Technical Monitor

by the

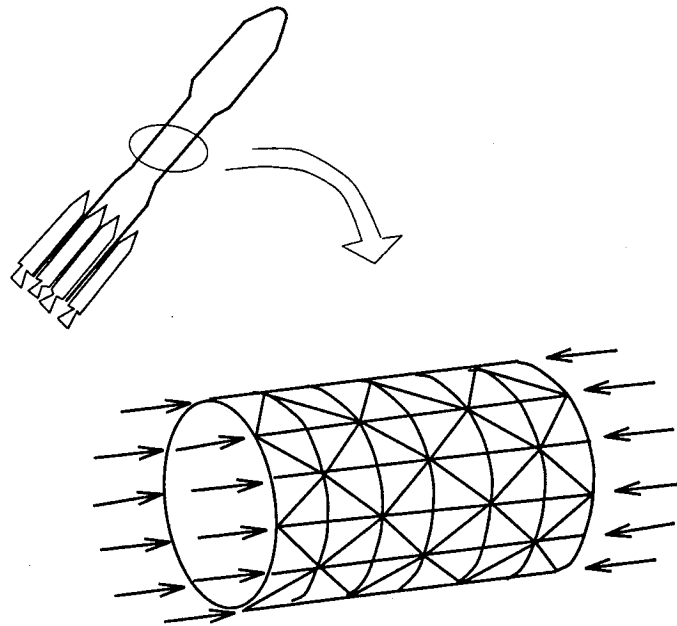
Department of Aerospace Engineering
College of Engineering and Technology
Old Dominion University

Principal Investigator:

Norman F. Knight, Jr., D. Sc.
Professor of Aerospace Engineering
Old Dominion University
Norfolk, Virginia 23529-0247
Telephone No. (757) 683-4265
FAX No. (757) 683-3200
Email: knight@aero.odu.edu

ANALYSIS AND DESIGN OF GENERAL STIFFENED COMPOSITE CIRCULAR CYLINDERS FOR GLOBAL BUCKLING WITH STRENGTH CONSTRAINTS

*Theoretical Foundations and
User's instructions for a FORTRAN Code*



Navin Jaunky
Department of Aerospace Engineering
Old Dominion University
Norfolk, VA 23529-0247

TABLE OF CONTENTS

TABLE OF CONTENTS	i
LIST OF FIGURES	ii
LIST OF FILES	iii
NOMENCLATURE	iv

Chapter		page
1	INTRODUCTION	1
2	THEORETICAL FOUNDATIONS	2
2.1	BUCKLING OF SIMPLY-SUPPORTED ORTHOTROPIC CYLINDERS	3
2.2	IMPROVED SMEARED STIFFENER THEORY	3
2.3	LOCAL BUCKLING OF SKIN SEGMENTS	5
2.3.1	Physical and Computational Domain	6
2.3.2	Rayleigh-Ritz Method	7
2.4	CRIPPLING OF STIFFENER SEGMENT	9
2.5	LOAD DISTRIBUTION BETWEEN SKIN AND STIFFENERS	10
2.6	STRAIN ANALYSIS	12
2.7	OPTIMIZATION OF GRID-STIFFENED CYLINDER	13
2.7.1	Design Problem Definition	14
2.7.2	Design Process Based on Genetic Algorithm	16
3	USER INSTRUCTIONS	17
3.1	ANALYSIS CODE	17
3.1.1	Example of Input and Output file	17
3.2	OPTIMIZATION CODE	19
3.2.1	Changing Type of Optimization	21
	REFERENCES	39

LIST OF FIGURES

1	Unit cell of grid-stiffened cylinder showing design variables.	40
2	Semi-infinite plate model for skin-stiffener element.	40
3	Typical profile for skin-stiffener element neutral surface.	41
4	Physical and computational domain.	41
5	Flow chart showing design optimization process.	42

LIST OF FILES

1	Example of input file (pan.inp)	23
2	Example of output file (pan.out)	24
3	Part of main program "main.f"	29
4	Part of subroutine "panel.f"	31
5	Modification to main program "main.f"	32
6	Modification to subprogram "panel.f"	33
7	Input file for optimization (inp.gen)	34
8	Input file for problem parameters (pan.inp)	34
9	Output file containing optimal designs (best.gen)	35
10	Output file containing convergence history (on.gen)	36
11	Information about first optimal design	37
12	Information about second optimal design	38

NOMENCLATURE

a	Axial stiffener spacing
b	Transverse stiffener spacing
h	Stiffener height
t	Skin laminate thickness
t_s	stiffener thickness
N_1, N_2, N_{12}	Design loads for cylinder
$LAMI$	Design variable for stacking sequence of skin laminate
$ICON$	Design variable for stiffening configuration
λ_G	Global buckling load factor
λ_{sk}	Buckling load factor of skin segment
$\lambda_1, \lambda_2, \lambda_3$	Crippling load factor of axial, transverse, and diagonal stiffener segment
$S_{xsk}, S_{ysk}, S_{xysk}$	Strain level factor for skin segment
S_1, S_2, S_2	Strain level factor for axial, transverse, and diagonal stiffener segment

Chapter 1

INTRODUCTION

The theoretical foundations and user instructions for a FORTRAN code for the design and analysis of composite grid-stiffened cylinders subjected to global and local buckling constraints, and strength constraints are presented using a discrete optimizer based on a genetic algorithm. An improved smeared stiffener theory is used for the global analysis. Local buckling of skin segments are assessed using a Rayleigh-Ritz method that accounts for material anisotropy. The local buckling of stiffener segments are also assessed. Constraints on the membrane strains in the skin and stiffener segments are imposed to include strength criteria in the grid-stiffened cylinder design. Design variables are the axial and transverse stiffener spacings, stiffener height and thickness, skin laminate stacking sequence, and stiffening configuration. The design optimization process is adapted to identify the best suited stiffening configurations and pattern for grid-stiffened composite cylinder with the length and radius of the cylinder, the design in-plane loads, and material properties as inputs.

The theoretical foundations for the analyses involved in the buckling of grid-stiffened circular cylinders are discussed briefly in Chapter 2. Instructions for setting up input files for the FORTRAN code are given in Chapter 3. To provide flexibilities in performing different types of optimization, instructions are also provided in Chapter 3 for modifying the code to adjust the number of design variables to facilitate a particular type of optimization.

Chapter 2

THEORETICAL FOUNDATIONS

The buckling analysis of grid-stiffened composite circular cylinders subjected to combined loads requires several key steps. Herein, acceptable designs are those which buckle globally and do not exhibit any local skin buckling or stiffener crippling, and the membrane strains in the skin and stiffener segments are below an acceptable level. The first step in the design process is to assess the global buckling response of a grid-stiffened shell. Once this global buckling response is determined, the second step is to determine the local skin buckling response for the quadrilateral and/or triangular skin segments between the stiffeners. The third step is to determine whether stiffener buckling or stiffener crippling has occurred at this global buckling load level. Finally the membrane strains in the skin and stiffener segment are determined.

The theoretical foundations for the various steps are

- Buckling of simply-supported orthotropic cylinders.
- Improved smeared stiffener theory ([1]).
- Buckling of panels with general parallelogram and triangular-shaped planform ([2, 3]).
- Crippling of stiffener segment ([4]).
- Load distribution between skin and stiffeners.
- Strain analysis.
- Optimization strategy.

and are discussed in this chapter.

2.1 BUCKLING OF SIMPLY-SUPPORTED ORTHOTROPIC CYLINDERS

The global buckling analysis is based on a Rayleigh-Ritz method using a first-order, shear-deformation theory and the improved smeared-stiffener modeling approach discussed in [1]. The cylinder is assumed to be simply supported and hence, the Rayleigh-Ritz method for the global analysis assumes the following Ritz functions for the axial displacement (u), the circumferential displacement (v), the transverse displacement (w), and the cross-sectional rotations ϕ_x and ϕ_y :

$$\begin{aligned}
 u &= \sum_{i=1}^N \left(A_{m_i n_i} \sin \frac{n_i y}{R} + B_{m_i n_i} \cos \frac{n_i y}{R} \right) \sin \frac{m_i \pi x}{L} \\
 v &= \sum_{i=1}^N \left(A_{m_i n_i} \sin \frac{n_i y}{R} + B_{m_i n_i} \cos \frac{n_i y}{R} \right) \cos \frac{m_i \pi x}{L} \\
 w &= \sum_{i=1}^N \left(A_{m_i n_i} \sin \frac{n_i y}{R} + B_{m_i n_i} \cos \frac{n_i y}{R} \right) \sin \frac{m_i \pi x}{L} \\
 \phi_x &= \sum_{i=1}^N \left(A_{m_i n_i} \sin \frac{n_i y}{R} + B_{m_i n_i} \cos \frac{n_i y}{R} \right) \cos \frac{m_i \pi x}{L} \\
 \phi_y &= \sum_{i=1}^N \left(A_{m_i n_i} \sin \frac{n_i y}{R} + B_{m_i n_i} \cos \frac{n_i y}{R} \right) \sin \frac{m_i \pi x}{L}
 \end{aligned} \tag{1}$$

where L and R are the length and radius of the cylindrical shell, respectively, and N is the number of terms in the Fourier series. The coordinate system for the cylinder is shown in Figure 1. The minimum potential energy principle is used with the Rayleigh-Ritz method, and include Sanders-Koiter shell theory ([5, 6]).

2.2 IMPROVED SMEARED STIFFENER THEORY

The improved smeared stiffener theory for stiffened cylinders, used here includes skin-stiffener interaction effects. Skin-stiffener interaction effects may lead to overestimation of buckling loads especially when the stiffener spacings are not small.

If a stiffened plate is bent while it is supported on all four edges, the neutral surface in the neighborhood of the stiffener will lie between the mid-plane of the skin and the centroid of the stiffener. It is convenient to think of this as a shift of the neutral surface from the centroid of the stiffener. Hence, the approximate

stiffness added by a stiffener to the skin stiffness will then be due to the skin-stiffener combination being bent about its neutral surface rather than due to the stiffener being bent about its own neutral surface or the skin neutral surface. The shifted location of the neutral surface is determined theoretically through a study of the local stress distribution near the skin-stiffener interface for a panel with a blade stiffener.

The neutral surface profile of the skin-stiffener combination is developed analytically using the minimum potential energy principle and statics conditions. The skin-stiffener interaction is accounted for by computing the bending and coupling stiffness due to the stiffener and the skin in the skin-stiffener region about a shifted neutral axis at the stiffener.

A grid-stiffened cylinder may be considered to be an assembly of repetitive units or unit cells (see Figure 1). Any stiffener segment in the unit cell may be isolated in a semi-infinite skin-stiffener model as shown in Figure 2 for a diagonal stiffener. The approach for obtaining the neutral surface in a semi-infinite stiffened panel is given in Reference [1].

A typical profile of the neutral surface for a skin-stiffener combination is shown in Figure 3. The distance y^* represents the distance from the centerline of the stiffener to the point where the neutral surface coincides with the mid-surface of the skin. The average of the neutral profile over the distance y^* is Z^* . The quantities y^* and Z^* are obtained numerically.

The smeared stiffnesses of a stiffened panel is obtained by mathematically converting the stiffened panel to an equivalent unstiffened panel (Ref. [7]). The smeared stiffnesses are developed on the basis that the strain energy of the stiffened panel should be the same as that of the equivalent unstiffened panel. These smeared stiffnesses can then be used in a Rayleigh-Ritz type analysis to solve for buckling loads of the stiffened panel. In Reference [7], the strain energy of the skin and stiffeners in the unit cell is obtained by using stiffnesses of the skin and the stiffeners which are computed about the mid-surface of the skin. Since, there is a shift in the neutral surface at the stiffener, the stiffness of the stiffeners and the skin segment directly

above it has to be computed about a shifted neutral surface so as to account for the skin-stiffener interactions.

The correction to the smeared stiffnesses due to the skin-stiffener interaction is herein introduced by computing the stiffness of the stiffener and the skin segment directly contiguous to it according to the following criteria.

1. If $y^* < t/4$, then the reference surface for the stiffener is Z_n .
2. If $y^* > t/4$, then the reference surface for the stiffener is Z^* .

In either case, the reference surface of the skin is taken to be its mid-surface. Other more elaborate and accurate schemes can be used to introduce the skin-stiffener interaction using the neutral surface profile. However, the one described herein is simple, and provides sufficiently accurate buckling loads for the preliminary structural design ([1]).

2.3 LOCAL BUCKLING OF SKIN SEGMENTS

The shape of a skin segment on a grid-stiffened panel depends on the stiffening configuration. If the stiffening configuration involves diagonal stiffener only, then the skin segment has a rhombic planform. If the stiffening configuration has diagonal stiffeners with axial or transverse stiffeners, then the skin segment has an isosceles triangular planform. For a general grid-stiffened panel, the skin segment has a right-angle triangular planform, and for an isogrid panel the skin segment has an equilateral triangular planform.

Buckling analyses for panel with these kinds of planforms is achieved through the use of "circulation function" and accounts for material anisotropy, different boundary conditions, and combined in-plane loading. A First-Order Shear-Deformation Theory is used. The shell theory that is used can be either Sanders-Koiter, Love, or Donnell theory. This is achieved through tracer coefficients.

2.3.1 Physical and Computational Domain

The buckling analysis of these local skin segments is enhanced by mapping their physical domain into a computational domain. Consider a general quadrilateral or triangular panel subjected to a state of combined in-plane loading where the loading and material properties are defined using the coordinate system $(x - y)$ shown Figure 4. The transformation from a physical domain to computational domain is necessary when dealing with general quadrilateral and triangular geometries in order to facilitate the computation of linear stiffness and geometric stiffness matrices and imposition of boundary conditions.

The physical domain $\mathcal{D}[x, y]$ is transformed to a computational domain $\mathcal{D}[\xi, \eta]$ as indicated in Figure 4 The mapping for a quadrilateral is

$$\begin{aligned} x(\xi, \eta) &= \sum_{i=1}^4 N_i(\xi, \eta) x_i \\ y(\xi, \eta) &= \sum_{i=1}^4 N_i(\xi, \eta) y_i \end{aligned} \quad (2)$$

where $x_i (i = 1, 2, 3, 4)$ and $y_i (i = 1, 2, 3, 4)$ are the physical coordinates of the i^{th} corner of the panel, ξ and η are the natural coordinates for the quadrilateral geometries, and $N_i (i = 1, 2, 3, 4)$ are the bilinear mapping functions given by

$$\begin{aligned} N_1(\xi, \eta) &= \frac{1}{4}(1 - \xi)(1 + \eta) \\ N_2(\xi, \eta) &= \frac{1}{4}(1 + \xi)(1 + \eta) \\ N_3(\xi, \eta) &= \frac{1}{4}(1 + \xi)(1 - \eta) \\ N_4(\xi, \eta) &= \frac{1}{4}(1 - \xi)(1 - \eta) \end{aligned}$$

The Jacobian of the transformation is

$$\mathbf{J} = \begin{bmatrix} \frac{\partial x}{\partial \xi} & \frac{\partial y}{\partial \xi} \\ \frac{\partial x}{\partial \eta} & \frac{\partial y}{\partial \eta} \end{bmatrix} \quad (3)$$

which is independent of the natural coordinates for general parallelogram-shaped geometries. This results in substantial computational savings in the overall formulation.

The mapping for a general triangle is

$$\begin{aligned}x(\xi, \eta, \rho) &= \xi x_1 + \eta x_2 + \rho x_3 \\y(\xi, \eta, \rho) &= \xi y_1 + \eta y_2 + \rho y_3\end{aligned}\tag{4}$$

where ξ , η and ρ are the area coordinates for the case of triangular geometries, and $x_i (i = 1, 2, 3)$ and $y_i (i = 1, 2, 3)$ are the physical coordinates of the i^{th} corner of the panel. Note that the third area coordinate will be expressed in terms of the other two or $\rho = (1 - \xi - \eta)$ based on the constraint that the sum of the area coordinates must be equal to one. The Jacobian of the transformation is independent of the area coordinates. The Jacobian, in either case, is used to relate derivatives in the two domains.

2.3.2 The Rayleigh-Ritz Method

The Rayleigh-Ritz method is an approximate method for solving a certain class of problems. Accordingly, trial functions with some unknown coefficients and satisfying the essential or geometric boundary conditions are introduced in the energy functional of the problem. The minimum conditions of this functional are then imposed, and resulting algebraic equations are solved for the unknown coefficients. These trial functions are called the ‘‘Ritz’’ functions.

The Ritz functions used here are expressed in terms of natural coordinates for the quadrilateral geometry or area coordinates for the triangular geometry for displacement field. The components of the displacement vector are three translations ($D_1, D_2, D_3 = u_0, v_0, w$) and two cross-sectional or bending rotations ($D_4, D_5 = \phi_x, \phi_y$) when considering transverse-shear deformation effects. Each displacement component is approximated independently by a different Ritz function. The approximation for the i^{th} component of the displacement vector is given by

$$\begin{aligned}D_i(\xi, \eta) &= \sum_{j=1}^N a_{ij} d_{ij} \\&= \sum_{j=1}^N a_{ij} \Gamma_i(\xi, \eta) f_j(\xi, \eta) \text{ for } i = 1, 2, 3, 4, 5\end{aligned}\tag{5}$$

where d_{ij} represents the j^{th} term in the N -term approximation for the i^{th} displacement component, a_{ij} are unknown coefficients to be determined, and $\Gamma_i(\xi, \eta)$ are the circulation functions.

The circulation functions Γ_i in Equation (5) are then used to impose different boundary conditions along each edge of the plate. Each term Γ_i is the product of three functions in the case of the triangular plate geometry and four functions in the case of the quadrilateral plate geometry. Each function is the equation of an edge of the triangular or quadrilateral plate as shown in Figure 4 raised to an independent exponent for each displacement component. Thus, the circulation functions for the quadrilateral plate are

$$\Gamma_i = (1 - \eta)^{p_i}(1 - \xi)^{q_i}(1 + \eta)^{r_i}(1 + \xi)^{s_i}$$

and for the triangular plate are

$$\Gamma_i = \xi^{p_i}\eta^{q_i}(1 - \xi - \eta)^{r_i} \quad (6)$$

For example, considering the quadrilateral plate case, p_i refers to edge 1, q_i refers to edge 2, r_i refers to edge 3, s_i refers to edge 4 as indicated in Figure 4. These exponents are used to impose different boundary conditions. If the i^{th} displacement component is free on a given edge, then the exponent for that edge will have a value of zero. If the i^{th} displacement component is constrained on a given edge, then the exponent for that edge will have a value of one. Only geometric boundary conditions are imposed in this approach. Thus, a simply supported condition for bending fields can be imposed on edge 1 by setting:

- $p_3 = 1$ for w , $p_4 = 0$ for ϕ_x , $p_5 = 0$ for ϕ_y

A clamped condition for bending fields can be imposed on edge 1 by setting:

- $p_3 = 1$ for w , $p_4 = 1$ for ϕ_x , $p_5 = 1$ for ϕ_y

A free-edge condition can be imposed on edge 1 by setting:

- $p_i = 0$ for u_0 , v_0 , w , ϕ_x and ϕ_y

The term f_j in Equation (5) is a polynomial function in ξ and η , and in its simplest form is a power series in ξ and η and is expressed as

$$f_j(\xi, \eta) = \xi^{m_j} \eta^{n_j}$$

$$m_j, n_j = (0, 0), (1, 0), (0, 1), (2, 0), (1, 1), (0, 2), \dots \quad (7)$$

The values of m_j and n_j are used basically to define terms in a two-dimensional Pascal's triangle. The number of terms N in Equation (5) defines the order of a complete function in two variables. The table below gives the value of N for polynomials of different degrees.

Table 1 Degree of polynomials with value of N

N	Degree of polynomials	N	Degree of polynomials
1	0	45	8
3	1	55	9
6	2	66	10
10	3	78	11
15	4	91	12
21	5	105	13
28	6	120	14
36	7	136	15

2.4 CRIPPLING OF STIFFENER SEGMENT

The local stiffener segment is analyzed to determine whether stiffener crippling will occur. Reference [4] provides a method for determining the buckling load of a stiffener segment. Accordingly, the stiffener segment at the nodes or intersection points of stiffeners are assumed to be clamped while the stiffener-skin attachment is assumed to be a simple support. From Ref. [4], the crippling load of the stiffener is N_{crip} and is given by

$$N_{crip} = \frac{\bar{s}_z}{2} \left[\sqrt{1 + \frac{4N_{cl}}{\bar{s}_z}} - 1 \right]$$

where

$$N_{cl} = t_s^3 \left[\frac{4\pi^2 E_{11}}{12L_1^2 [1 - (\nu_{12}^2 E_{22}/E_{11})]} + \frac{G_{12}}{h^2} \right] \quad (8)$$

where

$\bar{s}_z = \frac{5}{6}G_{13}t_s$, is a shear correction factor,

$L_1 = 2L$ is the length of the stiffener,

h is the height of the stiffener,

h is the height of the stiffener,

t_s is the thickness of the stiffener,

E_{11} is the longitudinal modulus of the stiffener material,

E_{22} is the transverse modulus of the stiffener material.

2.5 LOAD DISTRIBUTION BETWEEN SKIN AND STIFFENERS

The global buckling load is assumed to be a scalar multiple of the design load and has the form

$$(N_x, N_y, N_{xy}) = \lambda_G (N_1, N_2, N_{12}) \quad (9)$$

where N_1 , N_2 , and N_{12} are the applied in-plane prebuckling loads and represents the design load. Once the global buckling load factor (λ_G) has been determined using the improved smeared stiffener theory, the loads acting on the stiffener and skin segments have to be determined by distributing the loads based on the extensional stiffness of the skin and the stiffener.

The loads acting on the skin and stiffener segments are computed based on a global load factor of λ_G and these loads are used to determine the local buckling load factor of the skin, (λ_{sk}), local crippling factors of axial stiffener segment, (λ_1), transverse stiffener segment, (λ_2) and diagonal stiffener segment, (λ_3). These local buckling and crippling load factors describe the buckling characteristics of the stiffened cylinder and is as follows

- For $\lambda_{sk}, \lambda_1, \lambda_2, \lambda_3 \geq 1.0$, then the cylinder buckles globally at an axial load of $\lambda_G N_1$, i.e., $\lambda_{cr} = \lambda_G$.
- If one of $\lambda_{sk}, \lambda_1, \lambda_2, \lambda_3 < 1.0$, then the stiffened cylinder buckles locally. If $\lambda_{sk} < 1.0$, then skin buckling occurs, and if $\lambda_1 < 1.0$ then crippling of the axial

stiffener occurs. For this case, $\lambda_{cr} = \lambda_i \times \lambda_G$ where λ_i is < 1.0 , and subscript i can be any one of sk , 1, 2 or 3.

- If more than one of λ_{sk} , λ_1 , λ_2 and λ_3 are < 1.0 , then local buckling of the stiffened cylinder occurs and $\lambda_{cr} = \lambda_i \times \lambda_G$ where λ_i is the minimum of any of λ_{sk} , λ_1 , λ_2 or λ_3 with values < 1.0 .

The procedure ([8, 9] for distributing the applied loads for a general grid-stiffened circular cylinder are computed as follows:

$$\begin{aligned} (A_{11})_T &= \frac{2(A_{11})_1 h}{b} + \frac{2(A_{11})_3 h \sin^3 \theta}{b} + (A_{11})_s \\ (A_{22})_T &= \frac{2(A_{11})_2 h}{a} + \frac{2(A_{11})_3 h \cos^3 \theta}{a} + (A_{22})_s \\ (A_{66})_T &= \frac{2(A_{11})_3 h \cos \theta \sin^2 \theta}{a} + (A_{66})_s \end{aligned} \quad (10)$$

where $(A_{11})_T$ is total smeared axial extensional stiffness of the grid-stiffened panel, $(A_{22})_T$ is the total smeared transverse extensional stiffness of the grid-stiffened panel, $(A_{66})_T$ is the total smeared in-plane shear stiffness of the grid stiffened panel, $(A_{11})_1$, $(A_{11})_2$, $(A_{11})_3$ are the extensional stiffness of the axial, transverse and diagonal stiffeners, respectively, $(A_{ij})_s$ is the extensional stiffness of the skin, θ is the orientation of the diagonal stiffener, and h is the height of the stiffener. Second, the loads carried by the skin segment which could be either a general parallelogram-shaped geometry or a general triangular-shaped geometry, at the panel global buckling load are

$$\begin{aligned} (N_x)_{sk} &= \frac{(A_{11})_s}{(A_{11})_T} N_x = \frac{(A_{11})_s}{(A_{11})_T} \lambda_G N_1 \\ (N_y)_{sk} &= \frac{(A_{22})_s}{(A_{22})_T} N_y = \frac{(A_{22})_s}{(A_{22})_T} \lambda_G N_2 \\ (N_{xy})_{sk} &= \frac{(A_{66})_s}{(A_{66})_T} N_{xy} = \frac{(A_{66})_s}{(A_{66})_T} \lambda_G N_{12} \end{aligned} \quad (11)$$

These values then correspond to the design loads used for the in-plane prebuckling load in the skin-segment local buckling computation. If the critical buckling load factor of the skin segment λ_{sk} is greater than or equal to one, then the skin-segment

buckling load is greater than or equal to the global buckling load of the grid-stiffened panel. Third, the loads carried by each stiffener are computed. The load carried by the axial stiffener is

$$(N_x)_1 = \frac{(A_{11})_1}{(A_{11})_T} \lambda_G N_1 = \lambda_1 N_{crip} \quad (12)$$

where N_{crip} is determined using Equation (8). The critical buckling load factor, λ_1 , of the axial stiffener has to be greater than or equal to one. The load carried by the transverse stiffener is

$$(N_x)_2 = \frac{(A_{11})_2}{(A_{22})_T} \lambda_G N_2 = \lambda_2 N_{crip} \quad (13)$$

and the critical buckling load factor, λ_2 , of the transverse stiffener has to be greater than or equal to one. The load in the diagonal stiffeners has components from the axial, transverse, and in-plane shear loadings and is given by

$$(N_x)_3 = N_{dx} \sin \theta + N_{dy} \cos \theta + (N_{dxy})_x \cos \theta + (N_{dxy})_y \sin \theta = \lambda_3 N_{crip}$$

where

$$\begin{aligned} N_{dx} &= \frac{(A_{11})_3 \sin^3 \theta}{(A_{11})_T} \lambda_G N_1 \\ N_{dy} &= \frac{(A_{11})_3 \cos^3 \theta}{(A_{22})_T} \lambda_G N_2 \\ (N_{dxy})_x &= \frac{(A_{11})_3 \cos \theta \sin^2 \theta}{(A_{66})_T} \frac{b}{a} \lambda_G N_{12} \\ (N_{dxy})_y &= \frac{(A_{11})_3 \cos \theta \sin^2 \theta}{(A_{66})_T} \lambda_G N_{12} \end{aligned} \quad (14)$$

N_{dx} is the contribution from the axial in-plane loading, N_{dy} is the contribution from the transverse in-plane loading, $(N_{dxy})_x$ is the contribution from the in-plane shear loading along the edge where x is constant, and $(N_{dxy})_y$ is the contribution from the in-plane shear loading along the edge where y is constant. The critical buckling load factor, λ_3 , of the diagonal stiffener has to be greater than or equal to one.

2.6 STRAIN ANALYSIS

The critical buckling load factor of the stiffened cylinder is λ_{cr} where λ_{cr} takes on values as discussed in Section 2.5 and based on this load value the loads acting on the skin and stiffeners segments are obtained. For an axial load in the skin segment

of N_{xsk} , a circumferential load of N_{ysk} , a shear load of N_{xysk} and the loads in axial, transverse and diagonal stiffener segments of N_{x1} , N_{x2} and N_{x3} , respectively, the membrane strains in the skin and stiffener segments are

$$\begin{aligned}
 \epsilon_{xsk}^0 &= a_{11}^{(sk)} N_{xsk} + a_{12}^{(sk)} N_{ysk} + a_{16}^{(sk)} N_{xysk} \\
 \epsilon_{ysk}^0 &= a_{12}^{(sk)} N_{xsk} + a_{22}^{(sk)} N_{ysk} + a_{26}^{(sk)} N_{xysk} \\
 \gamma_{xysk}^0 &= a_{16}^{(sk)} N_{xsk} + a_{26}^{(sk)} N_{ysk} + a_{66}^{(sk)} N_{xysk} \\
 \epsilon_{x1}^0 &= a_{11}^{(1)} N_{x1} \\
 \epsilon_{x2}^0 &= a_{11}^{(2)} N_{x2} \\
 \epsilon_{x3}^0 &= a_{11}^{(3)} N_{x3}
 \end{aligned} \tag{15}$$

where ϵ_{xsk}^0 , ϵ_{ysk}^0 , and γ_{xysk}^0 , are the axial, circumferential, and shear membrane strains in the skin. ϵ_{x1}^0 , ϵ_{x2}^0 , and ϵ_{x3}^0 are the membrane strain in the axial, transverse, and diagonal stiffener segments respectively. The quantities $a_{ij}^{(sk)}$, $a_{11}^{(1)}$, $a_{11}^{(2)}$, and $a_{11}^{(3)}$ are axial flexibilities of the skin, axial, transverse, and diagonal stiffeners.

The strain level factors for the skin, axial, transverse, and diagonal stiffener segment are

$$\begin{aligned}
 S_{xsk} &= (\epsilon_{xsk}^0)_{al} / \epsilon_{xsk}^0 \\
 S_{ysk} &= (\epsilon_{ysk}^0)_{al} / \epsilon_{ysk}^0 \\
 S_{xysk} &= (\gamma_{xysk}^0)_{al} / \gamma_{xysk}^0 \\
 S_1 &= (\epsilon_{x1}^0)_{al} / \epsilon_{x1}^0 \\
 S_2 &= (\epsilon_{x2}^0)_{al} / \epsilon_{x2}^0 \\
 S_3 &= (\epsilon_{x3}^0)_{al} / \epsilon_{x3}^0
 \end{aligned} \tag{16}$$

where $(\epsilon_{xsk}^0)_{al}$, $(\epsilon_{ysk}^0)_{al}$, $(\gamma_{xysk}^0)_{al}$ and $(\epsilon_{xst}^0)_{al}$ are the allowable membrane strains in the skin and stiffeners, respectively.

2.7 OPTIMIZATION OF GRID-STIFFENED CYLINDERS

The design variables for a grid-stiffened composite shell are the axial and transverse stiffener spacings (a , b), the stiffening configuration (*ICON*), which is the

combination of axial, transverse and diagonal stiffeners, the skin laminate (*LAMI*), and the height (h), and thickness (t_s) of the stiffener. Except for the height of the stiffener, these design variables take on discrete values.

The genetic algorithm is a method for “evolving” a given design problem to a family of near-optimum designs (e.g., see References [10] and [11]). Stochastic processes are used to generate an initial population of individual designs and the process then applies principles of natural selection and survival of the fittest to find improved designs. Furthermore, since the discrete design procedure works with a population of designs it can explore a large design space and climb different hills. This is a major advantage as the converged solution contains many optima of comparable performance. The cost of having a large number of function evaluations is offset by the fact that a large number of optimum solutions are now available. The population or family of good designs produced by using the genetic algorithm may include the global optimal design, rather than a single design.

2.7.1 Design Problem Definition

The present design problem is to minimize the weight of a grid-stiffened composite circular cylindrical shell given the design loading condition, the length and radius of the cylinder, and the material properties for the skin and stiffeners. The design variables include stiffener spacings (a, b), the stacking sequence of the skin, stiffener layout, stiffener thickness (t_s), and stiffener height ($h_1 = h_2 = h_3 = h$) as shown in Figure 1. All stiffeners are assumed to be of the same height and thickness for manufacturing and assembly reasons. The design sought here is a cylinder of minimum weight in a certain design space which buckles globally at the design loads while the membrane strains in the skin and the stiffener segments do not exceed the allowable membrane strains $(\epsilon_{xsk}^0)_{al}$, $(\epsilon_{ysk}^0)_{al}$, $(\gamma_{xysk}^0)_{al}$ and $(\epsilon_{xst}^0)_{al}$ respectively. This design problem can be defined by setting up the optimization procedures in the following way. First, the global buckling load is assumed to be a scalar multiple of design loads and has the form

$$(N_x, N_y, N_{xy}) = \lambda_G(N_1, N_2, N_{12}) \quad (17)$$

where N_1 , N_2 , and N_{12} , are the applied in-plane prebuckling load. This values represent the design loads for the grid-stiffened cylinder. Second, the design constraints imposed on panel include

1. The critical buckling load should be greater than or equal to the design loads, that is, $\lambda_G \geq 1$.
2. Skin segments should not buckle at the critical buckling load, that is, $\lambda_{sk} \geq 1$.
3. Stiffener segments should not cripple at the critical buckling load, that is, $\lambda_1, \lambda_2, \lambda_3 \geq 1$.
4. The membrane strains in the skin segment should be less than or equal $(\epsilon_{xsk}^0)_{al}$, $(\epsilon_{ysk}^0)_{al}$, and $(\gamma_{xysk}^0)_{al}$ that is, $S_{xsk}, S_{ysk}, S_{xysk} \geq 1$.
5. The axial membrane strain in the stiffener segment should be greater than or equal $(\epsilon_{xst}^0)_{al}$, that is, $S_1, S_2, S_3 \geq 1$.

The general form of each constraint equation is written as

$$g_j = \begin{cases} (\frac{1}{\lambda_j} - 1) \leq 0.0 \\ (\frac{1}{S_j} - 1) \leq 0.0 \end{cases} \quad j = 1, \dots, N_c \quad (18)$$

Finally, the ‘‘Fitness’’ expression based on exterior penalty function approach is

$$\text{Fitness} = \left(\frac{Q}{F(\mathbf{X}, r_i)} \right) = \text{Max} \frac{Q}{W(\mathbf{X}) + r_i \sum_j^{N_c} [|g_j(\mathbf{X})| + g_j(\mathbf{X})]^2} \quad (19)$$

where \mathbf{X} = design variable vector

$F(\mathbf{X}, r_i)$ = Modified objective function

$W(\mathbf{X})$ = weight of of cylinder

$r_i \sum_j^{N_c} [|g_j(\mathbf{X})| + g_j(\mathbf{X})]^2$ = penalty function

Q = normalizing constant

N_c = Number of design constraints

r_i = penalty parameter

i = generation or iteration cycle in the optimization procedure.

2.7.2 Design Process Based on Genetic Algorithm

Implementation of the genetic algorithm is shown schematically in Figure 5. The design process begins with a random selection of a specified number of designs which comprise the initial population (i.e., first generation) for the genetic algorithm. Material properties, radius and length of the cylinder, boundary conditions of the skin segment, and design loadings are input to the analysis processor routine. The buckling analysis is performed which provides the critical eigenvalues for the global buckling response of the grid-stiffened cylinder, the local buckling response of the skin and stiffener segments, and the strain level factors of the skin and stiffener segments. The weight of the grid-stiffened cylinder is also computed. This procedure is repeated for each design configuration in the population. The “fitness” processor then evaluates the “fitness” of each design using Equation (19) and assigns a rank based on the fitness expression or objective function. The current population of design configurations is then processed by the genetic operators (crossover, mutation, and permutation) to create a new population of design configurations for the next generations which combines the most desirable characteristics of previous generations. Designs from previous generations may be replaced by new ones (i.e., children) except for the “most fit” designs (i.e., parents) which are always included in the next generation. The process is repeated until design convergence is obtained, which is defined herein by specifying a maximum number of generations (*NSTOP*) that may occur without improvement in the best design.

Chapter 3

USER INSTRUCTIONS

User instructions for using two FORTRAN codes are provided in this chapter. The first code is for analyzing a grid-stiffened cylinder subjected to combined in-plane loading. The code provides the global buckling load, local buckling load of skin and stiffener segments, and the strain level factors as output. Instructions for using this code are given in Section 3.1. The second code is for optimizing a grid-stiffened cylinder design subjected to global and local buckling constraints and strength constraints. Instructions for using this code and modifying it to obtain a particular type of optimization are given in Section 3.2.

3.1 ANALYSIS CODE

The analysis code is found in directory "cylinder/analysis" and a makefile is used to link all the subroutines together. The makefile may have to be modified to account for different computer system. Grid-stiffened cylinder with the unit cell geometry as shown in Figure 1 can be analyzed by using the code. Skin segments of the grid-stiffened cylinder are assumed to be simply-supported. Other boundary conditions of the skin segment can be accommodated through simple modifications to the source code. The executable for this code is "run" as specified in the makefile.

3.1.1 Examples for Input and Output file

An input file for a grid-stiffened cylinder with axial and diagonal stiffeners is given. The cylinder is 291.0 in. long, with a radius of 95.5 in., and has an axial and transverse stiffener spacings of 8.31428 in. and 14.4588 in., respectively. The height and thickness of the stiffener is 0.4125 in. and 0.09 in., respectively. The skin laminate has a ply stacking sequence of $[\pm 45/0_2]_{2s}$ with ply thickness of 0.008 in. The

ply orientations are measured from the x-axis in the counter-clockwise directions. The stiffener is made of unidirectional material. The material for the skin and stiffener is assumed to have the following nominal ply mechanical properties; $E_{11} = 20.2$ Msi; $E_{22} = 1.9$ Msi; $G_{12} = G_{13} = G_{23} = 0.73$ Msi and $\nu_{12} = 0.3$. The cylinder is subjected to an axial compression loading of $N_x = 1980$ lbs/in. The allowable strain are $(\epsilon_{xsk}^0) = 2428\text{E-}06$, and $(\epsilon_{xst}^0) = 1092\text{E-}06$. In this example $(\epsilon_{ysk}^0) = (\gamma_{xysk}^0) = 0.0$. The input file is named "pan.inp" and is given in List 1. Text after the character "!" are comments and need not be included in the actual file.

Some considerations for the input file are listed below.

1. The maximum number of plies in a laminate is 50, and the maximum number of material is 5.
2. When a stiffener type (axial, transverse, or diagonal) is not present, its thickness and ply thickness are entered as zero. But not the material properties and its height as shown for the transverse stiffener in the input file (List 1).
3. When analyzing cylinders stiffened in one axial direction only, one of the stiffener spacing is redundant. For example, an axially stiffened cylinder will have its stiffener spacing specified by the width of the unit cell only. The length of the unit cell is entered as the length of the cylinder. Cylinders stiffened in the circumferential or transverse directions are not considered herein.
4. The number of terms or modes (N) used in the analysis is taken from Table 1 for the local buckling of the skin. The maximum value for N is 100 as determined by parameter "nmod" in the file "panel.inc". Using a value of N between 55 and 78 is usually sufficient. The maximum number of terms (N) for the global buckling is 25 as determined by parameter "ncyl" in the file panel.inc ($N = \sqrt{ncyl}$).

Finally, if the user wishes to change the boundary conditions of the skin segment in the analysis, the subroutine "bclcal.f" has to be modified. The output file is "pan.out" and is given in List 2.

3.2 OPTIMIZATION CODE

The optimization code will optimize a grid-stiffened cylinder for minimum weight subjected to global and local buckling constraints, and strength constraints. and is found in directory “cylinder/optimize”. The executable for this code is “run” as specified in the makefile. The design variables are

1. Axial stiffener spacing (a).
2. Transverse stiffener spacing (b).
3. Stiffener height (h).
4. Stiffener thickness (t_s).
5. Skin laminate ($LAMI$).
6. Stiffening configuration ($IGEO$).

The number of design variable is defined by the parameter “n” in the main program “main.f” Each design variable can assume eight discrete values as allowed by the FORTRAN code. The eight discrete values of each design variable define the design space for optimization. The discrete values for a , b , h , and t_s are supplied through the file “inp.gen” which is read by the main program “main.f”. Part of the main program where the parameter “n”, the parameter for the population size “m” are defined, and the values for a , b , h , and t_s are read is shown in List 3. The discrete values for $LAMI$ and $IGEO$ are given in Table 2. The weight of the cylinder depends on the density of the material used. The density of the material, ρ , is hard-wired in subroutine “volume.f” and can be changed by adjusting the statement “rho = 0.057” in the subroutine.

Table 2 Design space for design variables *ICON* and *LAMI*.

Integer value	<i>LAMI</i>	<i>IGEO</i>
1	$[\pm 45/0]_{2s}$	axial stiffeners
2	$[\pm 45/90]_{2s}$	axial stiffeners*
3	$[\pm 45/0/90]_{2s}$	axial and transverse stiffeners
4	$[\pm 45/0_2]_{2s}$	diagonal stiffeners
5	$[\pm 45/90_2]_{2s}$	axial and diagonal stiffeners
6	$[\pm 45/0_2/90]_{2s}$	transverse and diagonal stiffeners
7	$[\pm 45/0/90_2]_{2s}$	axial, transverse and diagonal stiffeners
8	$[\pm 45/0_2/90_2]_{2s}$	no stiffeners

* Cylinders with circumferential stiffeners only are not considered.

The laminate stacking sequence corresponding to various discrete values of *LAMI* are hard-wired in subroutine "cskin.f", and can be changed by modifying subroutine "cskin.f". The ply thickness in subroutine "cskin.f" is kept constant for all laminates, and is read in "cskin.f". Subroutine "cskin.f" can be modified by the user to accommodate various laminate stacking sequences. The discrete values for *IGEO* are assigned in subroutine "panel.f" and part of the code where *IGEO* are being assigned is shown in List 4. Subroutine "geom.f" assigns the stiffening configuration based on the value of *IGEO* which is supplied by the main program "main.f".

Some parameters that may affect the optimization process are

- The population size "m" is hard-wired in "main.f". Usually $m > 2n$, and this condition has been found to work well, and $m \gg 2n$ is not recommended ([11]).
- The probabilities of crossover, mutation, and permutation have been hard-wired to 1.0, 0.1, and 0.95 in "main.f" ([11]).
- The termination criteria "NSTOP" is hard-wired in "main.f". The user has to experiment with the value of "NSTOP". Usually the code is run with a value of "NSTOP" and then with another value of "NSTOP" greater than the previous one. If there is no change in the optimal designs, then the second value of "NSTOP" provide a good value as a stopping criteria. For the problem under consideration, $NSTOP=25$, is usually sufficient.

- The penalty parameter r_i in Equation (19) can either increase at every i^{th} generation or can be constant for all generation. In subroutine "panel.f", r_i is kept constant at 1000. By commenting the line where "ainipen = 1000.0", the user can set

$$r_i = 1000 + i^2 \quad (20)$$

Keeping r_i constant works very well for the present optimization problem.

According to Lists 3 and 4, the code has been set up to optimize grid-stiffened panel with all design variables active.

3.2.1 Changing the Type of Optimzation

The user may want to optimize a grid-stiffened cylinder with less number of design variables. For example, the skin laminate and the stiffening configuration are fixed, and the only design variables are a , b , h , and t_s . An example of such an optimization is provided with the required input files, and the output files from the code are explained.

Consider the cylinder described in Sub-section 3.1.1, the cylinder is to be optimized for $N_x = 1980$ lbs/in., with design variables being a , b , h , and t_s . The skin laminate is $[\pm 45/0_2]_{2s}$ with a ply thickness of 0.008 in. Only axial and diagonal stiffeners are considered and therefore $IGEO = 5$. The axial stiffener spacing a and transverse stiffener spacing b is treated as one design variable i.e., (a, b) is a design variable. Values for (a, b) are provided such that the stiffening configuration closely approximates an isogrid configuration (i.e., $\theta \approx 30^\circ$). Hence, there are three design variables. In this example, the allowable strains are set to zero, and hence the strength constraints are inactive. List 5 and 6 show the appropriate modifications to "main.f" and "panel.f" respectively. In List 5, "n" has been changed to 3, and "m" has been changed to 8. While in List 6, a "!" modify" indicates the line that has been modified.

The code needs two input files, namely "inp.gen", and "pan.inp". The file "inp.gen" is read by program "main.f" and it defines the design space for the stiffener spacings, and the height and thickness of the stiffener. The file "pan.inp" provides the

problem parameters for the optimization problem and is read by subroutine "panel.f". Example for "inp.gen", and "pan.inp" are given in List 7 and 8 respectively.

The output files produced by the code are "best.gen", "on.gen", and "pan.out". The files "best.gen", and "on.gen" are produced by program "main.f", and the file "pan.out" is produced by subroutine "panel.f". The optimal designs ranked according to Equation (19) are stored in the file "best.f" and the convergence history of the optimization is stored in the file "on.gen". The file "best.gen" and "on.gen" for the above example is given in Lists 9 and 10 respectively.

The file "pan.out" stores the information about each design resulting from the analysis and is quite large. It is useful in obtaining the buckling loads and other information about the optimal designs stored in file "best.gen". To access information about an optimal design, use the value of its fitness (FS) in "best.gen" and locate that number (critlb) in "pan.out" using the search option of the unix editor being used. For example, the best design, which is the first design in "best.gen" has "FS=0.3512084E+00". Searching for the pattern "0.3512084E+00" in "pan.out" will bring the cursor to where information about the best design is written. List 11 and 12 give information about the first and second optimal designs which have been extracted from "pan.out".

LIST OF FILES

List 1: Example for Input file (pan.inp)

```

0.128 ! thickness of skin
1      ! Number of material
1,20.2e6,1.9e6,0.3,0.73e6 ! Material No., E11, E22, V12, G12
16     ! No. of plies
1,1,0.008,45.0 ! layer No., Material No., ply thickness, theta
2,1,0.008,-45.0
3,1,0.008,0.0
4,1,0.008,0.0
5,1,0.008,45.0
6,1,0.008,-45.0
7,1,0.008,0.0
8,1,0.008,0.0
9,1,0.008,0.0
10,1,0.008,0.0
11,1,0.008,-45.0
12,1,0.008,45.0
13,1,0.008,0.0
14,1,0.008,0.0
15,1,0.008,-45.0
16,1,0.008,45.0
0.09                                     !*axial stiffener thickness
1                                     ! Number of material
1,20.2e6,1.9e6,0.3,0.73e6 ! Material No., E11, E22, V12, G12
1                                     ! No. of layers
1,1,0.090,0.0 ! layer No., Material No., ply thickness, theta
0.0                                     !*transverse stiffener thickness
1                                     ! Number of material
1,20.2e6,1.9e6,0.3,0.73e6 ! Material No., E11, E22, V12, G12
1                                     ! No. of layers
1,1,0.0,0.0 ! layer No., Material No., ply thickness, theta
0.090                                     !*diagonal stiffener thickness
1                                     ! Number of material
1,20.2e6,1.9e6,0.3,0.73e6 ! Material No., E11, E22, V12, G12
1                                     ! No. of layers
1,1,0.090,0.0 ! layer No., Material No., ply thickness, theta
0.4125,0.4125,0.4125 ! height of X, Y, D-stiffener
291.0,95.5 ! length, radius of cylinder
8.31428,14.4588 ! length,width,orientation of U. cell
15 ! max m,n in Fourier series
45 ! # of modes considered for local buckling
1980.0,0.0,0.0 ! Nx, Ny, Nxy (loading condition)
2428.0e-06,0.0,0.0,1092.0e-06 ! skin_x, y, xy, stiff (allow. strains)

```

List 2: Example for Output file (pan.out)

SKIN LAMINATE DATA

STACK THICKNESS= 0.1280000000000000 in

NO. of MATERIAL types= 1

MAT.NO.	E1 (psi)	E2 (psi)	V12	G12 (psi)
1	0.2020E+08	0.1900E+07	0.3000	0.7300E+06

LAYER No.	MATERIAL No.	THK (in)	ORIENTATION (deg)
1	1	0.0080	45.0000
2	1	0.0080	-45.0000
3	1	0.0080	0.0000
4	1	0.0080	0.0000
5	1	0.0080	45.0000
6	1	0.0080	-45.0000
7	1	0.0080	0.0000
8	1	0.0080	0.0000
9	1	0.0080	0.0000
10	1	0.0080	0.0000
11	1	0.0080	-45.0000
12	1	0.0080	45.0000
13	1	0.0080	0.0000
14	1	0.0080	0.0000
15	1	0.0080	-45.0000
16	1	0.0080	45.0000

X-STIFFENER LAMINATE DATA

STACK THICKNESS= 8.999999999999997E-02in

NO. of MATERIAL types= 1

MAT.NO.	E1 (psi)	E2 (psi)	V12	G12 (psi)
1	0.2020E+08	0.1900E+07	0.3000	0.7300E+06

LAYER No.	MATERIAL No.	THK (in)	ORIENTATION (deg)
1	1	0.0900	0.0000

Y-STIFFENER LAMINATE DATA

STACK THICKNESS= 0.0000000000000000E+00in

NO. of MATERIAL types= 1

MAT.NO.	E1 (psi)	E2 (psi)	V12	G12 (psi)
---------	-------------	-------------	-----	--------------

1 0.2020E+08 0.1900E+07 0.3000 0.7300E+06

LAYER No.	MATERIAL No.	THK (in)	ORIENTATION (deg)
1	1	0.0000	0.0000

DIAGONAL-STIFFENER LAMINATE DATA

STACK THICKNESS= 8.999999999999997E-02in
NO. of MATERIAL types= 1

MAT.NO.	E1 (psi)	E2 (psi)	V12	G12 (psi)
1	0.2020E+08	0.1900E+07	0.3000	0.7300E+06

LAYER No.	MATERIAL No.	THK (in)	ORIENTATION (deg)
1	1	0.0900	0.0000

Height of X-stiffener = 0.4125000000000000
Height of Y-stiffener = 0.4125000000000000
Height of Dia-stiffener = 0.4125000000000000

Length = 291.00000000000000
Radius = 95.50000000000000

STIFFENER ORIENTATION (deg) = 29.90030151121361
UNIT CELL LENGTH (in) = 8.314280000000000
UNIT CELL WIDTH (in) = 14.458800000000000

No of MODES FOR CYLINDER = 15
No of MODES CONSIDERED = 45

* U *	* V *	* W *	*pX *	*pY *
0	0	0	0	0
1	0	1	0	1
0	1	0	1	0
2	0	2	0	2
1	1	1	1	1
0	8	0	8	0

LOADING MATRIX

1980.000	0.000
0.000	0.000

STRAIN ALLOWABLE

Max. axial strain in skin = 2.428000000000000E-03
Max. transverse strain in skin = 0.000000000000000E+00
Max. shear strain in skin = 0.000000000000000E+00

Max. axial strain in stiffener = 1.0920000000000001E-03

.....
END OF INPUT DATA
.....

SKIN STIFFNESS DATA

Extensional Stiffness (lbs)

1725572.065	365086.081	0.000
365086.081	544372.803	0.000
0.000	0.000	384943.176

Coupling Stiffness (lbs)

0.000	0.000	0.000
0.000	0.000	0.000
0.000	0.000	0.000

Bending Stiffness (lbs-in)

1904.344	647.714	94.496
647.714	896.388	94.496
94.496	94.496	674.825

Transverse shear stiffness (lbs/in)

0.77867E+05	0.00000E+00
0.00000E+00	0.77867E+05

STIFFENER	EXTENSIONAL	COUPLING	BENDING	SHEAR
STIFFNESS	(lbs)	(lbs in)	(lbs in ²)	(lbs)
1	0.7499E+06	-.2027E+06	0.6540E+05	0.2710E+05
2	0.0000E+00	0.0000E+00	0.0000E+00	0.0000E+00
3	0.7499E+06	-.2027E+06	0.6540E+05	0.2710E+05

<< ONLY AXIAL & DIAGONAL STIFFENERS >>

Stiffening Parameter (X) = 7.0050200635535451E-02

Stiffening Parameter (Y) = 0.0000000000000000E+00

Stiffening Parameter (D) = 2.8935348775449919E-02

cxc = 9.2134956352011789E-08

cxs = 0.0000000000000000E+00

sxc = -3.4502801522281621E-08

sxs = 0.0000000000000000E+00

znn = -1.8697911092877051E-02

zstar = -9.8630197802043167E-03

ystar = 0.7139400000000000

nstep = 10

cxc = 1.7963803460849354E-07

cxs = 1.5821236813778613E-07

sxc = -6.2975256903652235E-07

sxs = -1.2523730494538431E-07

znn = -3.6583424817610677E-02

zstar = -1.8291712342129864E-02

ystar = 8.2494266793107549E-02

nstep = 1

CORRECTED STIFFNESS

STIFFENER STIFFNESS	EXTENSIONAL (lbs)	COUPLING (lbs in)	BENDING (lbs in ²)	SHEAR (lbs)
1	0.7499E+06	-.1968E+06	0.6148E+05	0.2710E+05
2	0.0000E+00	0.0000E+00	0.0000E+00	0.0000E+00
3	0.7499E+06	-.1903E+06	0.5824E+05	0.2710E+05

EXTENSIONAL SMEARED STIFFNESS

Stiffeners			
116573.817	38857.468	0.000	
38857.468	117514.026	0.000	
0.000	0.000	38857.468	
stiffeners + skin			
1842145.881	403943.549	0.000	
403943.549	661886.829	0.000	
0.000	0.000	423800.644	

COUPLING SMEARED STIFFNESS

Stiffeners			
-30481.518	-9861.939	0.000	
-9861.939	-29824.800	0.000	
0.000	0.000	-9861.939	
stiffeners + skin			
-30481.518	-9861.939	0.000	
-9861.939	-29824.800	0.000	
0.000	0.000	-9861.939	

BENDING SMEARED STIFFNESS

Stiffeners			
9501.363	3017.777	0.000	
3017.777	9126.460	0.000	
0.000	0.000	3017.777	
stiffeners + skin			
11405.708	3665.491	94.496	
3665.491	10022.848	94.496	
94.496	94.496	3692.602	

SMEARED TRANSVERSE SHEAR STIFFNESS (lbs/in)

stiffeners		
5617.481	0.000	
0.000	5651.461	
stiffener + skin		
5617.481	0.000	
0.000	5651.461	

.....
BEGIN BUCKLING ANALYSIS
.....

lcons= 225
ierr 0

```

glam = 0.9713123932539653      ! Global lambda
skfx = 1800.514438239891      ! (Nx)_sk
skfy = 0.0000000000000000E+00 ! (Ny)_sk
skfxy = 0.0000000000000000E+00 ! (Nxy)_sk
stdfx = 236.9871816396951      ! N_dx
stdfy = 0.0000000000000000E+00 ! N_dy
stdfxyx = 0.0000000000000000E+00 ! (N_dxy)_x
stdfxyy = 0.0000000000000000E+00 ! (N_dxy)_y
stfx = 1913.152055822510      ! (N_x)_1
DETERMINANT = 60.10725583200000
skilam = 1.248682754551860      ! lambda_skin
riblx = 1.880641154677955      ! lambda_x_stiff
ribld = 30.42410048392902      ! lambda_d_stiff
rlam = 1.0000000000000000
xxl = 1.996763412355778        ! S_xsk
yyl = 0.0000000000000000E+00   ! S_ysk
xyl = 0.0000000000000000E+00   ! S_xysk
xstl = 1.037612920905549       ! S_1
xstl3 = 16.80356955513164      ! S_2
Volume = 1428.192546820781 ! (weight (lbs) density = 0.057 lbs/in^3
CPU TIME 8.131398

```

List 3: Part of main program "main.f"

```

C          GENETIC ALGORITHM
C
C      IS(I,J), I being the individual number and J its Jth  bits.
C      IS(I,J) bit string number I (old generation)
C      JS(I,J) bit string number I (new generation)
C      CRITLB(I) fitness associated to the individual I
C      FNS(I) normalized fitness of the individual I
C      M population size
C      NLA maximum number of layers
C      N number of bits in a string (=NLA/4)
C      PC probability of implementing crossover
C      PM probability of implementing mutation
C      PP probability of permutation
C      PRI probability of inversion
C      ITER iteration (generation) number
C
C
C*****
C      parameter (n=6,m=12,nn=m*2)
C
C      n = number of design variables
C      m = number of design in each group
C      nn= just for dimension ( parameter)
C
C      DIMENSION IS(nn,n), FNS(100), RD(n) ,JS(m,n),
C      &CRITLB(100),CRITZ(100),aas(8),bbs(8),hh1(8),tthk1(8),
C      &ISK(50,m),FSK(50),NGEN(50),alength(n)
C      real*4 tcp2(2)
C
C      COMMON/PIE/PI
C      COMMON/MATGEO/T,NLA
C      common /function/critlb
C
C      OPEN (UNIT=15, FILE='on.gen')
C      OPEN (UNIT=12, FILE='best.gen')
C      OPEN (UNIT=9 , FILE='inp.gen')
C
C      nla=16
C      N=NLA/4
C      n=15
C
C      Maximum number of generations
C
C      read(9,*)(aas(ij),ij=1,8)
C      read(9,*)(bbs(ij),ij=1,8)
C      read(9,*)(hh1(ij),ij=1,8)
C      read(9,*)(tthk1(ij),ij=1,8)
C
C      LTT=300
C

```

```

C      Genetic parameters
C
C      PC=1.00D+00
C      PM=0.10D+00
C      PP=0.95+00
C      M=16
C
C      NFT is the number of evaluations of the objective function
C      without improvement before the search stops.
C
C      NFT=150
C
C      Initialization of the stopping criterion
C
C      NCRIT=0
C      OPTI=0.D+00
C
C      NSTOP is the maximum number of generations without
C      improvement.
C
C      NSTOP=20
C
C      Initialization of the parameters of the subroutine STORE
C      before the first call.
C
C
C
C
C      call dtime(tcp2)
C      write(12,*)'CPU TIME =',tcp2(1)
C      CLOSE(12)
C      END

```

List 4: Part of subroutine "panel.f"

```

subroutine panel (io,is,critlb,ainipen,nn,nd,aas,bbs,hh1,
&               tthk1)
.
.
    include "opt.inc"
    include "panel.inc"
    integer is(nn,nd)
C
C    - - - - -
C    UNIT 5 FOR THE INPUT DATA FILE
C    - - - - -
    open(5,file='pan.inp')
    rewind 5
C
C    - - - - -
C    UNIT 6 IS FOR THE OUTPUT DATA FILE
C    - - - - -
    open(6,file='pan.out')
.
.
    clen = aas(is(io,1))
    cwid = bbs(is(io,2))
    h1    = hh1(is(io,3))
    h2    = h1
    h3    = h1
    thick = tthk1(is(io,4))
    igeo  = is(io,5)
    lami  = is(io,6)
    igeo  = is(io,6)
    call geom(sth1,sth2,sth3,igeo,thick)
    write(6,*)'-----'
    write(6,*)'Laminate = ',lami
    write(6,*)'Stiffener thickness = ',thick
    write(6,*)'Stiffener height   = ',h1
C
C    [1] READING ALL INPUT DATA FOR A LAMINATE
C           USING SUBROUTINE ISKIN
C    -----
    call iskin(sthk,nmsk,exsk,eysk,vsk,gsk,amatsk,nsk,
&             lnosk,msk,tsk,thesk)
C
    call cskin(sthk,nmsk,exsk,eysk,vsk,gsk,amatsk,nsk,
&             lnosk,msk,tsk,thesk,lami)
C
.
.
    write(6,51)critlb(io)
51  format('critlb = 'e14.7)
    write(6,*)'-----'
    return
end

```

List 5: Modifications to main program "main.f"

```

C          GENETIC ALGORITHM
C
C  IS(I,J), I being the individual number and J its Jth bits.
C  IS(I,J) bit string number I (old generation)
C  JS(I,J) bit string number I (new generation)
C  CRITLB(I) fitness associated to the individual I
C  FNS(I) normalized fitness of the individual I
C  M population size
C  NLA maximum number of layers
C  N number of bits in a string (=NLA/4)
C  PC probability of implementing crossover
C  PM probability of implementing mutation
C  PP probability of permutation
C  PRI probability of inversion
C  ITER iteration (generation) number
C
C*****
C      parameter (n=3,m=8,nn=m*2)
C
C      n = number of design variables
C      m = number of design in each group
C      nn= just for dimension ( parameter)
C
C      DIMENSION IS(nn,n), FNS(100), RD(n) ,JS(m,n),
C      &CRITLB(100),CRITZ(100),aas(8),bbs(8),hh1(8),tthk1(8),
C      &ISK(50,m),FSK(50),NGEN(50),alength(n)
C      real*4 tcp2(2)
C
C      COMMON/PIE/PI
C      COMMON/MATGEO/T,NLA
C      common /function/critlb
C
C      OPEN (UNIT=15, FILE='on.gen')
C      OPEN (UNIT=12, FILE='best.gen')
C      OPEN (UNIT=9 , FILE='inp.gen')
C
C      .
C      .
C      .
C
C      read(9,*)(aas(ij),ij=1,8)
C      read(9,*)(bbs(ij),ij=1,8)
C      read(9,*)(hh1(ij),ij=1,8)
C      read(9,*)(tthk1(ij),ij=1,8)
C
C      .
C      .
C      .
C
C      END

```

List 6: Modifications to subroutine "panel.f"

```

subroutine panel (io,is,critlb,ainipen,nn,nd,aas,bbs,hh1,
&                tthk1)
.
.
.
      include "opt.inc"
      include "panel.inc"
      integer is(nn,nd)
C
C      - - - - -
C      UNIT 5 FOR THE INPUT DATA FILE
C      - - - - -
      open(5,file='pan.inp')
      rewind 5
C
C      - - - - -
C      UNIT 6 IS FOR THE OUTPUT DATA FILE
C      - - - - -
      open(6,file='pan.out')
.
.
.
      clen  = aas(is(io,1))      ! modify
      cwid  = bbs(is(io,1))      ! modify
      igeo  = 5                  ! modify
      lami  = 4                  ! modify
      h1    = hh1(is(io,2))      ! modify
      h2    = h1                 ! modify
      h3    = h1                 ! modify
      thick = tthk1(is(io,3))    ! modify
C
      call geom(sth1,sth2,sth3,igeo,thick)
      write(6,*)'-----'
      write(6,*)'Laminate =',lami
      write(6,*)'Stiffener thickness = ',thick
      write(6,*)'Stiffener height   = ',h1
C      -----
C      [1] READING ALL INPUT DATA FOR A LAMINATE
C           USING SUBROUTINE ISKIN
C      -----
      call iskin(sthk,nmsk,exsk,eysk,vsk,gsk,amatsk,nsk,
&                lnosk,msk,tsk,thesk)
C
      call cskin(sthk,nmsk,exsk,eysk,vsk,gsk,amatsk,nsk,
&                lnosk,msk,tsk,thesk,lami)
C
.
.
.
      END

```

List 7: Input file for optimization (inp.gen).

```

7.4615385,7.6578947,7.86486,8.08333,8.31428,8.559,
      8.818181,9.09375      ! a
12.904760,13.334316,13.637386,13.954510,14.458800,
      14.815906,15.385749,15.790637      ! b
0.40,0.4125,0.425,0.4375,0.45,0.4625,0.475,0.4875      ! h
0.048,0.054,0.06,0.066,0.072,0.078,0.084,0.090      ! t

```

List 8: Input file for problem parameters (pan.inp).

```

1      ! Number of material
1,20.2e6,1.9e6,0.3,0.73e6 ! Material No., E11, E22, V12, G12
0.008 ! ply thickness for skin laminate
1      !*Number of material (X-stiffener)
1,20.2e6,1.9e6,0.3,0.73e6 ! Material No., E11, E22, V12, G12
1      ! Number of plies
1,1,0.0 ! layer No., material No., theta
1      !*Number of material (Y-stiffener)
1,20.2e6,1.9e6,0.3,0.73e6 ! Material No., E11, E22, V12, G12
1      ! Number of plies
1,1,0.0 ! layer No., material No., theta
1      !*Number of material (D-stiffener)
1,20.2e6,1.9e6,0.3,0.73e6 ! Material No., E11, E22, V12, G12
1      ! Number of plies
1,1,0.0 ! layer No., material No., theta
291.0,95.5 ! length, radius of cylinder
15      ! max m,n in Fourier series
45      ! # of modes considered for local buckling
1980.0,0.0,0.0,0.0 ! Nx, Ny, Nxy
0.0,0.0,0.0,0.0 ! skin_x, _y, _xy, stiff_x (strain allowable)

```


List 9: Output file containing optimal designs (best.gen).

```

POPULATION SIZE= 8 Crossover PROB.=1.000
MUTATION PROB.=0.100 PERMUTATION PROB.=0.950
BESTS DESIGNS AFTER 246 EVALUATIONS OF THE OF
  FS= 0.3512084E+00 GENERATION= 15
7 3 8
  FS= 0.3500683E+00 GENERATION= 8
5 2 8
  FS= 0.3499497E+00 GENERATION= 13
6 3 8
  FS= 0.3494749E+00 GENERATION= 9
8 3 8
  FS= 0.3489305E+00 GENERATION= 4
5 3 8
  FS= 0.3478998E+00 GENERATION= 34
8 5 6
  FS= 0.3478000E+00 GENERATION= 11
5 4 8
  FS= 0.3477422E+00 GENERATION= 33
6 5 8
  FS= 0.3456823E+00 GENERATION= 1
2 3 8
  FS= 0.3455608E+00 GENERATION= 7
.
.
.
CPU TIME = 1985.198

```

List 10: Onput file containing convergence history (best.gen).

population size= 8 crossover prob.=1.000
 mutation prob.=0.100 permutation prob.=0.950

Iteration	Average	Best
1	0.1474611E+00	0.3456823E+00
2	0.1024948E+00	0.3456823E+00
3	0.1993546E+00	0.3456823E+00
4	0.2728501E+00	0.3489305E+00
5	0.2851492E+00	0.3489305E+00
6	0.3256674E+00	0.3489305E+00
7	0.2783510E+00	0.3489305E+00
8	0.2561589E+00	0.3500683E+00
9	0.3033118E+00	0.3500683E+00
10	0.2970200E+00	0.3500683E+00
11	0.3478100E+00	0.3500683E+00
12	0.3478156E+00	0.3500683E+00
13	0.2627671E+00	0.3500683E+00
14	0.2576738E+00	0.3500683E+00
15	0.3180880E+00	0.3512084E+00
16	0.3490608E+00	0.3512084E+00
17	0.3021455E+00	0.3512084E+00
18	0.3403848E+00	0.3512084E+00
19	0.3053899E+00	0.3512084E+00
20	0.2841141E+00	0.3512084E+00
21	0.3408947E+00	0.3512084E+00
22	0.3505790E+00	0.3512084E+00
23	0.3286393E+00	0.3512084E+00
24	0.3287967E+00	0.3512084E+00
25	0.3507364E+00	0.3512084E+00
26	0.3414941E+00	0.3512084E+00
27	0.3363042E+00	0.3512084E+00
28	0.3312716E+00	0.3512084E+00
29	0.3270619E+00	0.3512084E+00
30	0.3008105E+00	0.3512084E+00
31	0.3288947E+00	0.3512084E+00
32	0.3504603E+00	0.3512084E+00
33	0.3406868E+00	0.3512084E+00
34	0.3283831E+00	0.3512084E+00

FINAL POPULATION AFTER 246 EVALUATIONS OF THE O.F.

List 11: Information about first optimal design from (pan.out).

```

-----
Laminate =                4
Stiffener thickness =    8.999999999999997E-02
Stiffener height   =    0.4250000000000000

STIFFENER ORIENTATION (deg) = 29.81872703828845
UNIT CELL LENGTH      (in)  = 8.818180999999999
UNIT CELL WIDTH       (in)  = 15.385749000000000
<< ONLY AXIAL & DIAGONAL STIFFENERS >>
Stiffening Parameter (X) = 6.7824713502575448E-02
Stiffening Parameter (Y) = 0.0000000000000000E+00
Stiffening Parameter (D) = 2.7831146619772991E-02
IFLAG =                5
znn = -1.8748481539636742E-02
zstar = -9.8976731692590435E-03
ystar = 0.7602874500000001
nstep =                10
znn = -3.6390656669926545E-02
zstar = -1.8195328248661609E-02
ystar = 8.7768143721372954E-02
nstep =                1
lcons=                225
ierr =                0
Global lambda =        1.004465200334541
penalty factor =      100000.00000000000
skfx =        1865.845124687763
skfy =        0.0000000000000000E+00
skfxy =       0.0000000000000000E+00
stdfx =        243.7657369767708
stdfy =        0.0000000000000000E+00
stdfxyx =      0.0000000000000000E+00
stdfxyy =      0.0000000000000000E+00
stfx =        1982.569736920487
DETERMINANT =        67.83715975128450
skilam =        1.075033581289790
riblx =        1.698565494963615
ribld =        27.73106058929319
rlam =        1.0000000000000000
xxl =        0.0000000000000000E+00
yyl =        0.0000000000000000E+00
xyl =        0.0000000000000000E+00
xstl1 =      0.0000000000000000E+00
xstl3 =      0.0000000000000000E+00
Volume =       1423.555983291840
critlb =       0.3512084E+00
-----

```

List 12: Information about second optimal design from (pan.out).

```

-----
Laminate =                4
Stiffener thickness =    8.9999999999999997E-02
Stiffener height   =    0.4125000000000000

STIFFENER ORIENTATION (deg) = 29.90030151121361
UNIT CELL LENGTH      (in)  = 8.314280000000000
UNIT CELL WIDTH      (in)  = 14.458800000000000
<< ONLY AXIAL & DIAGONAL STIFFENERS >>
Stiffening Parameter (X) = 7.0050200635535451E-02
Stiffening Parameter (Y) = 0.0000000000000000E+00
Stiffening Parameter (D) = 2.8935348775449919E-02
IFLAG =                5
znn = -1.8697911092877051E-02
zstar = -9.8630197802043167E-03
ystar = 0.7139400000000000
nstep =                10
znn = -3.6583424817610677E-02
zstar = -1.8291712342129864E-02
ystar = 8.2494266793107549E-02
nstep =                1
lcons=                225
ierr                0
Global lambda =      1.001613221328421
penalty factor =    100000.00000000000
skfx =      1856.682854104444
skfy =      0.0000000000000000E+00
skfxy =      0.0000000000000000E+00
stdfx =      244.3801768249596
stdfy =      0.0000000000000000E+00
stdfxxy =      0.0000000000000000E+00
stdfxyy =      0.0000000000000000E+00
stfx =      1972.834287745410
DETERMINANT =      60.10725583200000
skilam =      1.210907572842309
riblx =      1.823747951708783
ribld =      29.50370983966332
rlam =      1.0000000000000000
xxl =      0.0000000000000000E+00
yyl =      0.0000000000000000E+00
xyl =      0.0000000000000000E+00
xstl1 =      0.0000000000000000E+00
xstl3 =      0.0000000000000000E+00
Volume =      1428.192546820781
critlb =      0.3500683E+00
-----

```

References

- [1] Jaunky, N., Knight, N. F. and Ambur, D. R., "An Improved Smeared Theory for Buckling Analysis of Grid-Stiffened Composite Panels," *Composite: Part B* (formerly *International Journal for Composite engineering*), Vol. 27B, No. 5, 1996, pp. 519-526.
- [2] Jaunky, N., Knight, N. F. and Ambur, D. R., "Buckling of Arbitrary Quadrilateral Anisotropic Plates," *AIAA Journal*, Vol. 33, May 1995, pp. 938-944.
- [3] Jaunky, N., Knight, N. F. and Ambur, D. R., "Buckling Analysis of General Triangular Anisotropic Plates using Polynomials," *AIAA Journal*, Vol. 33, December 1995, pp. 2414-2417.
- [4] Reddy, A. D., Valisetty, Rao R., and Rehfield, L. W., "Continuous Filament Wound Composite Concepts for Aircraft Fuselage Structures," *Journal of Aircraft*, Vol. 22, No. 3, March 1985, pp. 249-255.
- [5] Sanders, J. L. Jr., "An Improved First Approximation Theory for Thin Shells," NASA Report R-24, 1959.
- [6] Koiter, W. T., "A Consistent First Approximation in General Theory of Thin Elastic Shells," *The Theory of Thin Elastic Shells*, Proceedings IUTAM Symposium, Delft, 1959, pp. 12-33, 1960, Amsterdam, the Netherlands, North-Holland Publishing Company.
- [7] Jaunky, N., "Elastic Buckling of Stiffened Composite Curved Panel," Old Dominion University, Norfolk, Virginia, Masters's Thesis, August 1991.
- [8] Jaunky, N., "Buckling Analysis and Optimum Design of Multidirectionally Stiffened Composite Curved Panel," Old Dominion University, Norfolk, VA, Ph. D. Dissertation, December 1995.
- [9] Phillips, J. L. and Gurdal, Z., "Structural Analysis and Optimum Design of Geodesically Stiffened Composite Panels," Report CCMS-90-05, Center for Composite Materials and Structures, Virginia Polytechnic Institute and State University, Blacksburg, VA, July 1990.
- [10] Nagendra, S., Haftka, R. T., and Gurdal, Z., "Design of a Blade Stiffened Composite Panel by Genetic Algorithm," Proceedings of the 34th AIAA/ASME/ASCE/AHS/ASC Structures, Structural Dynamics and Materials Conference, AIAA Paper No. 93-1584-CP, April 1993, La Jolla, CA, pp. 2418-2436.
- [11] Leriche, R., and Haftka, R. T., "Optimization of Laminate Stacking Sequence for Buckling Load Maximization by Genetic Algorithm," *AIAA Journal*, Vol. 31, No. 5, May 1993, pp. 951-956.

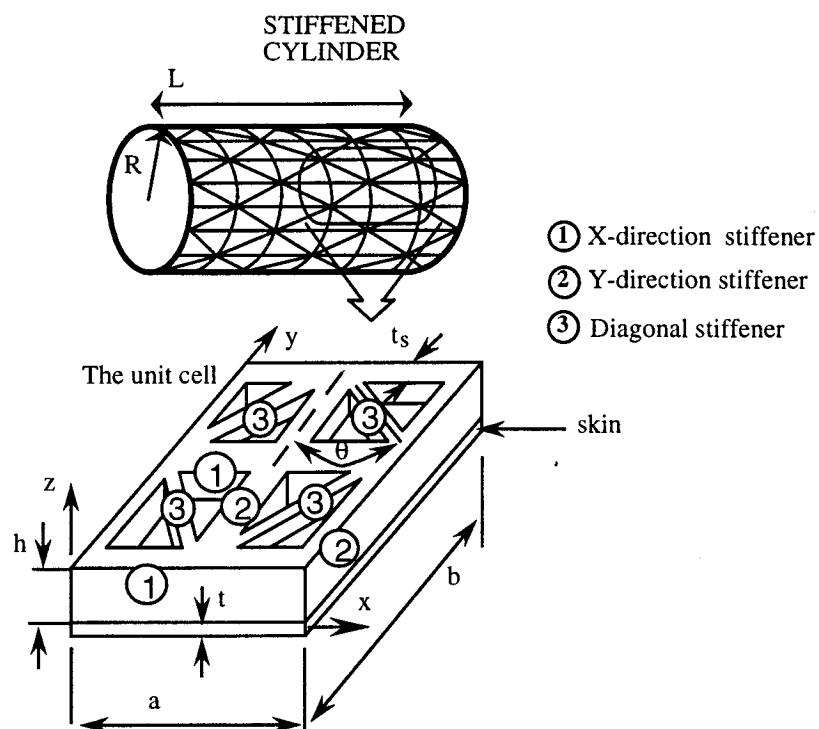


Figure 1 Unit cell of a grid-stiffened cylinder showing design variables.

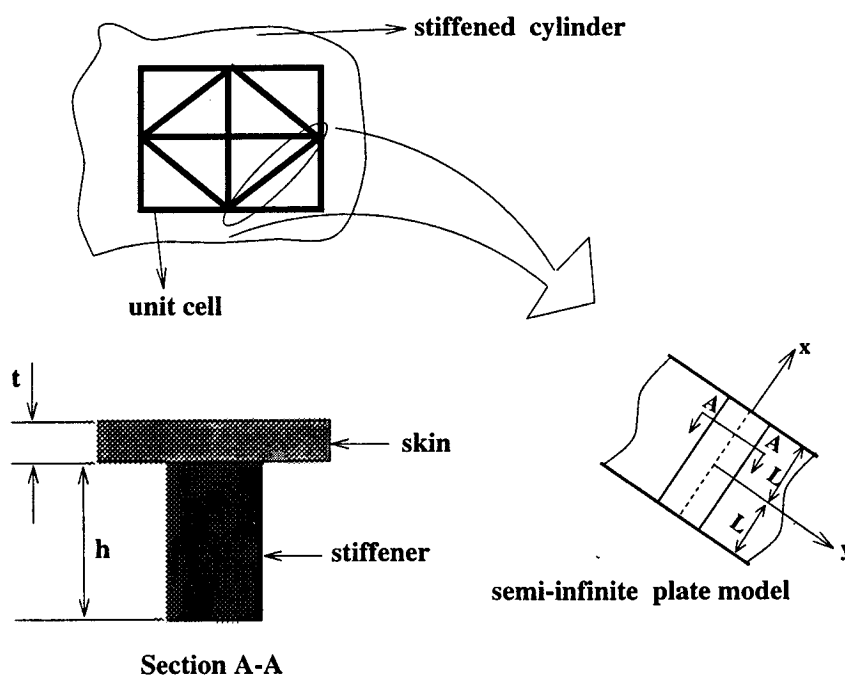


Figure 2 Semi-infinite plate model for skin-stiffener element.

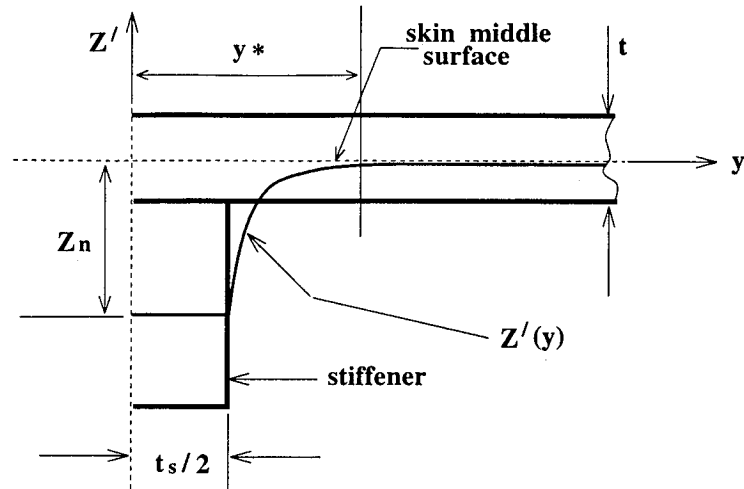


Figure 3 Typical profile for skin-stiffener element neutral surface.

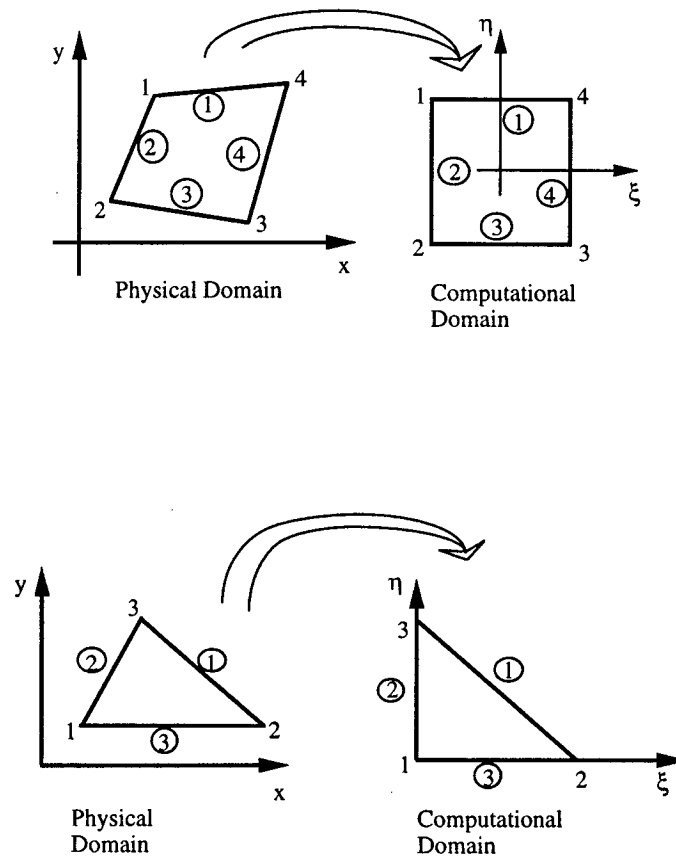


Figure 4 Physical and computational domain for plate geometries.

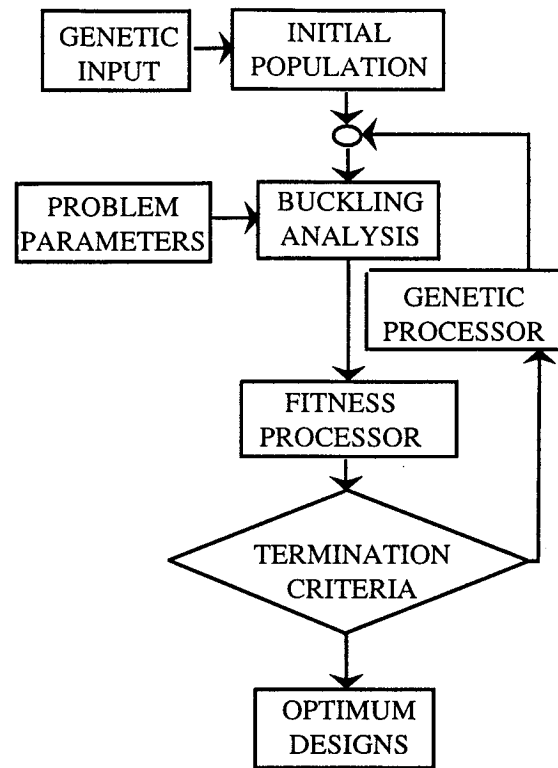


Figure 5 Flow chart showing the design optimization process.

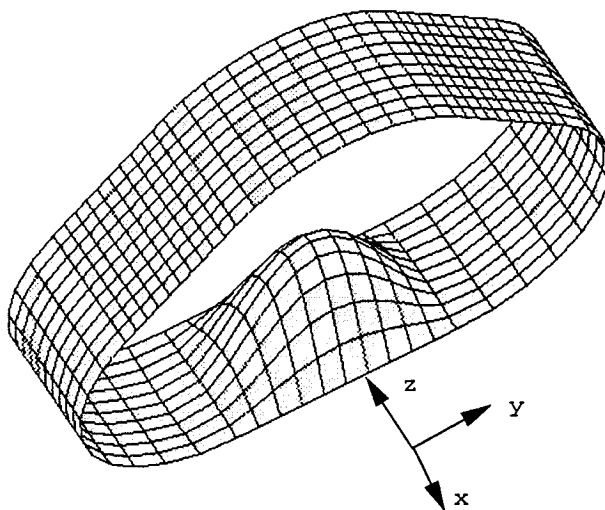
APPENDIX C

Documentation for the Analysis Code for the Buckling of Variable-Curvature Anisotropic Panels

- Theoretical Foundations
- User Instructions
- Sample Problems

BUCKLING ANALYSIS OF ANISOTROPIC VARIABLE-CURVATURE PANELS AND SHELLS

*Theoretical Foundations and
User's instructions for a FORTRAN Code*



Navin Jaunky
Department of Aerospace Engineering
Old Dominion University
Norfolk, VA 23529-0247

TABLE OF CONTENTS

TABLE OF CONTENTS	i
LIST OF FIGURES	ii
LIST OF FILES	iii
LIST OF TABLES	iv
NOMENCLATURE	v

Chapter	page
1 INTRODUCTION	1
2 THEORETICAL FOUNDATIONS	2
2.1 GEOMETRY OF VARIABLE CURVATURE PANEL	3
2.2 BEZIER POLYNOMIALS	3
2.3 CONTINUITIES ALONG SEGMENT JUNCTURES	4
2.4 MINIMUM POTENTIAL ENERGY PRINCIPLE	6
3 USER INSTRUCTIONS	8
3.1 APPLICATION OF BOUNDARY CONDITIONS	8
3.2 CYLINDRICAL PANEL	9
3.3 WING LEADING-EDGE PANEL	10
3.4 NON-CIRCULAR FUSELAGE	11
REFERENCES	19

LIST OF FIGURES

1	Coordinate system and geometry of shell with variable curvature.	22
2	Control points for joining shell segments.	22
3	Geometry and boundary conditions of curved composite panel.	23
4	Geometry, dimensions and boundary conditions of composite wing leading-edge panel.	23
5	Boundary conditions for quarter symmetric model of composite wing leading-edge panel.	24
6	Buckling load interaction curve for the composite wing-leading edge panel. ..	24
7	Geometry of non-circular fuselage.	25
8	Boundary conditions for quarter symmetric model of non-circular fuselage. ..	25

LIST OF FILES

1	Input files for cylindrical panel.	13
2	Input file for wing leading-edge panel (full model).	15
3	Input file for wing leading-edge panel (quarter symmetric model).	17
4	Input file for non-circular fuselage (isotropic).	18

LIST OF TABLES

1	Size of stiffness matrices for panel and shell for increasing number of segments.	20
2	Comparison of buckling loads results for composite curved panel.	20
3	Comparisons of buckling loads results for wing leading-edge panel.	21
4	Comparisons of buckling loads results for non-circular fuselage.	21

Nomenclature

u_0, v_0	displacement along axial and transverse directions
w	displacement along radial direction
ϕ_x, ϕ_y	rotations of normals to middle surface or curvatures
x, y, z	axial, circumferential, and normal coordinates
$f_i(n, \nu)$	Bezier polynomial of order n
q_{ij}	Bezier control points
ξ, η	non-dimensional coordinates
L	length of segment
S_I	width of segment I
R	radius of curvature

**ANALYSIS AND DESIGN OF FUSELAGE STRUCTURES
INCLUDING RESIDUAL STRENGTH PREDICTION METHODOLOGY**

- FINAL REPORT -

for

NASA Grant NAG-1-1588

Submitted to:

Structural Mechanics Branch
Structures Division
NASA Langley Research Center
Hampton, Virginia 23681-0001
Dr. James H. Starnes, Jr., Technical Monitor

by the

Department of Aerospace Engineering
College of Engineering and Technology
Old Dominion University

Principal Investigator:

Norman F. Knight, Jr., D. Sc.
Professor of Aerospace Engineering
Old Dominion University
Norfolk, Virginia 23529-0247
Telephone No. (757) 683-4265
FAX No. (757) 683-3200
Email: knight@aero.odu.edu

June 11, 1998

ANALYSIS AND DESIGN OF FUSELAGE STRUCTURES INCLUDING RESIDUAL STRENGTH PREDICTION METHODOLOGY

Final Report for NASA Grant NAG-1-1588

by

Norman F. Knight, Jr.
Department of Aerospace Engineering
College of Engineering and Technology
Old Dominion University

SUMMARY

The goal of this research project is to develop and assess methodologies for the design and analysis of fuselage structures accounting for residual strength. Two primary objectives are included in this research activity: development of structural analysis methodology for predicting residual strength of fuselage shell-type structures; and the development of accurate, efficient analysis, design and optimization tool for fuselage shell structures. Assessment of these tools for robustness, efficient, and usage in a fuselage shell design environment will be integrated with these two primary research objectives.

This research activity extended over a period of four years from January 1, 1994 until December 31, 1997 with a no-cost extension granted until March 31, 1998. Over the course of the grant, the principal investigator, graduate students, a post doctoral research assistant, and two research scientists were supported at various levels and during different time periods. This research produced nine conference papers, seven archival journal papers, one NASA report, one Ph. D. dissertation and four Master's theses. The research computer codes developed under this grant have been documented (see appendices), and a distribution CD with FORTRAN source code, sample problems, and postscript versions of the documentation is provided.

BACKGROUND

The design of aerospace structures generally results in light-weight structural designs, advanced structural materials and fabrication concepts, and highly stressed systems. The goals of aerospace structural design are to meet the design requirements for the operating conditions and flight envelope of the vehicle, adequate service life and damage tolerance, and reasonable manufacturing cost. Aerospace fuselage structures are generally subject to internal pressure loadings, thermal cycling, bending, axial, and shear loadings, and fatigue over its intended life cycle. Fuselage structures involve flat and curved stiffened and unstiffened panels with and without cutouts that are interconnected by frames, stringers and bulkheads. Damage tolerance issues associated with fuselage structures have been studied by several researchers. The two most common in fuselage structures are longitudinal cracks under hoop stresses induced by internal pressure loading and circumferential cracks

intersections are only coarsely approximately. Discrete stiffener modeling of these panels provided approximately the same level of detail in the response prediction at a fraction of the modeling and computational costs. Use of the smeared stiffener theory in STAGS was also considered; however, this formulation does not account for any skin-stiffener interaction – it simply modifies the skin stiffness by uniformly “smearing” the stiffener stiffness across the skin and accounts for eccentricity of the stiffeners. An improved theory is needed for preliminary design and analysis tools.

Shell Theories. As part of our studies on the design of cylindrical panels, various shell theories were examined including the Sanders-Koiter theory, the Love theory, and the Donnell theory (see D1). All are implemented using “tracer” coefficients in the analysis. In nearly all cases considered, the buckling results from each theory were in very good agreement. However, for angle-ply laminates with increasing anisotropy and certain winding angles, the results predicted by the Donnell theory were significantly different than those obtained using the Sanders-Koiter or Love theory. This was confirmed by STAGS finite element analyses. As the winding angle changes, changes in the buckling mode shape occur for which Donnell’s theory is not accurate. As we move towards the automated design optimization process, these changes in behavior and their impact on the spatial discretization requirements need to be understood. Results from these investigations are reported in a journal paper that has recently been accepted for publication (see JP6).

Further studies on the influence of which shell theory to use for buckling of cylindrical shells were conducted using the PANDA2 computer code from Dr. David Bushnell of the Lockheed-Martin Advanced Technology Center. These studies verified the previous results for axially compressed cylinders. In addition other loading conditions were considered: external pressure, in-plane shear loading and hydrostatic loading. In each of these loading cases, Donnell’s theory and Sander’s theory were found to be in good agreement for all values of the fiber winding angle considered (see T3).

Variational Formulation. The original plan was to develop a variational formulation of a damaged structure; however, it became necessary to develop a better understanding of other local discontinuities and their influence on local stress distributions which then contribute to the prebuckling stress state. Close examination of the skin-stiffener intersection region revealed that the traditional assumptions used in smeared stiffener theory for preliminary design and sizing of stiffened panels constrained for global overall buckling did not account for any interaction between the skin and the stiffener. This local stiffness discontinuity results in a shift of the neutral surface of the stiffened panel away from the skin middle surface as the stiffener is approached. As a result, the load redistribution between the skin and the stiffener is changed. The formulation and its comparison with traditional smeared stiffener theory is given in four publications (see CP3, JP3, R1 and D1).

Progressive Failure Analysis. This activity formed the basis of another Master’s thesis (Mr. David W. Sleight, a NASA employee) under the direction of Dr. Knight (see T1). The progressive failure analysis methodology involved the use of COMET and its generic constitutive processor (GCP) for the evaluation of point stress failure criteria, degradation of ply-level material properties, re-calculation of new laminate stiffnesses, and saving the

path-dependent historical material data. The methodology employed various solution procedures and processors from COMET which have functionally equivalent routines in the current version of STAGS.

The basic steps of the progressive failure methodology includes the following steps. First, a nonlinear solution is obtained at a given load step while holding the material data constant during the nonlinear iteration. Then the stress recovery step is performed using the element stress resultants (these should be the best available since they are provided by the element developer). Next using these stress resultants, the midplane strains and changes in curvature are computed and used to calculate the point strains and stresses through the thickness of the laminate - only in-plane components are used. Given these point values, various failure criteria can be assessed including maximum strain, Christensen's criteria, and Hashin's criteria. Next, the ply discounting method is used to degrade lamina material data and new laminate stiffness coefficients are computed. Historical data are saved and the next iteration begins.

Several standard test cases with available experimental data were used to verify the methodology and its implementation. These included the rail-shear problem and the tension-loaded open hole problem. Then compression loaded panels were analyzed and the use of these failure models on failure load prediction was performed. Overall good performance of the progressive failure analysis methodology was obtained as reported in the 1997 conference paper (see CP5). Sensitivity of the results to material allowable values is also noted. In most cases nominal values were used since experimentally determined values were unavailable.

Migration of this methodology to the STAGS finite element code should be possible provided that the STAGS code has the GCP features available in COMET. There are three critical aspects of this type of analysis. Two are mechanics related: failure mode representation and detection and material degradation modeling. The third aspect is the organization and preservation of the path-dependent historical data (similar to an elastoplastic analysis). The details of the COMET implementation are in Mr. Sleight's Master's thesis.

Shell Analysis for Design and Optimization

Shell analysis for design and optimization at the preliminary design stage must consider trade-offs between computational effort and accuracy. The analysis tasks are embedded within the design optimization iteration process and are frequently performed tens or hundreds or even thousands of times for a given design problem. Even though the computer systems are significantly more powerful today than even five years ago, there still are insufficient computational resources to embed detailed finite element structural models within the design optimization loop. This limitation is due in part to the fact that often times the design optimization procedure requires a geometry change which then requires a finite element model change which then requires an engineer in the loop.

To this end, robust and cost-effective analysis methods are being developed and integrated into design optimization programs. This research grant considers three independent strategies. The first strategy is the use of VICON (or VICON-OPT) which is based on extensions to the early work in PASCO and VIPASA. It features exact stiffness matrices

for the structural model and has a very accurate eigenvalue solver. This strategy is applicable to prismatic structures in general. The second strategy is to develop a new family of analysis and design tools for general grid-stiffened composite plate and shell structures. Significant amount of effort is devoted to this strategy. The third strategy is to explore the use of PANDA2 for the design and optimization of sandwich plates and shells accounting for local failures in the sandwich structure as well as possibly postbuckling strength. Various aspects of these three strategies are summarized next.

VICON Program. The VICON computer program for stress and buckling analysis of composite panels has been under development for a number of years. It makes use of exact stiffness matrices that produce accurate results for any prismatic assembly of flat plates without any user requirement to generate a finite element grid. It is also computationally efficient achieving results as much as an order of magnitude faster than conventional general purpose finite element codes. This efficiency has allowed the development of a design capability where the dimensions of a panel (plate breadths, layer thicknesses and ply angles) may be adjusted to achieve a minimum mass panel.

The VICON computer program for analysis and design of plate assemblies has been improved in both capability and efficiency. A six-week period was spent by Dr. Anderson at the University of Wales working with the co-developers of the program. The new capabilities that have been developed under this grant were combined with the new capabilities developed at the University of Wales to result in one program having the combined capabilities developed at both sites. In discussions with Professor Fred Williams, developed a new approach to sensitivity calculations that should result in increased accuracy and faster solution times than current method. This was implemented in the program and evaluated while at the University of Wales. Other efficiency improvements developed under the grant were given extensive evaluation and checks and a number of bugs fixed to insure compatibility with new features of the program developed at the University of Wales.

Treatment of Curved Plates. A number of different shell theories have been examined to determine the feasibility of incorporating an exact stiffness matrix for a curved plate into the VICON program. Use will be made of a numerical method developed for flat plates having transverse shear deformation that is in the present program. It is necessary that the equations have a certain format for the existing method to be directly applicable. It has been found that the theories based on either physical strains or tensor strains and neglecting inplane shear and transverse loadings for the inplane equilibrium will satisfy this format requirement. The present program which treats only flat plates exactly is based on tensor strains with the same neglect of the inplane shear and transverse loadings on inplane equilibrium. The theories for the curved plate can be implemented by simple modifications of a 10×10 matrix in the existing program. The work was accomplished by a Master's graduate student (Mr. David McGowan, a NASA employee) under the direction of Dr. M. S. Anderson. He defended his thesis during the Spring 1997 semester (see T2) and co-authored a 1997 conference paper on it as well (see CP6).

Effect of Axial Load Application Point. The equations necessary for the calculation of the additional bending that occurs for this case have been developed and implemented

in the program. The location of the load application point can be prescribed in input data and through linking equations can be made a function of the dimensions of the panel so that changes that might occur during the design process can be included.

Panels having Postbuckled Strength. The original plan was to try to use the program PBUCKLE to account for post buckling strength of a panel structure. In looking at the capabilities of PBUCKLE it appeared to be limited to certain specific cross-sections rather than the general capability of VICON. An alternate idea has been implemented that retains the generality of VICON and has the following features:

1. The designer can choose a load level, less than ultimate, at which buckling will occur.
2. The designer can choose which part of the panel will undergo significant buckling.
3. The method is quite simple and executes in the same time as would be required to design a buckle free panel.
4. The method requires an assumption of the reduction of the inplane stiffnesses of the plates that have been selected to buckle at less than ultimate load. A good estimate of this reduction can be obtained from published results on the post buckling response of individual plates.

The method is just reaching its final stages of development and has been applied to the design of a metal zee-stiffened panel having a buckling load two thirds of its ultimate load. The optimized mass of this panel was found to be about 12% less than if it were required to be a non-buckling design at ultimate load. The panel was analyzed with the STAGS program to check the validity of the simplifying assumptions made in the VICON analysis. The ultimate load determined by the STAGS analysis was 10% higher than the design load which is encouraging that the proposed method might be a valid way to design panels having postbuckling strength. These results were reported in a 1997 conference paper by Dr. Anderson (see CP7).

Grid-Stiffened Composite Panels. A collection of analysis tools has been developed which include a Rayleigh-Ritz approach for linear buckling analysis of the overall panel, Rayleigh-Ritz approach for linear buckling of the skin segments locally, and stiffener crippling assessment. As part of the design process, a global buckling analysis capability was developed. Based on these global buckling load levels, the skin segments and stiffener segments were individually analyzed to determine if their "local" buckling load exceeded the buckling load determined at the global level. If so, then this configuration was an acceptable design and its weight was computed. If not, then this configuration was penalized as an unacceptable design.

These analysis methods account for anisotropic material behavior, transverse shear deformation effects, and skin-stiffener interaction at the global level through an improved smeared stiffener theory. Local buckling analyses were developed to handle different plan-form shapes of the skin segments between stiffeners. These methods address general quadrilateral and triangular shaped skin segments and have been verified with classical solutions and finite element calculations. Two conference papers (CP1, CP2) and two journal papers (JP1, JP2) reported this work. Special attention was also given to the smeared stiffener modeling theory used in the global buckling analysis. A new improved theory was devel-

oped and implemented. A 1995 conference paper (CP3), 1996 journal paper (JP3), and 1995 NASA report (R1) resulted from this effort.

These analysis tools are integrated together and combined with a genetic algorithm for the "evolution" of a family of best designs. The implementation of the genetic algorithm used in this research is based on the software obtained from Prof. R. Haftka of the University of Florida and is gratefully acknowledged. The genetic algorithm or GA is ideal for this class of structures because of the inherent discrete nature of the design variables. That is, discrete choices exist for stiffener pattern (axial, transverse, diagonal, or selected combinations), skin lamination pattern, material type, and stiffener spacings. Integration of these various analysis methods with a design strategy based on the genetic algorithm was developed and documented (see Appendix A). These results were reported in a 1996 conference paper (CP4) and a 1998 journal paper (JP4). This research effort formed the basis of Mr. Navin Jaunky's Ph. D. dissertation under Dr. Knight's direction and was completed in December 1995 (see D1). Dr. Jaunky has continued with this research grant since that time as a post-doctoral research associate.

The source code, sample problems, and documentation (same as Appendix A) are available on a compact disk (CD).

Grid-Stiffened Composite Circular Cylinders. This research effort is focussed on the optimal design of general stiffened circular cylinders. In addition to the global buckling constraints, an exploratory study has been performed to determine the effect of strength constraints in finding an optimal design. Strain allowables are incorporated in to the analysis and compared with the computed strains in the stiffeners and panel skins for each design configuration during each generation of the genetic algorithm execution. Preliminary results indicate that the optimal design configuration without strength constraints generally leads to a grid-stiffened cylinder which in itself is very redundant in its load paths. Design configurations with strength constraints are essentially the same as those without the strength constraints except for a slight weight penalty for the case of only axial loads. For the combined load cases (e.g., hoop loads or torsion), this is not the case. Integration of these various analysis methods with a design strategy based on the genetic algorithm was developed and documented (see Appendix B). These results were reported in a 1997 conference paper (CP8), and a journal paper (galley proofs have been reviewed, publication is pending, JP5).

The source code, sample problems, and documentation (same as Appendix B) are available on a compact disk (CD).

Variable-Curvature Shell Structures. A concerted effort has been expended to verify the formulation and implementation of the variable-radius shell analysis without complete success. Representation of the variable radius has been attempted using a segmented or superelement approach based on the tools developed previously under this grant. This approach required the development of an assembly procedure and special "joining" functions along segment junctures. Using this approach, the buckling response appears to be artificially "stiffened" perhaps because of the approximations used along the segment junctures.

As an alternate approach, a global function representation of the shell radius has been attempted using a Legendre polynomial of order one. This would permit the modeling of a

shell with a linear change in curvature as a function of the circumferential coordinate. The present analysis method for buckling of anisotropic shells with variable curvature uses a segment approach where displacement fields within each segment are represented by Bezier polynomials and a first-order shear-deformation theory is used. In general, segments can be used in both axial and circumferential directions, however the present implementation considers only segments in the circumferential direction. Continuity of displacement at the junctures of adjacent segments are imposed using C^0 and C^1 conditions obtained from the properties of the Bezier control points. The shell with variable curvature is assumed to consist of two or more curved panels of constant curvature which is representative of fuselage or wing structures.

Results are presented for a composite cylindrical panel subjected axial compression, a non-circular fuselage segment subjected to axial compression, and a composite wing leading-edge variable-curvature panel subjected to combined axial compression and shear. Sanders-Koiter shell theory is used in these studies. Buckling loads from the present analysis are compared with those obtained from the STAGS finite element code. The STAGS finite element model consists of the 410 element, and curved surfaces are approximated as an assembly of flat surfaces. Buckling loads obtained from finite element solutions are determined to be four percent lower than those of the present analysis. Implementation of this method has been verified and documented (see Appendix C). These results were reported in a 1998 conference paper (CP9), and a journal paper will be submitted to the *Composite Structures* journal in the near future.

The source code, sample problems, and documentation (same as Appendix C) are available on a compact disk (CD).

Sandwich Plates and Shells. Sandwich construction techniques offer many advantages that can be exploited for advanced vehicles such as the HSCT. Recently PANDA2 has been extended to handle panels with sandwich wall construction by including the additional failure modes. Using this tool, various sandwich panel designs were assessed, and dominant designing failure modes based on the various mathematical models were identified. An exploratory study of the design of sandwich panels was performed using the PANDA2 software system with the cooperation of a research scientist, Dr. David Bushnell.

The status of analysis methods available was introduced, and analysis needs and refinements were defined. Assessment of sandwich panels, and their known potential failure modes and mechanisms will be performed using PANDA2 and their impact on the design process is identified.

PANDA2 analysis is based on a global single layer approach wherein the sandwich core material is treated as just another layer in the laminate for determining global buckling behavior. Local analyses of failure modes account for core materials and the different face sheets, if applicable, in an analytical approach using solutions from Plantema, Vinson and PANDA2's models. Failure modes include face wrinkling, face dimpling, core shear crimping, core transverse shear stress failure, core crushing and tension, and face sheet pull-off. Of the approximations built into PANDA2, those associated with the transverse shear effects and the single-term buckling solution used in the PANDA-type (closed-form) analysis appear to be the more limiting factors in the analysis of sandwich structures.

This work was accomplished by a Master's graduate student (Mr. Hao Jiang) under

the direction of Dr. Knight (see T3). He should defend his thesis during the Summer 1998 semester and a copy of his thesis will be forwarded to the technical monitor at that time.

PUBLICATIONS SPONSORED BY NAG-1-1588

The following conference papers, archival journal papers, NASA reports, Master's theses and dissertations resulted either in part or totally from the research effort sponsored by this grant. Copies of these papers have already been provided to the technical monitor when they appeared in the open literature.

Conference Papers

- CP1 Jaunky, Navin, Knight, N. F., Jr., and Ambur, D. R., "Buckling of Arbitrary Quadrilateral Anisotropic Plates," AIAA Paper No. 94-1369. Proceedings of the 35th AIAA/ASME/ASCE/AHS/ASC Structures, Structural Dynamics, and Materials Conference, Hilton Head, SC, April 18-20, 1994.
- CP2 Jaunky, Navin, Knight, N. F., Jr., and Ambur, D. R., "Buckling of General Triangular Anisotropic Plates Using Polynomials," AIAA Paper No. 95-1456. Proceedings of the 36th AIAA/ASME/ASCE/AHS/ASC Structures, Structural Dynamics, and Materials Conference, New Orleans, LA, April 10-12, 1995.
- CP3 Jaunky, Navin, Knight, N. F., Jr., and Ambur, D. R., "An Improved Smeared Theory for Buckling Analysis of Grid-Stiffened Composite Panels," Proceedings of the Tenth International Conference on Composite Materials - Volume V: Structures, Vancouver, British Columbia, Canada, August 14-18, 1995, pp. V-51 to V-58.
- CP4 Jaunky, N., Knight, N. F., Jr. and Ambur, D. R., "Optimal Design of Grid-Stiffened Composite Panels Using Global and Local Buckling Analyses," AIAA Paper No. 96-1581. Proceedings of the 37th AIAA/ASME/ASC/AHS/ASCE Structures, Structural Dynamics, and Materials Conference, Salt Lake City, UT, April 15-17, 1996.
- CP5 Sleight, David W., Knight, N. F., Jr., and Wang, J. T., "Evaluation of a Progressive Failure Analysis Methodology for Laminated Composite Structures," AIAA Paper No. 97-1187. Proceedings of the 38th AIAA/ASME/ASCE/AHS/ASC Structures, Structural Dynamics, and Materials Conference, Kissimmee, FL, April 10-12, 1997.
- CP6 McGowan, David M., and Anderson, Melvin S., "Development of Curved Plate Elements for the Exact Buckling Analysis of Composite Plate Assemblies," AIAA Paper No. 97-1305. Proceedings of the 38th AIAA/ASME/ASCE/AHS/ASC Structures, Structural Dynamics, and Materials Conference, Kissimmee, FL, April 10-12, 1997.
- CP7 Anderson, Melvin S., "Design of Panels Having Postbuckling Strength," AIAA Paper No. 97-1240. Proceedings of the 38th AIAA/ASME/ASCE/AHS/ASC Structures, Structural Dynamics, and Materials Conference, Kissimmee, FL, April 10-12, 1997.
- CP8 Jaunky, N., Knight, N. F., Jr. and Ambur, D. R., "Optimal Design of General Stiffened Composite Circular Cylinders for Global Buckling with Strength Constraints," AIAA Paper No. 97-1402. Proceedings of the 38th AIAA/ASME/ASCE/AHS/ASC Structures, Structural Dynamics, and Materials Conference, Kissimmee, FL, April 7-10, 1997.

- CP9 Jaunky, N., Knight, N. F., Jr. and Ambur, D. R., "Buckling Analysis of Anisotropic Curved Panels and Shells with Variable Curvature," AIAA Paper No. 98-1772. Proceedings of the 39th AIAA/ASME/ASCE/AHS/ASC Structures, Structural Dynamics, and Materials Conference, Long Beach, CA, April 20-23, 1998.

Archival Journal Papers

- JP1 Jaunky, Navin, Knight, N. F., Jr., and Ambur, D. R., "Buckling of Arbitrary Quadrilateral Anisotropic Plates," *AIAA Journal*, Vol. 33, No. 5, May 1995, pp. 938-944.
- JP2 Jaunky, Navin, Knight, N. F., Jr., and Ambur, D. R., "Buckling of General Triangular Anisotropic Plates Using Polynomials," *AIAA Journal*, Vol. 33, No. 12, December 1995, pp. 2414-2417.
- JP3 Jaunky, Navin, Knight, N. F., Jr., and Ambur, D. R., "Formulation of an Improved Smeared Theory for Buckling Analysis of Grid-Stiffened Composite Panels," *International Journal of Composite Engineering*, Vol. 27B, No. 5, 1996, pp. 519-526.
- JP4 Jaunky, N., Knight, N. F., Jr. and Ambur, D. R., "Optimal Design of Grid-Stiffened Composite Panels Using Global and Local Buckling Analyses," *Journal of Aircraft*, Vol. 35, No. 3, May-June 1998, pp. 478-486.
- JP5 Jaunky, N., Knight, N. F., Jr. and Ambur, D. R., "Optimal Design of General Stiffened Composite Circular Cylinders for Global Buckling with Strength Constraints," Accepted for publication in *Composite Structures*, galley proofs returned, April 1998.
- JP6 Jaunky, N. and Knight, N. F., Jr., "An Assessment of Shell Theories for Buckling of Cylindrical Panels Loaded in Axial Compression," Accepted for publication in *International Journal of Solid and Structures*, May 1998.
- JP7 Jaunky, N., Knight, N. F., Jr. and Ambur, D. R., "Buckling Analysis of Anisotropic Variable-Curvature Panels and Shells," submitted for review to *Composite Structures*, May 1998.

NASA Reports

- R1 Jaunky, Navin, Knight, N. F., Jr., and Ambur, D. R., *Formulation of an Improved Smeared Theory for Buckling Analysis of Grid-Stiffened Composite Panels*, NASA TM-110162, 1995.

Doctoral Dissertation

- D1 Jaunky, Navin, "Buckling Analysis of Optimum Design of Multidirectionally Stiffened Composite Circular Shells," Ph. D. Dissertation, Department of Aerospace Engineering, Old Dominion University, Norfolk, VA, December 1995.

Master's Theses

- T1 Sleight, David W., "Progressive Failure Analysis Methodology for Laminated Composite Structures," Master's Thesis, Department of Aerospace Engineering, Old Dominion University, Norfolk, VA, August 1996.
- T2 McGowan, David M., "Development of Curved-Plate Elements for the Exact Buckling Analysis of Composite Plate Assemblies Including Transverse Shear Effects," Master's

Thesis, Department of Aerospace Engineering, Old Dominion University, Norfolk, VA, May 1997.

- T3 Jiang, Hao, "Analysis and Design of Sandwich Plates and Shells using PANDA2," Master's Thesis, Department of Aerospace Engineering, Old Dominion University, Norfolk, VA, June 1998.

APPENDIX A

Documentation for the Analysis and Design Code for the Buckling of Grid-Stiffened Panels

- Theoretical Foundations
- User Instructions
- Sample Problems

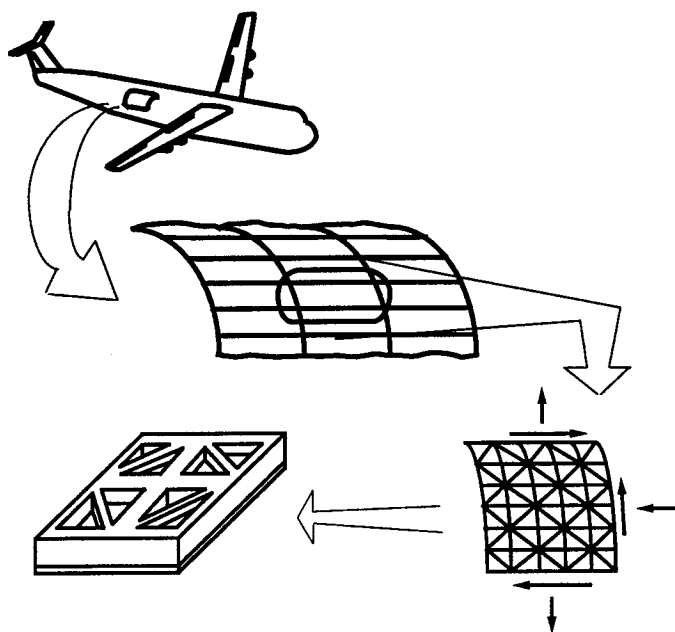
APPENDIX B

Documentation for the Analysis and Design Code for the Buckling of Grid-Stiffened Cylinders

- Theoretical Foundations
- User Instructions
- Sample Problems

ANALYSIS AND DESIGN OF GRID-STIFFENED PANELS FOR BUCKLING

*Theoretical Foundations and
User's instructions for a FORTRAN Code*



Navin Jaunky
Department of Aerospace Engineering
Old Dominion University
Norfolk, VA 23529-0247

TABLE OF CONTENTS

TABLE OF CONTENTS	i
LIST OF FIGURES	ii
LIST OF FILES	iii

Chapter	page
1 INTRODUCTION	1
2 THEORETICAL FOUNDATIONS	2
2.1 IMPROVED SMEARED STIFFENER THEORY	2
2.2 LOCAL BUCKLING OF SKIN SEGMENTS	4
2.2.1 Physical and Computational Domain	4
2.2.2 Rayleigh-Ritz Method	5
2.3 CRIPPLING OF STIFFENER SEGMENT	7
2.4 OPTIMIZATION OF GRID-STIFFENED PANEL	8
2.4.1 Panel Design Procedure	8
2.4.2 Design Problem Definition	9
2.4.3 Design Process Based on Genetic Algorithm	12
3 USER INSTRUCTIONS	18
3.1 ANALYSIS CODE	18
3.1.1 Example of Input and Output file	18
3.2 OPTIMIZATION CODE	19
3.2.1 Changing Type of Optimization	21
REFERENCES	38

LIST OF FIGURES

2.1	Semi-infinite plate model for skin-stiffener element.	14
2.2	Typical profile for skin-stiffener element neutral surface.	14
2.3	Physical and computational domain.	15
2.4	Unit cell showing design variables.	16
2.5	Flow chart showing design optimization process.	17

LIST OF FILES

1. Example of input file (pan.inp)	23
2. Example of output file (pan.out)	24
3. Part of main program “main.f”	28
4. Part of subroutine “panel.f”	30
5. Modification to main program “main.f”	31
6. Modification to subprogram “panel.f”	32
7. Input file for optimization (inp.gen)	33
8. input file for problem parameters (pan.inp)	33
9. Output file containing optimal designs (best.gen)	34
10. Output file containing convergence history (on.gen)	35
11. Information about first optimal design	36
12. Information about second optimal design	37

Chapter 1

INTRODUCTION

The theoretical foundation and user instructions for a FORTRAN code for the design and analysis of composite grid-stiffened circular cylindrical panels exhibiting global buckling are presented. Buckling analysis of composite grid-stiffened panel is performed by an analytical tool using an improved smeared stiffener theory ([1]) for the global buckling analysis, and a Rayleigh-Ritz-type buckling analysis for skin segment with general parallelogram-shaped ([2]) and general triangular planform ([3]) to assess local skin buckling. Crippling of stiffener segments are assessed by a method given in Reference [4].

The integration of this analysis method with a design optimization process for discrete design variable, such as the genetic algorithm ([5]) is done to obtain a design optimization tool for grid-stiffened panel. The optimization tool ([6]) provides optimal designs for a buckling resistant grid-stiffened panel for a given set of in-plane design loads, boundary conditions of the panel, panel material properties, and the length, width, and radius of the panel. The design variables are the height and thickness of the stiffener, the axial and transverse stiffener spacings, the skin laminate and the stiffening configuration (isogrid, orthogrid, etc.).

The theoretical foundation for the analyses involved in the buckling of grid-stiffened panel are discussed briefly in Chapter 2. Instructions for setting up input files for the FORTRAN code are given in Chapter 3. To provide flexibilities in performing different types of optimization, instructions are also provided in Chapter 3 for modifying the code to adjust the number of design variables to facilitate a particular type of optimization.

Chapter 2

THEORETICAL FOUNDATIONS

The theoretical foundations for the improved smeared stiffener theory ([1]), buckling of panels with general parallelogram and triangular-shaped planform ([2, 3]), and crippling of stiffener segments ([4]) are discussed in this chapter. The optimization strategy for buckling of grid-stiffened panel with global and local buckling constraints are also discussed in this chapter.

2.1 IMPROVED SMEARED STIFFENER THEORY

The improved smeared stiffener theory for stiffened panels, used here includes skin-stiffener interaction effects. Skin-stiffener interaction effects may lead to overestimation of buckling loads especially when the stiffener spacings are not small.

If a stiffened plate is bent while it is supported on all four edges, the neutral surface in the neighborhood of the stiffener will lie between the mid-plane of the skin and the centroid of the stiffener. It is convenient to think of this as a shift of the neutral surface from the centroid of the stiffener. Hence, the approximate stiffness added by a stiffener to the skin stiffness will then be due to the skin-stiffener combination being bent about its neutral surface rather than due to the stiffener being bent about its own neutral surface or the skin neutral surface. The shifted location of the neutral surface is determined theoretically through a study of the local stress distribution near the skin-stiffener interface for a panel with a blade stiffener.

The neutral surface profile of the skin-stiffener combination is developed analytically using the minimum potential energy principle and statics conditions. The skin-stiffener interaction is accounted for by computing the bending and coupling stiffness due to the stiffener and the skin in the skin-stiffener region about a shifted neutral axis at the stiffener.

A grid-stiffened panel may be considered to be an assembly of repetitive units or unit cells (see Figure 2.1). Any stiffener segment in the unit cell may be isolated in a

semi-infinite skin-stiffener model as shown in Figure 2.1 for a diagonal stiffener. The approach for obtaining the neutral surface in a semi-infinite stiffened panel is given in Reference [1].

A typical profile of the neutral surface for a skin-stiffener combination is shown in Figure 2.2. The distance y^* represents the distance from the centerline of the stiffener to the point where the neutral surface coincides with the mid-surface of the skin. The average of the neutral profile over the distance y^* is Z^* . The quantities y^* and Z^* are obtained numerically.

The smeared stiffnesses of a stiffened panel is obtained by mathematically converting the stiffened panel to an equivalent unstiffened panel (Ref. [7]). The smeared stiffnesses are developed on the basis that the strain energy of the stiffened panel should be the same as that of the equivalent unstiffened panel. These smeared stiffnesses can then be used in a Rayleigh-Ritz type analysis to solve for buckling loads of the stiffened panel. In Reference [7], the strain energy of the skin and stiffeners in the unit cell is obtained by using stiffnesses of the skin and the stiffeners which are computed about the mid-surface of the skin. Since, there is a shift in the neutral surface at the stiffener, the stiffness of the stiffeners and the skin segment directly above it has to be computed about a shifted neutral surface so as to account for the skin-stiffener interactions.

The correction to the smeared stiffnesses due to the skin-stiffener interaction is herein introduced by computing the stiffness of the stiffener and the skin segment directly contiguous to it according to the following criteria.

1. If $y^* < t/4$, then the reference surface for the stiffener is Z_n .
2. If $y^* > t/4$, then the reference surface for the stiffener is Z^* .

In either case, the reference surface of the skin is taken to be its mid-surface. Other more elaborate and accurate schemes can be used to introduce the skin-stiffener interaction using the neutral surface profile. However, the one described herein is simple, and provides sufficiently accurate buckling loads for the preliminary structural design ([1]).

2.2 LOCAL BUCKLING OF SKIN SEGMENTS

The shape of a skin segment on a grid-stiffened panel depends on the stiffening configuration. If the stiffening configuration involves diagonal stiffener only, then the skin segment has a rhombic planform. If the stiffening configuration has diagonal stiffeners with axial or transverse stiffeners, then the skin segment has an isosceles triangular planform. For a general grid-stiffened panel, the skin segment has a right-angle triangular planform, and for an isogrid panel the skin segment has an equilateral triangular planform.

Buckling analyses for panel with these kinds of planforms is achieved through the use of "circulation function" and accounts for material anisotropy, different boundary conditions, and combined in-plane loading. A First-Order Shear-Deformation Theory is used. The shell theory that is used can be either Sanders-Koiter, Love, or Donnell theory. This is achieved through tracer coefficients.

2.2.1 Physical and Computational Domain

The buckling analysis of these local skin segments is enhanced by mapping their physical domain into a computational domain. Consider a general quadrilateral or triangular panel subjected to a state of combined in-plane loading where the loading and material properties are defined using the coordinate system $(x - y)$ shown Figure 2.3. The transformation from a physical domain to computational domain is necessary when dealing with general quadrilateral and triangular geometries in order to facilitate the computation of linear stiffness and geometric stiffness matrices and imposition of boundary conditions.

The physical domain $\mathcal{D}[x, y]$ is transformed to a computational domain $\mathcal{D}[\xi, \eta]$ as indicated in Figure 2.3. The mapping for a quadrilateral is

$$\begin{aligned} x(\xi, \eta) &= \sum_{i=1}^4 N_i(\xi, \eta) x_i \\ y(\xi, \eta) &= \sum_{i=1}^4 N_i(\xi, \eta) y_i \end{aligned} \quad (1)$$

where $x_i (i = 1, 2, 3, 4)$ and $y_i (i = 1, 2, 3, 4)$ are the physical coordinates of the i^{th} corner of the panel, ξ and η are the natural coordinates for the quadrilateral geometries, and $N_i (i = 1, 2, 3, 4)$ are the bilinear mapping functions given by

$$\begin{aligned}
N_1(\xi, \eta) &= \frac{1}{4}(1 - \xi)(1 + \eta) \\
N_2(\xi, \eta) &= \frac{1}{4}(1 + \xi)(1 + \eta) \\
N_3(\xi, \eta) &= \frac{1}{4}(1 + \xi)(1 - \eta) \\
N_4(\xi, \eta) &= \frac{1}{4}(1 - \xi)(1 - \eta)
\end{aligned}$$

The Jacobian of the transformation is

$$\mathbf{J} = \begin{bmatrix} \frac{\partial x}{\partial \xi} & \frac{\partial y}{\partial \xi} \\ \frac{\partial x}{\partial \eta} & \frac{\partial y}{\partial \eta} \end{bmatrix} \quad (2)$$

which is independent of the natural coordinates for general parallelogram-shaped geometries. This results in substantial computational savings in the overall formulation.

The mapping for a general triangle is

$$\begin{aligned}
x(\xi, \eta, \rho) &= \xi x_1 + \eta x_2 + \rho x_3 \\
y(\xi, \eta, \rho) &= \xi y_1 + \eta y_2 + \rho y_3
\end{aligned} \quad (3)$$

where ξ , η and ρ are the area coordinates for the case of triangular geometries, and x_i ($i = 1, 2, 3$) and y_i ($i = 1, 2, 3$) are the physical coordinates of the i^{th} corner of the panel. Note that the third area coordinate will be expressed in terms of the other two or $\rho = (1 - \xi - \eta)$ based on the constraint that the sum of the area coordinates must be equal to one. The Jacobian of the transformation is independent of the area coordinates. The Jacobian, in either case, is used to relate derivatives in the two domains.

2.2.2 The Rayleigh-Ritz Method

The Rayleigh-Ritz method is an approximate method for solving a certain class of problems. Accordingly, trial functions with some unknown coefficients and satisfying the essential or geometric boundary conditions are introduced in the energy functional of the problem. The minimum conditions of this functional are then imposed, and resulting algebraic equations are solved for the unknown coefficients. These trial functions are called the “Ritz” functions.

The Ritz functions used here are expressed in terms of natural coordinates for the quadrilateral geometry or area coordinates for the triangular geometry for displacement

field. The components of the displacement vector are three translations ($D_1, D_2, D_3 = u_0, v_0, w$) and two cross-sectional or bending rotations ($D_4, D_5 = \phi_x, \phi_y$) when considering transverse-shear deformation effects. Each displacement component is approximated independently by a different Ritz function. The approximation for the i^{th} component of the displacement vector is given by

$$\begin{aligned} D_i(\xi, \eta) &= \sum_{j=1}^N a_{ij} d_{ij} \\ &= \sum_{j=1}^N a_{ij} \Gamma_i(\xi, \eta) f_j(\xi, \eta) \quad \text{for } i = 1, 2, 3, 4, 5 \end{aligned} \quad (4)$$

where d_{ij} represents the j^{th} term in the N -term approximation for the i^{th} displacement component, a_{ij} are unknown coefficients to be determined, and $\Gamma_i(\xi, \eta)$ are the circulation functions.

The circulation functions Γ_i in Equation (4) are then used to impose different boundary conditions along each edge of the plate. Each term Γ_i is the product of three functions in the case of the triangular plate geometry and four functions in the case of the quadrilateral plate geometry. Each function is the equation of an edge of the triangular or quadrilateral plate as shown in Figure 2.3 raised to an independent exponent for each displacement component. Thus, the circulation functions for the quadrilateral plate are

$$\Gamma_i = (1 - \eta)^{p_i} (1 - \xi)^{q_i} (1 + \eta)^{r_i} (1 + \xi)^{s_i}$$

and for the triangular plate are

$$\Gamma_i = \xi^{p_i} \eta^{q_i} (1 - \xi - \eta)^{r_i} \quad (5)$$

For example, considering the quadrilateral plate case, p_i refers to edge 1, q_i refers to edge 2, r_i refers to edge 3, s_i refers to edge 4 as indicated in Figure 2.3. These exponents are used to impose different boundary conditions. If the i^{th} displacement component is free on a given edge, then the exponent for that edge will have a value of zero. If the i^{th} displacement component is constrained on a given edge, then the exponent for that edge will have a value of one. Only geometric boundary conditions are imposed in this approach. Thus, a simply supported condition for bending fields can be imposed on edge 1 by setting:

- $p_3 = 1$ for w , $p_4 = 0$ for ϕ_x , $p_5 = 0$ for ϕ_y

A clamped condition for bending fields can be imposed on edge 1 by setting:

- $p_3 = 1$ for w , $p_4 = 1$ for ϕ_x , $p_5 = 1$ for ϕ_y

A free-edge condition can be imposed on edge 1 by setting:

- $p_i = 0$ for u_0 , v_0 , w , ϕ_x and ϕ_y

The term f_j in Equation (4) is a polynomial function in ξ and η , and in its simplest form is a power series in ξ and η and is expressed as

$$f_j(\xi, \eta) = \xi^{m_j} \eta^{n_j}$$

$$m_j, n_j = (0, 0), (1, 0), (0, 1), (2, 0), (1, 1), (0, 2), \dots \quad (6)$$

The values of m_j and n_j are used basically to define terms in a two-dimensional Pascal's triangle. The number of terms N in Equation (4) defines the order of a complete function in two variables. The table below gives the value of N for polynomials of different degrees.

Table 1 Degree of polynomials with value of N

N	Degree of polynomials	N	Degree of polynomials
1	0	45	8
3	1	55	9
6	2	66	10
10	3	78	11
15	4	91	12
21	5	105	13
28	6	120	14
36	7	136	15

2.3 CRIPPLING OF STIFFENER SEGMENT

The local stiffener segment is analyzed to determine whether stiffener crippling will occur. Reference [4] provides a method for determining the buckling load of a stiffener segment. Accordingly, the stiffener segment at the nodes or intersection points of stiffeners are assumed to be clamped while the stiffener-skin attachment is assumed to be a simple support. From Ref. [4], the crippling load of the stiffener is N_{crip} and is given by

$$N_{crip} = \frac{\bar{s}_z}{2} \left[\sqrt{1 + \frac{4N_{cl}}{\bar{s}_z}} - 1 \right]$$

where

$$N_{cl} = t_s^3 \left[\frac{4\pi^2 E_{11}}{12L_1^2 [1 - (\nu_{12}^2 E_{22}/E_{11})]} + \frac{G_{12}}{h^2} \right] \quad (7)$$

where

$\bar{s}_z = \frac{5}{6}G_{13}t_s$, is a shear correction factor,

$L_1 = 2L$ is the length of the stiffener,

h is the height of the stiffener,

t_s is the thickness of the stiffener,

E_{11} is the longitudinal modulus of the stiffener material,

E_{22} is the transverse modulus of the stiffener material.

2.4 OPTIMIZATION OF GRID-STIFFENED PANEL

The analysis and design of grid-stiffened composite panels subjected to combined loads require several key steps. In the present optimization procedure, acceptable designs are those which buckle globally and do not exhibit any local skin buckling or stiffener crippling. The first step is to assess the global buckling response of the grid-stiffened panel. Once this global buckling response is determined, the second step is to determine the local skin buckling response for general quadrilateral and/or triangular skin segments that occur locally between stiffeners. The third step is to determine whether stiffener buckling or stiffener crippling has occurred at this global load level. This sequence of steps is performed repeatedly in a design cycle until an optimum or near-optimum design is obtained. The genetic algorithm is used herein and the buckling analyses involved in the global and local buckling of grid-stiffened panels have been discussed in Sections 2.1 and 2.2.

2.4.1 Panel Design Procedure

The design of grid-stiffened composite panels requires that many of the design variables, such as stiffener spacing and stiffener thicknesses may only take on certain discrete values rather than vary continuously over the design space, and often a “family” of good designs is needed rather than a single-point design due to manufacturing requirements. Gradient-based methods for structural optimization are not appropriate in this case.

The genetic algorithm is a method for “evolving” a given design problem to a family of near-optimum designs ([5]). Based on Darwin’s theory of survival-of-the-fittest, the genetic algorithm involves the random creation of a design population that “evolves” towards some definition of fitness. The genetic algorithm is attractive due to their simplicity of approach in discrete variable combinatorics. The genetic algorithm can be used

directly to solve unconstrained optimization problems, while constrained optimization must first be transformed to an unconstrained optimization problem (e.g., use of an exterior penalty function). Stochastic processes are used to generate an initial population of individual designs and the process then applies principles of natural selection and survival of the fittest to find improved designs. Furthermore, since the discrete design procedure works with a population of designs it can explore a large area of the design space and climb different hills. This is a major advantage as the converged solution contains many optima of comparable performance. The cost of having a large number of function evaluations is offset by the fact that a large number of optima solutions are now available. In a gradient-based optimization procedure, only a single-point design, usually the extremum to the starting point, is obtained. The genetic algorithm produces a population or family of good designs which may include the global optimal design, rather than a single design. Hence, it is an appropriate tool for designing general grid-stiffened panels.

2.4.2 Design Problem Definiton

The present design problem is to minimize the weight per unit area of a grid-stiffened composite panel given the design loading condition, the length and width of the panel, the material properties for the skin and stiffeners, and the boundary conditions of the panel. The design variables include stiffener spacings (a, b), the stacking sequence of the skin, stiffener layout or stiffening configuration, stiffener thickness (t_s), and stiffener height ($h_1 = h_2 = h_3 = h$) as shown in Figure 2.4. The axial and transverse directions of the panel are along the x and y axis respectively. All stiffeners are assumed to be of the same height and thickness for manufacturing and assembly reasons. The design sought here is a panel of minimum weight in a certain design space which buckles globally at the design loads. The design is defined by setting up the optimization procedures in the following way. First, the global buckling load is assumed to be a scalar multiple of design loads and has the form

$$N_x = \lambda_G N_1, \quad N_y = \lambda_G N_2, \quad N_{xy} = \lambda_G N_{12} \quad (8)$$

where N_1, N_2, N_{12} are the applied in-plane prebuckling loads. These values represent the design loads for the grid-stiffened panel. Second, the design constraints imposed on panel include

1. The critical buckling load should be greater than or equal to the design loads, that is, $\lambda_G \geq 1$.
2. Skin segments should not buckle at the critical buckling load, that is, $\lambda_{sk} \geq 1$.
3. Stiffener segments should not cripple at the critical buckling load, i.e., $\lambda_1, \lambda_2, \lambda_3 \geq 1$ where $\lambda_1, \lambda_2, \lambda_3$ is the crippling load factor of the x-direction stiffener, y-direction stiffener and diagonal stiffener, respectively.

The general form of each constraint equation is written as

$$g_j = \left(\frac{1}{\lambda_j} - 1 \right) \leq 0.0 \quad j = 1, \dots, N_c \quad (9)$$

Finally, the "Fitness" expression based on exterior penalty function approach is

$$\text{Fitness} = \left(\frac{Q}{F(\mathbf{X}, r_i)} \right) = \text{Max} \frac{Q}{W(\mathbf{X}) + r_i \sum_j^{N_c} [|g_j(\mathbf{X})| + g_j(\mathbf{X})]^2} \quad (10)$$

where

\mathbf{X} = design variable vector

$F(\mathbf{X}, r_i)$ = modified objective function

$W(\mathbf{X})$ = weight of panel per unit area

$r_i \sum_j^{N_c} [|g_j(\mathbf{X})| + g_j(\mathbf{X})]^2$ = penalty function

Q = normalizing constant

N_c = number of design constraints

r_i = penalty parameter

i = generation or iteration cycle in the optimization procedure.

Once the global buckling load factor has been determined using the improved smeared stiffener theory, the loads acting on the stiffener and skin segments have to be determined by distributing the loads based on the extensional stiffness of the skin and the stiffener. The procedure for distributing the applied loads for a general grid-stiffened panel involves three steps. First, the extensional stiffness coefficients for grid-stiffened panel are computed as follows (Ref. [7]):

$$\begin{aligned} (A_{11})_T &= \frac{2(A_{11})_1 h}{b} + \frac{2(A_{11})_3 h \sin^3 \theta}{b} + (A_{11})_s \\ (A_{22})_T &= \frac{2(A_{11})_2 h}{a} + \frac{2(A_{11})_3 h \cos^3 \theta}{a} + (A_{22})_s \\ (A_{66})_T &= \frac{2(A_{11})_3 h \cos \theta \sin^2 \theta}{a} + (A_{66})_s \end{aligned} \quad (11)$$

where $(A_{11})_T$ is total smeared axial extensional stiffness of the grid-stiffened panel, $(A_{22})_T$ is the total smeared transverse extensional stiffness of the grid-stiffened panel, $(A_{66})_T$ is the total smeared in-plane shear stiffness of the grid stiffened panel, $(A_{11})_1$, $(A_{11})_2$, $(A_{11})_3$ are the extensional stiffness of the axial, transverse and diagonal stiffeners, respectively, $(A_{ij})_s$ is the extensional stiffness of the skin, θ is the orientation of the diagonal stiffener, and h is the height of the stiffener. Second, the loads carried by the skin segment which could be either a general parallelogram-shaped geometry or a general triangular-shaped geometry, at the panel global buckling load are

$$\begin{aligned}(N_x)_{sk} &= \frac{(A_{11})_s}{(A_{11})_T} N_x = \frac{(A_{11})_s}{(A_{11})_T} \lambda_G N_1 \\ (N_y)_{sk} &= \frac{(A_{22})_s}{(A_{22})_T} N_y = \frac{(A_{22})_s}{(A_{22})_T} \lambda_G N_2 \\ (N_{xy})_{sk} &= \frac{(A_{66})_s}{(A_{66})_T} N_{xy} = \frac{(A_{66})_s}{(A_{66})_T} \lambda_G N_{12}\end{aligned}\quad (12)$$

These values then correspond to the design loads used for the in-plane prebuckling load in the skin-segment local buckling computation. If the critical buckling load factor of the skin segment λ_{sk} is greater than or equal to one, then the skin-segment buckling load is greater than or equal to the global buckling load of the grid-stiffened panel. Third, the loads carried by each stiffener are computed. The load carried by the axial stiffener is

$$(N_x)_1 = \frac{(A_{11})_1}{(A_{11})_T} \lambda_G N_1 = \lambda_1 N_{crip} \quad (13)$$

where N_{crip} is determined using Equation (7). The critical buckling load factor, λ_1 , of the axial stiffener has to be greater than or equal to one. The load carried by the transverse stiffener is

$$(N_x)_2 = \frac{(A_{11})_2}{(A_{22})_T} \lambda_G N_2 = \lambda_2 N_{crip} \quad (14)$$

and the critical buckling load factor, λ_2 , of the transverse stiffener has to be greater than or equal to one. The load in the diagonal stiffeners has components from the axial, transverse, and in-plane shear loadings and is given by

$$(N_x)_3 = N_{dx} \sin \theta + N_{dy} \cos \theta + (N_{dxy})_x \cos \theta + (N_{dxy})_y \sin \theta = \lambda_3 N_{crip}$$

where

$$\begin{aligned}N_{dx} &= \frac{(A_{11})_3 \sin^3 \theta}{(A_{11})_T} \lambda_G N_1 \\ N_{dy} &= \frac{(A_{11})_3 \cos^3 \theta}{(A_{22})_T} \lambda_G N_2\end{aligned}$$

$$\begin{aligned}
(N_{dxy})_x &= \frac{(A_{11})_3 \cos \theta \sin^2 \theta}{(A_{66})_T} \frac{b}{a} \lambda_G N_{12} \\
(N_{dxy})_y &= \frac{(A_{11})_3 \cos \theta \sin^2 \theta}{(A_{66})_T} \lambda_G N_{12}
\end{aligned} \tag{15}$$

N_{dx} is the contribution from the axial in-plane loading, N_{dy} is the contribution from the transverse in-plane loading, $(N_{dxy})_x$ is the contribution from the in-plane shear loading along the edge where x is constant, and $(N_{dxy})_y$ is the contribution from the in-plane shear loading along the edge where y is constant. The critical buckling load factor, λ_3 , of the diagonal stiffener has to be greater than or equal to one.

The weight per unit area of the grid-stiffened panel is

$$W = \frac{\rho}{ab} (w_1 + w_2 + w_3 + w_s)$$

where

$$\begin{aligned}
w_1 &= 2 h a t_s \\
w_2 &= 2 h b t_s \\
w_3 &= 2 h t \sqrt{a^2 + b^2} \\
w_s &= a b t_{skin}
\end{aligned} \tag{16}$$

w_1 is the volume of the axial stiffeners in the unit cell, w_2 is the volume of the transverse stiffeners in the unit cell, w_3 is the volume of the diagonal stiffeners in the unit cell, w_s is the volume of the skin in the unit cell, t_{skin} is the thickness of skin, and ρ is the mass density of the material.

2.4.3 Design Process Based on Genetic Algorithm

Implementation of the genetic algorithm is shown schematically in Figure 2.5. The design process begins with a random selection of a specified number of designs which comprise the initial population (i.e., first generation) for the genetic algorithm. Material properties, length and width of panel, boundary conditions of the stiffened panel, and design loadings are input to the analysis processor routine. The buckling analysis is performed which provides the critical eigenvalues for the global buckling response of the grid-stiffened panel and the local buckling response of the skin and stiffener segments, which also computes the weight per unit area of the grid-stiffened panel. This procedure is repeated for each design configuration in the population. The “fitness” processor then evaluates the “fitness” of each design using Equation (10) and assigns a rank based on the

fitness expression or objective function. The current population of design configurations is then processed by the genetic operators (crossover, mutation, and permutation) to create a new population of design configurations for the next generations which combine the most desirable characteristics of previous generations. Designs from previous generations may be replaced by new ones (i.e., children) except for the “most fit” designs (i.e., parents) which are always included in the next generation. The process is repeated until design convergence is obtained, which is defined herein by specifying a maximum number of generations (*NSTOP*) that may occur without improvement in the best design.

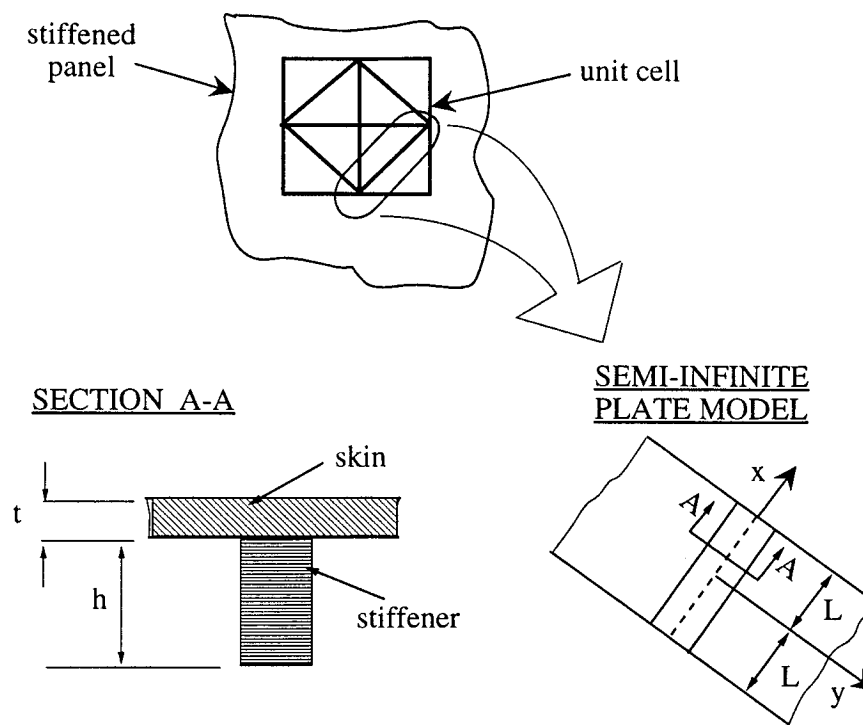


Figure 2.1 Semi-infinite plate model for skin-stiffener element.

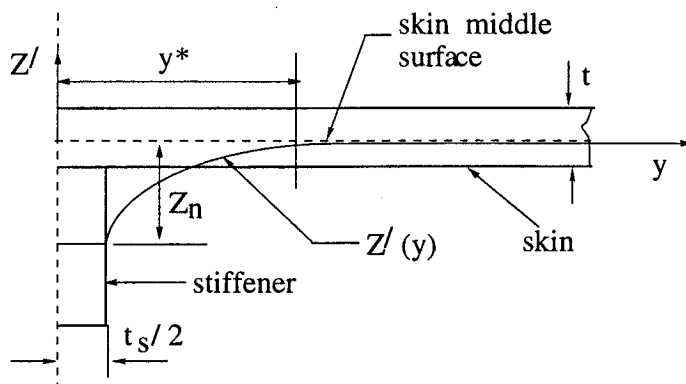


Figure 2.2 Typical profile for skin-stiffener element neutral surface.

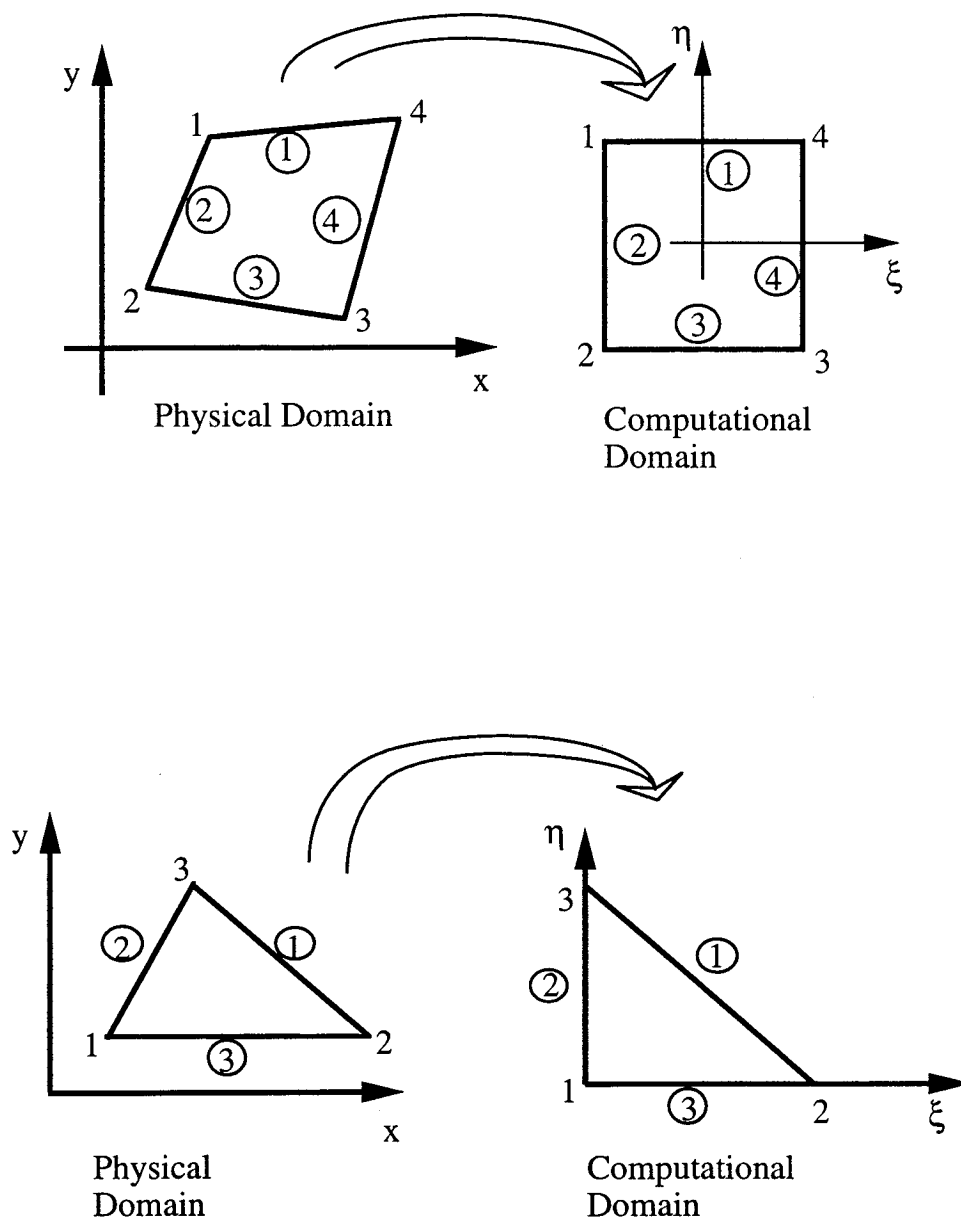


Figure 2.3 Physical and computational domain for plate geometries.

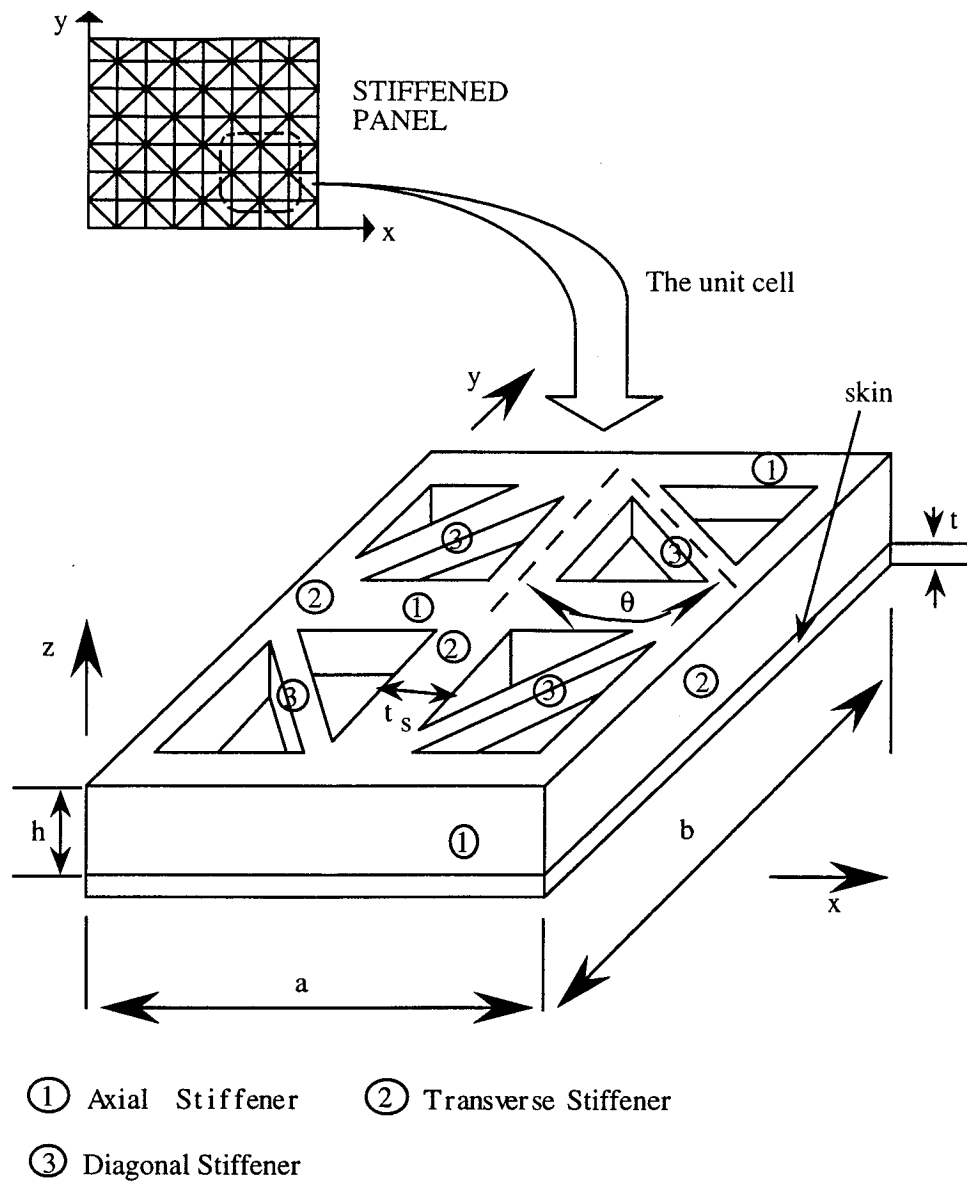


Figure 2.4 Unit cell showing design variables.

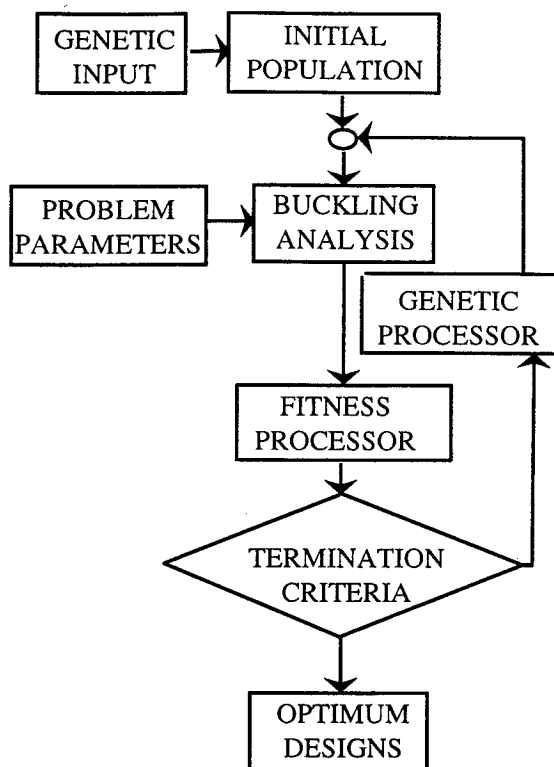


Figure 2.5 Flow chart showing the design optimization process.

Chapter 3

USER INSTRUCTIONS

User instructions for using two FORTRAN codes are provided in this chapter. The first code is for analyzing a grid-stiffened panel subjected to combined in-plane loading. The code provides the global buckling load, and local buckling load of skin and stiffener segments as output. Instructions for using this code are given in Section 3.1. The second code is for optimizing a grid-stiffened panel design subjected to global and local buckling constraints. Instructions for using this code and modifying it to obtain a particular type of optimization are given in Section 3.2.

3.1 ANALYSIS CODE

The analysis code is found in directory “panel/grid” and a makefile is used to link all the subroutines together. The makefile may have to be modified to account for different computer system. Grid-stiffened panel with the unit cell geometry as shown in Figure 2.4 can be analyzed by using the code. Skin segments of the grid-stiffened panel are assumed to be simply-supported. Other boundary conditions of the skin segment can be accommodated through simple modifications to the source code. The executable for this code is “run” as specified in the makefile.

3.1.1 Examples for Input and Output file

An input file for a flat grid-stiffened panel with axial and diagonal stiffeners is given. The panel is 20.0 in. long and 56.0 in wide, and has an axial and transverse stiffener spacings of 3.3333 in. and 5.89473 in., respectively. The height and thickness of the stiffener is 0.5 in. and 0.06 in., respectively. The skin laminate has a ply stacking sequence of [60/0/60] with ply thickness of 0.006 in. The ply orientations are measured from the x-axis in the counter-clockwise directions. The stiffener is made of unidirectional material. The material for the skin and stiffener is assumed to have the following nominal ply mechanical properties; $E_{11} = 20.2$ Msi; $E_{22} = 1.9$ Msi; $G_{12} = G_{13} = G_{23} = 0.73$ Msi and $\nu_{12} = 0.3$. The panel is simply supported and is subjected to axial compression

loading of $N_x = 400$ lbs/in. The input file is named "pan.inp" and is given in List 1. Text after the character "!" are comments and need not be included in the actual file.

Some considerations for the input file are listed below.

1. The maximum number of plies in a laminate is 50, and the maximum number of material is 5.
2. When a stiffener type (axial, transverse, or diagonal) is not present, its thickness and ply thickness are entered as zero. But not the material properties and its height as shown for the transverse stiffener in the above input file.
3. The dimension of the panel is read as (x, y) coordinate of each node (see Figure 2.3). The radius of the panel is read by specifying the radius at each node. For a flat panel, the radius is input as a very large number.
4. When analyzing panels stiffened in one direction only, one of the stiffener spacing is redundant. For example, an axially stiffened panel will have its stiffener spacing specified by the width of the unit cell only. The length of the unit cell is entered as the length of the panel.
5. The number of terms or modes (N) used in the analysis is taken from Table 1. The maximum value for N is 150 as determined by parameter "nmod" in the file "panel.inc". Using a value of N between 55 and 78 is usually sufficient.

Finally, if the user wishes to change the boundary conditions of the skin segment in the analysis, the subroutine "bclocal.f" has to be modified. The output file is "pan.out" and is given in List 2.

3.2 OPTIMIZATION CODE

The optimization code will optimize a grid-stiffened panel for minimum weight subjected to global and local buckling constraints, and is found in directory "panel/optimize". The executable for this code is "run" as specified in the makefile. The design variables are

1. Axial stiffener spacing (a).
2. Transverse stiffener spacing (b).

3. Stiffener height (h).
4. Stiffener thickness (t_s).
5. Skin laminate ($LAMI$).
6. Stiffening configuration ($IGEO$).

The number of design variable is defined by the parameter “n” in the main program “main.f”. Each design variable can assume eight discrete values as allowed by the FORTRAN code. The eight discrete values of each design variable define the design space for optimization. The discrete values for a , b , h , and t_s are supplied through the file “inp.gen” which is read by the main program “main.f”. Part of the main program where the parameter “n”, and the parameter for the population size “m” are defined, the values for a , b , h , and t_s are read is shown in List 3. The discrete values for $LAMI$ and $IGEO$ are given in Table 2.

Table 2 Design space for design variables $ICON$ and $LAMI$.

Integer value	$LAMI$	$IGEO$
1	$[\pm 45/0]_{2s}$	axial stiffeners
2	$[\pm 45/90]_{2s}$	transverse stiffeners
3	$[\pm 45/0/90]_{2s}$	axial and transverse stiffeners
4	$[\pm 45/0_2]_{2s}$	diagonal stiffeners
5	$[\pm 45/90_2]_{2s}$	axial and diagonal stiffeners
6	$[\pm 45/0_2/90]_{2s}$	transverse and diagonal stiffeners
7	$[\pm 45/0/90_2]_{2s}$	axial, transverse and diagonal stiffeners
8	$[\pm 45/0_2/90_2]_{2s}$	no stiffeners

The laminate stacking sequence corresponding to various discrete values of $LAMI$ are hard-wired in subroutine “cskin.f”, and can be changed by modifying subroutine “cskin.f”. The ply thickness in subroutine “cskin.f” is kept constant for all laminates, and is read in “cskin.f”. Subroutine “cskin.f” can be modified by the user to accommodate various laminate stacking sequences. The discrete values for $IGEO$ are assigned in subroutine “panel.f” and part of the code where $IGEO$ are being assigned is shown in List 4. Subroutine “geom.f” assigns the stiffening configuration based on the value of $IGEO$ which is supplied by the main program “main.f”.

Some parameters that may affect the optimization process are

- The population size “m” is hard-wired in “main.f”. Usually $m > 2n$, and this condition has been found to work well, and $m \gg 2n$ is not recommended.
- The probabilities of crossover, mutation, and permutation have been hard-wired to 1.0, 0.1, and 0.95 in “main.f”. These values work very well for the optimization problem under consideration.
- The termination criteria “NSTOP” is hard-wired in “main.f”. The user has to experiment with the value of “NSTOP”. Usually the code is run with a value of “NSTOP” and then with another value of “NSTOP” greater than the previous one. If there is no change in the optimal designs, then the second value of “NSTOP” provide a good value as a stopping criteria. For the problem under consideration, NSTOP=25, is usually sufficient.
- The penalty parameter r_i in Equation (10) can either increase at every i^{th} generation or can be constant for all generation. In subroutine “panel.f”, r_i is kept constant at 1000. By commenting the line where “ainipen = 1000.0”, the user can set

$$r_i = 1000 + i^2 \quad (17)$$

Keeping r_i constant works very well for the present optimization problem.

According to Lists 3 and 4, the code has been set up to optimize grid-stiffened panel with all design variables active.

3.2.1 Changing the Type of Optimization

The user may want to optimize a grid-stiffened panel with less number of design variables. For example, the skin laminate, and the stiffening configuration may be fixed, and the only design variables are a , b , h , and t_s . An example of such an optimization is provided with the required input files, and the output files from the code are explained.

Consider the panel described in Sub-section 3.1.1, the panel is to be optimized for $N_x = 400$ lbs/in., with design variables being a , b , h , and t_s . The skin laminate is [60/0/60]_s with a ply thickness of 0.006 in. Only axial and diagonal stiffeners are considered and therefore $IGEO = 5$. The axial stiffener spacing a and transverse stiffener spacing b is treated as one design variable i.e., (a, b) is a design variable. Values for (a, b) are provided such that the stiffening configuration closely approximates an isogrid configuration (i.e.,

$\theta \approx 30^\circ$). Hence, there are three design variables. List 5 and 6 show the appropriate modifications to “main.f” and “panel.f” respectively. In List 5, “n” has been changed to 3, and “m” has been changed to 8. While in List 6, a “! modify” indicates the line that has been modified.

The code needs two input files, namely “inp.gen”, and “pan.inp”. The file “inp.gen” is read by program “main.f” and it defines the design space for the stiffener spacings, and the height and thickness of the stiffener. The file “pan.inp” provides the problem parameters for the optimization problem and is read by subroutine “panel.f”. Example for “inp.gen”, and “pan.inp” are given in List 7 and 8 respectively.

The output files produced by the code are “best.gen”, “on.gen”, and “pan.out”. The files “best.gen”, and “on.gen” are produced by program “main.f”, and the file “pan.out” is produced by subroutine “panel.f”. The optimal designs ranked according to Equation (10) are stored in the file “best.f” and the convergence history of the optimization is stored in the file “on.gen”. The file “best.gen” and “on.gen” for the above example is given in Lists 9 and 10 respectively.

The file “pan.out” stores the information about each design resulting from the analysis and is quite large. It is useful in obtaining the buckling loads and other information about the optimal designs stored in file “best.gen”. To access information about an optimal design, use the value of its fitness (FS) in “best.gen” and locate that number (critlb) in “pan.out” using the search option of the unix editor being used. For example, the best design, which is the first design in “best.gen” has “FS= 0.7669355E+03”. Searching for the pattern “0.7669355E+03” in “pan.out” will bring the cursor to where information about the best design is written. List 11 and 12 give information about the first and second optimal designs which have been extracted from “pan.out”.

LIST OF FILES

List 1: Example for Input file (pan.inp)

```

0.036          ! thickness of skin
1              ! Number of material
1,20.2e6,1.9e6,0.3,0.73e6 ! Material No., E11, E22, v12, G12
6              ! No. of plies
1,1,0.006,60.0 ! layer No., Material No., ply thickness, theta
2,1,0.006,0.0
3,1,0.006,-60.0
4,1,0.006,-60.0
5,1,0.006,0.0
6,1,0.006,60.0
0.060          ! axial stiffener thickness
1              ! Number of material
1,20.2e6,1.9e6,0.3,0.73e6 ! Material No., E11, E22, v12, G12
1              ! No. of plies
1,1,0.060,0.0  ! layer No., Material No., ply thickness, theta
0.0            ! transverse stiffener thickness
1              ! Number of material
1,20.2e6,1.9e6,0.3,0.73e6 ! Material No., E11, E22, v12, G12
1              ! No. of plies
1,1,0.0,0.0    ! layer No., Material No., ply thickness, theta
0.060          ! diagonal stiffener
1              ! Number of material
1,20.2e6,1.9e6,0.3,0.73e6 ! Material No., E11, E22, v12, G12
1              ! No. of plies
1,1,0.060,0.0  ! layer No., Material No., ply thickness, theta
0.5,0.5,0.5    ! height of axial, transverse, and diagonal stiffener
0.0,0.0,1.0e12 ! (x,y), radius for node 1 for 20 in. by 56 in. panel
20.0,0.0,1.0e12 ! (x,y), radius for node 2 for 20 in. by 56 in. panel
20.0,56.0,1.0e12 ! (x,y), radius for node 3 for 20 in. by 56 in. panel
0.0,56.0,1.0e12 ! (x,y), radius for node 4 for 20 in. by 56 in. panel
1,0,1,0        ! B.C's of U for panel
0,1,0,1        ! B.C's of V for panel
1,1,1,1        ! B.C's of W for panel
0,0,0,0        ! B.C's of Px for panel
0,0,0,0        ! B.C's of Py for panel
3.333333,5.89473 ! length, width of unit cell
55             ! # of modes considered (N)
400.0,0.0,0.0  ! Nx, Ny, Nxy (loading condition)

```

List 2: Example of output file (pan.out)

SKIN LAMINATE DATA

STACK THICKNESS= 3.5999999999999997E-02in

NO. of MATERIAL types= 1

MAT.NO.	E1 (psi)	E2 (psi)	V12	G12 (psi)
---------	-------------	-------------	-----	--------------

1	0.2020E+08	0.1900E+07	0.3000	0.7300E+06
---	------------	------------	--------	------------

LAYER No.	MATERIAL No.	THK (in)	ORIENTATION (deg)
1	1	0.0060	60.0000
2	1	0.0060	0.0000
3	1	0.0060	-60.0000
4	1	0.0060	-60.0000
5	1	0.0060	0.0000
6	1	0.0060	60.0000

X-STIFFENER LAMINATE DATA

STACK THICKNESS= 5.9999999999999998E-02in

NO. of MATERIAL types= 1

MAT.NO.	E1 (psi)	E2 (psi)	V12	G12 (psi)
---------	-------------	-------------	-----	--------------

1	0.2020E+08	0.1900E+07	0.3000	0.7300E+06
---	------------	------------	--------	------------

LAYER No.	MATERIAL No.	THK (in)	ORIENTATION (deg)
1	1	0.0600	0.0000

Y-STIFFENER LAMINATE DATA

STACK THICKNESS= 0.0000000000000000E+00in

NO. of MATERIAL types= 1

MAT.NO.	E1 (psi)	E2 (psi)	V12	G12 (psi)
---------	-------------	-------------	-----	--------------

1	0.2020E+08	0.1900E+07	0.3000	0.7300E+06
---	------------	------------	--------	------------

LAYER No.	MATERIAL No.	THK (in)	ORIENTATION (deg)
1	1	0.0000	0.0000

DIAGONAL-STIFFENER LAMINATE DATA

STACK THICKNESS= 5.9999999999999998E-02in

NO. of MATERIAL types= 1

MAT.NO.	E1	E2	V12	G12
---------	----	----	-----	-----

	(psi)	(psi)	(psi)
1	0.2080E+08	0.1880E+07	0.3000 0.7400E+06

LAYER	MATERIAL	THK	ORIENTATION
No.	No.	(in)	(deg)
1	1	0.0600	0.0000

Height of X-stiffener = 0.5000000000000000
 Height of Y-stiffener = 0.5000000000000000
 Height of Dia-stiffener = 0.5000000000000000

Node #	X	Y	RADIUS
1	0.000	0.000	1000000000000.000
2	20.000	0.000	1000000000000.000
3	20.000	56.000	1000000000000.000
4	0.000	56.000	1000000000000.000

BOUNDARY CONDITIONS					
Edge	U	V	W	Px	Py
1	1	0	1	0	0
2	0	1	1	0	0
3	1	0	1	0	0
4	0	1	1	0	0

STIFFENER ORIENTATION (deg) = 29.48715171286544
 UNIT CELL LENGTH (in) = 3.3333330000000000
 UNIT CELL WIDTH (in) = 5.8947300000000000

No of MODES CONSIDERED = 55

* U *	* V *	* W *	*pX *	*pY *
0	0	0	0	0
1	0	1	0	1
0	1	0	1	0
2	0	2	0	2
1	1	1	1	1
0	9	0	9	0

LOADING MATRIX

400.000	0.000
0.000	0.000

.....
 END OF INPUT DATA

SKIN STIFFNESS DATA

Extensional Stiffness (lbs)

319210.997	102680.460	0.000
102680.460	319210.997	0.000

	0.000	0.000	108265.268
Coupling Stiffness (lbs)			
	0.000	0.000	0.000
	0.000	0.000	0.000
	0.000	0.000	0.000
Bending Stiffness (lbs-in)			
	29.504	12.073	5.245
	12.073	37.478	15.469
	5.245	15.469	12.676
Transverse shear stiffness (lbs/in)			
	0.21900E+05	0.00000E+00	
	0.00000E+00	0.21900E+05	

STIFFENER STIFFNESS	EXTENSIONAL (lbs)	COUPLING (lbs in)	BENDING (lbs in ²)	SHEAR (lbs)
1	0.6060E+06	-.1624E+06	0.5615E+05	0.2190E+05
2	0.0000E+00	0.0000E+00	0.0000E+00	0.0000E+00
3	0.6240E+06	-.1672E+06	0.5781E+05	0.2220E+05

<< ONLY AXIAL & DIAGONAL STIFFENERS >>

Stiffening Parameter (X) = 0.7183978195291273
 Stiffening Parameter (Y) = 0.0000000000000000E+00
 Stiffening Parameter (D) = 0.2029944179752305

X-stiffener

znn = -0.1288619996825681
 zstar = -1.3159971231018306E-02
 ystar = 1.6169244000000000
 nstep = 56

D-stiffener

znn = -0.1294158431233926
 zstar = -1.5048423842671259E-02
 ystar = 3.292702233808636
 nstep = 99

CORRECTED STIFFNESS

STIFFENER STIFFNESS	EXTENSIONAL (lbs)	COUPLING (lbs in)	BENDING (lbs in ²)	SHEAR (lbs)
1	0.6060E+06	-.1547E+06	0.5198E+05	0.2190E+05
2	0.0000E+00	0.0000E+00	0.0000E+00	0.0000E+00
3	0.6240E+06	-.1581E+06	0.5292E+05	0.2220E+05

EXTENSIONAL SMEARED STIFFNESS

Stiffeners

230840.070	78957.215	0.000
78957.215	246923.403	0.000
0.000	0.000	78957.215

stiffeners + skin

550051.067	181637.676	0.000
------------	------------	-------

181637.676	566134.400	0.000
0.000	0.000	187222.484

COUPLING SMEARED STIFFNESS

Stiffeners		
-58876.790	-20008.824	0.000
-20008.824	-62573.722	0.000
0.000	0.000	-20008.824
stiffeners + skin		
-58876.790	-20008.824	0.000
-20008.824	-62573.722	0.000
0.000	0.000	-20008.824

BENDING SMEARED STIFFNESS

Stiffeners		
19776.506	6696.980	0.000
6696.980	20943.508	0.000
0.000	0.000	6696.980
stiffeners + skin		
19806.010	6709.053	5.245
6709.053	20980.986	15.469
5.245	15.469	6709.656

SMEARED TRANSVERSE SHEAR STIFFNESS (lbs/in)

stiffeners		
11137.905		0.000
0.000		11594.610
stiffener + skin		
11137.905		0.000
0.000		11594.610

.....
BEGIN BUCKLING ANALYSIS
.....

Global Lamda = 1.007544806578725
 (Nx)_sk = 233.0447616099682
 (Ny)_sk = 0.0000000000000000E+00
 (Nxy)_sk = 0.0000000000000000E+00
 (Nx)_1 = 892.3931403986120
 Ndx_1 = 109.5527510697837
 Ndx_2 = 0.0000000000000000E+00
 (Ndx)_x = 0.0000000000000000E+00
 (Ndx)_y = 0.0000000000000000E+00
 DETERMINANT = 9.824549017545001
 skilam = 1.024367601996003
 riblx = 2.062871407188981
 ribld = 34.25216887196387
 Volume (lbs/ft²) (rho = 0.057 lbs/in³) = 0.5487635861376152
 CPU TIME 3.071758

List 3: Part of main program "main.f"

```

C          GENETIC ALGORITHM
C
C          IS(I,J), I being the individual number and J its Jth bits.
C          IS(I,J) bit string number I (old generation)
C          JS(I,J) bit string number I (new generation)
C          CRITLB(I) fitness associated to the individual I
C          FNS(I) normalized fitness of the individual I
C          M population size
C          NLA maximum number of layers
C          N number of bits in a string (=NLA/4)
C          PC probability of implementing crossover
C          PM probability of implementing mutation
C          PP probability of permutation
C          PRI probability of inversion
C          ITER iteration (generation) number
C
C
C*****
C          parameter (n=6,m=14,nn=m*2)
C
C          n = number of design variables
C          m = number of design in each group
C          nn= just for dimension ( parameter)
C
C          DIMENSION IS(nn,n), FNS(100), RD(n) ,JS(m,n),
C          &CRITLB(100),CRITZ(100),aas(8),bbs(8),hh1(8),tthk1(8),
C          &ISK(50,m),FSK(50),NGEN(50),alength(n)
C          real*4 tcp2(2)
C          common/genpara/n,m,nn
C          common /stap/alength,area
C          COMMON/PIE/PI
C          COMMON/MATGEO/T,NLA
C          common /function/critlb
C
C          OPEN (UNIT=15, FILE='on.gen')
C          OPEN (UNIT=12, FILE='best.gen')
C          OPEN (UNIT=9 , FILE='inp.gen')
C
C          nla=16
C          N=NLA/4
C          n=15
C
C          Maximum number of generations
C
C          read(9,*)(aas(ij),ij=1,8)
C          read(9,*)(bbs(ij),ij=1,8)
C          read(9,*)(hh1(ij),ij=1,8)
C          read(9,*)(tthk1(ij),ij=1,8)
C
C          LTT=300
C

```

```

C      Genetic parameters
C
C      PC=1.00D+00
C      PM=0.10D+00
C      PP=0.95+00
C      M=16
C
C      NFT is the number of evaluations of the objective function
C      without improvement before the search stops.
C
C      NFT=150
C
C      Initialization of the stopping criterion
C
C      NCRIT=0
C      OPTI=0.D+00
C
C      NSTOP is the maximum number of generations without
C      improvement.
C
C      NSTOP=15
C
C      Initialization of the parameters of the subroutine STORE
C      before the first call.
C
C
C
C      call dtime(tcp2)
C      write(12,*)'CPU TIME =',tcp2(1)
C      CLOSE(12)
C      END

```

List 4: Part of subroutine "panel.f"

```

subroutine panel (io,is,critlb,ainipen,nn,nd,aas,bbs,hh1,
&                tthk1)
.
.
.
      include "opt.inc"
      include "panel.inc"
      dimension is(nn,nd)
C
C      - - - - -
C      UNIT 5 FOR THE INPUT DATA FILE
C      - - - - -
      open(5,file='pan.inp')
      rewind 5
C
C      - - - - -
C      UNIT 6 IS FOR THE OUTPUT DATA FILE
C      - - - - -
      open(6,file='pan.out')
.
.
.
      clen = aas(is(io,1))
      cwid = bbs(is(io,2))
      h1    = hh1(is(io,3))
      h2    = h1
      h3    = h1
      thick = tthk1(is(io,4))
      lami  = is(io,5)
      igeo  = is(io,6)
      call geom(sth1,sth2,sth3,igeo,thick)
      write(6,*)'-----'
      write(6,*)'Laminate =',lami
      write(6,*)'Stiffener thickness = ',thick
      write(6,*)'Stiffener height   = ',h1
C
C      -----
C      [1] READING ALL INPUT DATA FOR A LAMINATE
C           USING SUBROUTINE ISKIN & STSKIN
C      -----
      call iskin(sthk,nmsk,exsk,eysk,vsk,gsk,amatsk,nsk,
&               lnosk,msk,tsk,thesk)
C
      call cskin(sthk,nmsk,exsk,eysk,vsk,gsk,amatsk,nsk,
&               lnosk,msk,tsk,thesk,lami)
C
.
.
.
      write(6,51)critlb(io)
51  format('critlb = 'e14.7)
      write(6,*)'-----'
      return
end

```

List 5: Modifications to main program "main.f"

```

C          GENETIC ALGORITHM
C
C          IS(I,J), I being the individual number and J its Jth bits.
C          IS(I,J) bit string number I (old generation)
C          JS(I,J) bit string number I (new generation)
C          CRITLB(I) fitness associated to the individual I
C          FNS(I) normalized fitness of the individual I
C          M population size
C          NLA maximum number of layers
C          N number of bits in a string (=NLA/4)
C          PC probability of implementing crossover
C          PM probability of implementing mutation
C          PP probability of permutation
C          PRI probability of inversion
C          ITER iteration (generation) number
C
C*****
C          parameter (n=3,m=8,nn=m*2)
C
C          n = number of design variables
C          m = number of design in each group
C          nn= just for dimension ( parameter)
C
C          DIMENSION IS(nn,n), FNS(100), RD(n) ,JS(m,n),
C          &CRITLB(100),CRITZ(100),aas(8),bbs(8),hh1(8),tthk1(8),
C          &ISK(50,m),FSK(50),NGEN(50),alength(n)
C          real*4 tcp2(2)
C          common/genpara/n,m,nn
C          common /stap/alength,area
C          COMMON/PIE/PI
C          COMMON/MATGEO/T,NLA
C          common /function/critlb
C
C          OPEN (UNIT=15, FILE='on.gen')
C          OPEN (UNIT=12, FILE='best.gen')
C          OPEN (UNIT=9 , FILE='inp.gen')
C
C          nla=16
C          N=NLA/4
C          n=15
C
C          Maximum number of generations
C
C          read(9,*)(aas(ij),ij=1,8)
C          read(9,*)(bbs(ij),ij=1,8)
C          read(9,*)(hh1(ij),ij=1,8)
C          read(9,*)(tthk1(ij),ij=1,8)
C
C          .
C          .
C          .
C          END

```

List 6: Modifications to of subroutine "panel.f"

```

subroutine panel (io,is,critlb,ainipen,nn,nd,aas,bbs,hh1,
&                tthk1)
.
.
.
      include "opt.inc"
      include "panel.inc"
      dimension is(nn,nd)
C
C      - - - - -
C      UNIT 5 FOR THE INPUT DATA FILE
C      - - - - -
      open(5,file='pan.inp')
      rewind 5
C
C      - - - - -
C      UNIT 6 IS FOR THE OUTPUT DATA FILE
C      - - - - -
      open(6,file='pan.out')
.
.
.
      clen  = aas(is(io,1))           ! modify
      cwid  = bbs(is(io,1))           ! modify
      h1    = hh1(is(io,2))           ! modify
      h2    = h1                      ! modify
      h3    = h1                      ! modify
      thick = tthk1(is(io,3))         ! modify
      igeo = 5                        ! modify
      call geom(sth1,sth2,sth3,igeo,thick)
      write(6,*)'-----'
C      write(6,*)'Laminate =',lami           ! modify
      write(6,*)'Stiffener thickness = ',thick
      write(6,*)'Stiffener height   = ',h1
C
C      -----
C      [1] READING ALL INPUT DATA FOR A LAMINATE
C           USING SUBROUTINE ISKIN & STSKIN
C      -----
      call iskin(sthk,nmsk,exsk,eysk,vsk,gsk,amatsk,nsk,      ! modify
&               lnosk,msk,tsk,thesk)                        ! modify
C
      call cskin(sthk,nmsk,exsk,eysk,vsk,gsk,amatsk,nsk,      ! modify
&               lnosk,msk,tsk,thesk,lami)                    ! modify
C
.
.
.
      write(6,51)critlb(io)
51  format('critlb = 'e14.7)
      write(6,*)'-----'
      return
      end

```


List 7: Input file for optimization (inp.gen)

```

6.667,5.71428,5.00,4.444,4.444,4.0,3.6363,3.33333 ! a
11.2,10.1818,8.61538,8.0,7.4666,7.0,6.2222,5.894 ! b
0.49375,0.50000,0.50625,0.51250,0.51875,0.52500,0.53125,0.53750 ! h
0.060,0.066,0.072,0.078,0.084,0.090,0.096,0.102 ! t

```

List 8: Input file for problem parameters (pan.inp)

```

0.036 ! skin thickness
1      ! Number of material
1,20.2e6,1.9e6,0.3,0.73e6 ! material No., E11, E22, v12, G12
6      ! number of plies
1,1,0.006,60.0      ! layer No., material no., ply thickness, theta
2,1,0.006,0.0
3,1,0.006,-60.0
4,1,0.006,-60.0
5,1,0.006,0.0
6,1,0.006,60.0
1      ! Number of material (X-stiffener)
1,20.2e6,1.9e6,0.3,0.73e6 ! material No., E11, E22, v12, G12
1      ! number of plies
1,1,0.0      ! layer No., material no., theta
1      ! Number of material (Y-stiffener)
1,20.2e6,1.9e6,0.3,0.73e6 ! material No., E11, E22, v12, G12
1      ! number of plies
1,1,0.0      ! layer No., material no., theta
1      ! Number of material (D-stiffener)
1,20.2e6,1.9e6,0.3,0.73e6 ! material No., E11, E22, v12, G12
1      ! number of plies
1,1,0.0      ! layer No., material no., theta
0.0,0.0,1.0e12 ! x,y,r of node 1
20.0,0.0,1.0e12 ! x,y,r of node 2
20.0,56.0,1.0e12 ! x,y,r of node 3
0.0,56.0,1.0e12 ! x,y,r of node
1,0,1,0      ! B.c's of U
0,1,0,1      ! B.c's of V
1,1,1,1      ! B.c's of W
0,0,0,0      ! B.c's of Px
0,0,0,0      ! B.c's of Py
55           ! # of modes considered
400.0,0.0,0.0 ! Nx, Ny, Nxy

```

List 9: Output file containing optimal designs (best.gen)

```
POPULATION SIZE= 8 Crossover PROB.=1.000
MUTATION PROB.=0.100 PERMUTATION PROB.=0.950
BESTS DESIGNS AFTER 211 EVALUATIONS OF THE OF
  FS= 0.7669355E+03 GENERATION= 15
8 3 1
  FS= 0.1063876E+03 GENERATION= 1
8 1 1
  FS= 0.6040214E+01 GENERATION= 1
8 5 5
  FS= 0.8574801E+00 GENERATION= 1
7 8 5
  FS= 0.5234697E+00 GENERATION= 1
6 4 4
  FS= 0.1314688E+00 GENERATION= 1
4 8 3
  FS= 0.4932792E-01 GENERATION= 1
2 6 1
  FS= 0.3394876E-01 GENERATION= 1
2 3 8
  FS= 0.3239560E-01 GENERATION= 1
1 1 3
CPU TIME = 516.6477
```

List 10: Output file containing convergence history (on.gen)

```

population size= 8  crossover prob.=1.000
mutation prob.=0.100  permutation prob.=0.950
Iteration   Average      Best
1    0.4257929E+02  0.1063876E+03
2    0.5292514E+02  0.1063876E+03
3    0.8050877E+02  0.1063876E+03
4    0.6810519E+02  0.1063876E+03
5    0.1045733E+03  0.1063876E+03
6    0.9221518E+02  0.1063876E+03
7    0.9460207E+02  0.1063876E+03
8    0.8101215E+02  0.1063876E+03
9    0.7896147E+02  0.1063876E+03
10   0.6563631E+02  0.1063876E+03
11   0.5746792E+02  0.1063876E+03
12   0.8395988E+02  0.1063876E+03
13   0.6175915E+02  0.1063876E+03
14   0.5932686E+02  0.1063876E+03
15   0.1258099E+03  0.7669355E+03
16   0.2046968E+03  0.7669355E+03
17   0.2256355E+03  0.7669355E+03
18   0.1188792E+03  0.7669355E+03
19   0.2204189E+03  0.7669355E+03
20   0.2373301E+03  0.7669355E+03
21   0.4233659E+03  0.7669355E+03
22   0.2582285E+03  0.7669355E+03
23   0.6843670E+03  0.7669355E+03
24   0.3967787E+03  0.7669355E+03
25   0.3142109E+03  0.7669355E+03
26   0.1357727E+03  0.7669355E+03
27   0.1403906E+03  0.7669355E+03
28   0.2964355E+03  0.7669355E+03
29   0.3865364E+03  0.7669355E+03

```

FINAL POPULATION AFTER 211 EVALUATIONS OF THE

O.F.

List 11: Information about first optimal design from "pan.out"

```

-----
Stiffener thickness = 5.999999999999998E-02
Stiffener height = 0.5062500000000000
SKIN LAMINATE
LAYER MATERIAL THK ORIENTATION
No. No. (in) (deg)
1 1 0.0600 0.0000
STIFFENER ORIENTATION (deg) = 29.49017008775938
UNIT CELL LENGTH (in) = 3.3333300000000000
UNIT CELL WIDTH (in) = 5.8940000000000000
<< ONLY AXIAL & DIAGONAL STIFFENERS >>
Stiffening Parameter (X) = 0.7274678814806318
Stiffening Parameter (Y) = 0.0000000000000000E+00
Stiffening Parameter (D) = 0.1996764909471687
X-stiffener
znn = -0.1317762672296654
zstar = -1.3303185398854778E-02
ystar = 1.6167200000000000
nstep = 56
D-stiffener
znn = -0.1312237003831008
zstar = -1.5189387389525246E-02
ystar = 3.292386964576168
nstep = 99
Global Lamda = 1.034195740432642
(Nx)_sk = 238.2547676115182
(Ny)_sk = 0.0000000000000000E+00
(Nxy)_sk = 0.0000000000000000E+00
(Nx)_1 = 912.3437009050962
Ndx_1 = 108.8378075805412
Ndx_2 = 0.0000000000000000E+00
(Ndxy)_x = 0.0000000000000000E+00
(Ndxy)_y = 0.0000000000000000E+00
skilam = 1.002140728935756
riblx = 2.002348947521088
ribld = 33.41810771983094
Volume (lbs/ft^2) (rho=0.0570)= 0.5519452823098701
critlb = 0.7669355E+03
-----

```

List 12: Information about second optimal design from "pan.out"

```

-----
Stiffener thickness = 5.999999999999998E-02
Stiffener height   = 0.4937500000000000
SKIN LAMINATE
LAYER      MATERIAL      THK      ORIENTATION
No.        No.          (in)     (deg)
  1         1          0.0600     0.0000
STIFFENER ORIENTATION (deg) = 29.49017008775938
UNIT CELL LENGTH      (in) = 3.3333300000000000
UNIT CELL WIDTH       (in) = 5.8940000000000000
<< ONLY AXIAL & DIAGONAL STIFFENERS >>
Stiffening Parameter (X) = 0.7095057115675297
Stiffening Parameter (Y) = 0.0000000000000000E+00
Stiffening Parameter (D) = 0.1947462072200780
X-stiffener
znn = -0.1278212016698681
zstar = -1.3189737836119143E-02
ystar = 1.5878500000000000
nstep = 55
D-stiffener
znn = -0.1272756072256236
zstar = -1.4851388047712849E-02
ystar = 3.292386964576168
nstep = 99
Global Lamda = 0.9691460449089669
(Nx)_sk = 225.6313101069534
(Ny)_sk = 0.0000000000000000E+00
(Nxy)_sk = 0.0000000000000000E+00
(Nx)_1 = 864.0049748708219
Ndx_1 = 103.0712516679092
Ndx_2 = 0.0000000000000000E+00
(Ndxy)_x = 0.0000000000000000E+00
(Ndxy)_y = 0.0000000000000000E+00
skilam = 1.058207774362076
riblx = 2.147540224369275
ribld = 35.85353200238720
Volume (lbs/ft^2) (rho=0.0570)= 0.5456130037343178
critlb = 0.1063876E+03
-----

```

References

- [1] Jaunky, N., Knight, N. F. and Ambur, D. R., "An Improved Smeared Theory for Buckling Analysis of Grid-Stiffened Composite Panels," *Composite: Part B* (formerly *International Journal for Composite engineering*), Vol. 27B, No. 5, 1996, pp. 519-526.
- [2] Jaunky, N., Knight, N. F. and Ambur, D. R., "Buckling of Arbitrary Quadrilateral Anisotropic Plates," *AIAA Journal*, Vol. 33, May 1995, pp. 938-944.
- [3] Jaunky, N., Knight, N. F. and Ambur, D. R., "Buckling Analysis of General Triangular Anisotropic Plates using Polynomials," *AIAA Journal*, Vol. 33, December 1995, pp. 2414-2417.
- [4] Reddy, A. D., Valisetty, Rao R., and Rehfield, L. W., "Continuous Filament Wound Composites Concepts for Aircraft Fuselage Structures," *AIAA Journal of Aircraft*, Vol. 22, No. 3, March 1985, pp. 249-255.
- [5] Nagendra, S., Haftka, R. T., and Gurdal, Z., "Design of a Blade Stiffened Composite Panel by Genetic Algorithm," Proceedings of the 34th AIAA/ASME/ASCE/AHS/ASC Structures, Structural Dynamics and Materials Conference, AIAA Paper No. 93-1584-CP, April 1993, La Jolla, CA, pp. 2418-2436.
- [6] Jaunky, N., Knight, N. F. and Ambur, D. R., "Optimal Design of Grid-stiffened Composite Panels Using Global and Local Buckling Analyses," Proceedings of the 37th AIAA/ASME/ASCE/AHS/ASC Structures, Structural Dynamics and Materials Conference, AIAA Paper No. 96-1581-CP, Salt Lake City, Utah, April 96, pp. 2315-2325.
- [7] Jaunky, N., "Elastic Buckling of Stiffened Composite Curved Panel," Old Dominion University, Norfolk, Virginia, Master's Thesis, August 1991.

Chapter 1

INTRODUCTION

The theoretical foundations and user instructions for a FORTRAN code for the buckling analysis for anisotropic variable curvature panels are presented. The variable curvature panel is assumed to consist of two or more panels of constant curvature where each panel may have a different curvature. Bezier polynomials are used as Ritz functions. Displacement (C^0), and slope (C^1) continuities between segments are imposed by manipulation of the Bezier control points. A first-order shear-deformation theory is used in the buckling formulation.

Chapter 2 gives an account of the theoretical foundations of the buckling analysis. Instructions for setting up input files for the FORTRAN code are given in Chapter 3 for three structure cases. Examples of input files for the structural cases considered are also given. Finite element results of the structural cases considered are given so as to provide a comparison between results from the present analysis and those of finite element simulations.

Chapter 2

THEORETICAL FOUNDATIONS

The present analysis method for buckling of anisotropic shells with variable curvature uses a segment approach where displacement fields within each segment are represented by Bezier polynomials and a first-order, shear-deformation theory is used. In general, segments can be used in both axial and circumferential directions, however the present implementation considers only segments in the circumferential direction. This restriction is based on the typical frame spacing for fuselage structures and on limiting general buckling to frames rather than across frames. Continuity of displacement at the junctures of adjacent segments are imposed using C^0 and C^1 conditions obtained from the properties of the Bezier control points ([1]). The shell with variable curvature is assumed to consist of two or more curved panels of constant curvature which is representative of fuselage or wing structures.

The following sections

- Geometry of variable curvature panel.
- Bezier polynomials.
- Continuities along segment junctures.
- Minimum potential energy

describe the formulation of the buckling analysis.

2.1 GEOMETRY OF VARIABLE CURVATURE PANEL

The coordinate system and the displacement directions for a noncircular shell is shown in Figure 1. Any point in the wall of the shell is specified by means of curvilinear coordinate system x , y and z , where x is the axial coordinate fixed to mid-surface, y is the circumferential coordinate which follows the median line of the transverse cross section, and z is the radial coordinate normal to both x and y . The noncircular shell is assumed to consist of two or more segments in the circumferential direction each of constant radius. The normal and tangent vectors of the two segments at a juncture are equal as shown in Figure 1, where $\vec{n}_1 = \vec{n}_2$ and $\vec{t}_1 = \vec{t}_2$.

2.2 BEZIER POLYNOMIALS

Bezier polynomials are used in the axial and circumferential directions to represent the displacement fields. The Bezier polynomial in terms of an independent variable is given by

$$f_i(n, \nu) = \frac{n!}{(i-1)!(n-i+1)!} \nu^{i-1} (\nu-1)^{n-i+1} \quad (1)$$

where n denotes the order of the polynomial and $0 \leq \nu \leq 1$. For a Bezier polynomial of order n , there are $(n+1)$ control points. The values of the control points will determine the variation of $f_i(n, \nu)$ within the interval of $0 \leq \nu \leq 1$. Any point on the surface of the segment is given by a parametric function in two variables of the form

$$P_{rs}(\xi, \eta) = \sum_{r=1}^X \sum_{s=1}^Y f_r(\xi) f_s(\eta) q_{rs} \quad (2)$$

where the coordinates ξ and η are defined as

$$\begin{aligned} \xi &= x / L \\ \eta &= (y - y_i) / (y_{i+1} - y_i) \end{aligned} \quad (3)$$

with $0 \leq \xi, \eta \leq 1$, X and Y are the number of control points in the axial and circumferential direction respectively, and q_{rs} are the Bezier control points or coefficients.

The displacement vector can be written as

$$\begin{Bmatrix} u_0 \\ v_0 \\ w \\ \phi_x \\ \phi_y \end{Bmatrix}_j = \begin{bmatrix} P_{rs} & 0 & 0 & 0 & 0 \\ 0 & P_{rs} & 0 & 0 & 0 \\ 0 & 0 & P_{rs} & 0 & 0 \\ 0 & 0 & 0 & P_{rs} & 0 \\ 0 & 0 & 0 & 0 & P_{rs} \end{bmatrix}_j \begin{Bmatrix} q_{1rs} \\ q_{2rs} \\ q_{3rs} \\ q_{4rs} \\ q_{5rs} \end{Bmatrix}_j \quad (4)$$

where u_0 and v_0 are the axial and transverse membrane displacements, respectively, w is the normal displacement, and ϕ_x and ϕ_y are the bending rotations. There are five degrees of freedom ($NDOF=5$) per control point and the range of subscript j is 1, 2, 3, ... (XY). The control points for each degree of freedom can be used to impose boundary conditions on each degree of freedom on each segment.

2.3 CONTINUITIES ALONG SEGMENT JUNCTURES

Continuity of displacement functions along segment junctures are obtained by using the relations between control points of the adjacent segment based on C^0 and C^1 continuities. Figure 2 shows two adjacent segments and the control points that are involved in the C^0 and C^1 continuities for the case of eleven control points in the axial direction and six control points in the transverse directions, i.e., $X = 11$ and $Y = 6$. The control points shown in Figure 2 are for one degree of freedom and therefore subscript 1,2, ...,5 in $q_{1rs}, q_{2rs}, \dots, q_{5rs}$ of Equation (4) have been dropped. In the I^{th} segment, control points q_{k6} and q_{k5} are related to control points q_{k1} and q_{k2} of the $(I+1)^{th}$ segment, where $k = 1,2, \dots, 11$ according to

$$\begin{aligned} q_{k6} &= q_{k1} \quad \text{for } C^0 \text{ continuity} \\ q_{k6} &= \frac{S_I q_{k5} + S_{I+1} q_{k2}}{S_I + S_{I+1}} \quad \text{for } C^1 \text{ continuity} \end{aligned} \quad (5)$$

where S_I and S_{I+1} are the width of the I^{th} and $(I+1)^{th}$ segment, respectively. Using these conditions the unknowns q_{k1} and q_{k2} are expressed in terms of q_{k5} and q_{k6} , which the master control points.

The procedure for slaving q_{k1} and q_{k2} to q_{k5} and q_{k6} is demonstrated below considering only control points with subscript k and only one degree of freedom.

Equation (5) can be written as

$$\begin{aligned} q_{k1}^{(I+1)} - q_{k6}^{(I)} &= 0 \\ a_{k2}^{(I+1)} q_{k2}^{(I+1)} + a_{k5}^{(I)} q_{k5}^{(I)} - q_{k6}^{(I)} &= 0 \end{aligned} \quad (6)$$

where superscript $(I+1)$ and (I) have been added to denote segment $(I+1)$ and (I) , respectively. Equation (6) can be written in matrix form as

$$\begin{bmatrix} 1 & 0 & 0 & -1 & \vdots & 0 & \cdots & 0 \\ 0 & a_{k2}^{(I+1)} & a_{k5}^{(I)} & -1 & \vdots & 0 & \cdots & 0 \end{bmatrix} \begin{Bmatrix} q_{k1}^{(I+1)} \\ q_{k2}^{(I+1)} \\ \vdots \\ q_{k5}^{(I)} \\ q_{k6}^{(I)} \\ q_{k3}^{(I+1)} \\ \vdots \\ q_{k6}^{(I+1)} \\ q_{k1}^{(I)} \\ \vdots \\ q_{k4}^{(I)} \end{Bmatrix} = \begin{Bmatrix} 0 \\ 0 \end{Bmatrix} \quad (7)$$

In matrix notation form Equation (7) can be written as

$$\begin{bmatrix} [\mathbf{C}_e] & [\mathbf{C}_r] & \vdots & [\mathbf{0}] \end{bmatrix} \begin{Bmatrix} \{\mathbf{D}_e\} \\ \vdots \\ \{\mathbf{D}_r\} \end{Bmatrix} = [\mathbf{0}] \quad (8)$$

Using Equation (8), a transformation matrix $[\mathbf{T}]$ is developed, and

$$\begin{Bmatrix} \{\mathbf{D}_e\} \\ \{\mathbf{D}_r\} \end{Bmatrix} = \begin{bmatrix} [\mathbf{C}_{er}]_{2 \times 2} & [\mathbf{0}]_{2 \times 8} \\ [\mathbf{I}]_{10 \times 10} \end{bmatrix} \{\mathbf{D}_r\} = [\mathbf{T}] \{\mathbf{D}_r\} \quad (9)$$

where $[\mathbf{C}_{er}] = -[\mathbf{C}_e]^{-1}[\mathbf{C}_r]$. These matrices have to be set up for $k = 1, 2, 3, \dots, 11$, and for every degree of freedom. The complete matrices $[\mathbf{C}_{er}]$, $[\mathbf{C}_e]$, and $[\mathbf{C}_r]$ including each k and degree of freedom contains some populated blocks and matrix multiplication and inversion can be performed by manipulating the blocks for computational efficiency. The modified stiffness matrix $[\mathbf{K}]$ is given by

$$[\mathbf{K}] = [\mathbf{T}]^T [\mathbf{K}] [\mathbf{T}] \quad (10)$$

The above matrix multiplication is performed by manipulating the populated blocks in matrix $[\mathbf{T}]$ for computational efficiency.

Since the buckling analysis involves first-order, shear-deformation, only C^0 continuity is required in the variational formulation. However the advantage of also imposing C^1 continuity is not only to obtain a more accurate analysis but also to reduce the size of the stiffness and geometric stiffness matrices when a larger number of segments are used to represent the shell that is being analyzed. Table 1 shows the size of the matrices as indicated by the parameter *ISIZE* with the number of segments for different conditions of continuities when $X = 11$ and $Y = 6$. *ISIZE* is the number of terms in the matrix and also the number of unknown coefficients to be determined. If the segments are joined to approximate a closed shell, the size of the final matrices is less than that for a panel. The size of the stiffness and geometric stiffness matrices after assembly is given by the expression

$$ISIZE = NDOF \times X \times Y \times NSEG - NDOF \times 2 \times X \times MJOIN \quad (11)$$

for C^0 and C^1 continuities, where *ISIZE* is the matrix size or number of unknown coefficients, *NSEG* is the number of segments, and $MJOIN = NSEG - 1$ for a panel and $MJOIN = NSEG$ for a closed shell, i.e., *MJOIN* is the number of junctures.

2.4 MINIMUM POTENTIAL ENERGY PRINCIPLE

The linear stiffness matrices are derived from the strain energy which is given by

$$U = \frac{1}{2} \int_A \{\epsilon\}^T \begin{bmatrix} A_{ij} & B_{ij} & 0 \\ B_{ij} & D_{ij} & 0 \\ 0 & 0 & C_{pq} \end{bmatrix} \{\epsilon\} dA \quad (12)$$

where A_{ij} is the extensional stiffness coefficient matrix, B_{ij} is the coupling stiffness coefficient matrix, D_{ij} is the bending stiffness coefficient matrix and C_{pq} is the transverse shear stiffness coefficient matrix. The strain vector is $\{\epsilon\}$ and given by

$$\{\epsilon\}^T = \{\epsilon_x^0 \ \epsilon_y^0 \ \gamma_{xy}^0 \ \kappa_x \ \kappa_y \ \kappa_{xy} \ \gamma_{xz} \ \gamma_{yz}\}^T \quad (13)$$

The strain-displacement relations are

$$\begin{aligned} \epsilon_x^0 &= \frac{\partial u_0}{\partial x} \\ \epsilon_y^0 &= \frac{\partial v_0}{\partial y} + \frac{w_0}{R} \end{aligned}$$

$$\begin{aligned}
\gamma_{xy}^0 &= \frac{\partial u_0}{\partial y} + \frac{\partial v_0}{\partial x} \\
\kappa_x &= \frac{\partial \phi_x}{\partial x} \\
\kappa_y &= \frac{\partial \phi_y}{\partial y} \\
\kappa_{xy} &= \frac{\partial \phi_x}{\partial y} + \frac{\partial \phi_y}{\partial x} + \frac{C_2}{2R} \left(\frac{\partial v_0}{\partial x} - \frac{\partial u_0}{\partial y} \right) \\
\gamma_{xz}^0 &= \phi_x + \frac{\partial w_0}{\partial x} \\
\gamma_{yz}^0 &= \phi_y + \frac{\partial w_0}{\partial y} - C_1 \frac{v_0}{R}
\end{aligned} \tag{14}$$

Here C_1 and C_2 are “tracer” coefficients used to implement different strain-displacement relations or shell theories. Accordingly when $C_1 = C_2 = 1$, the first approximation of Sanders-Koiter shell theory [2, 3] is obtained, and when $C_1 = 1$, $C_2 = 0$, Love’s shell theory [4] including transverse shear deformations is obtained. Finally, when $C_1 = 0$ and $C_2 = 0$, Donnell’s shell theory [5] including transverse shear deformation is obtained.

The geometric stiffness matrix is derived from the work done, (W_d) , by the applied prebuckling loading and is given by

$$W_d = \int_A (\bar{N}_x \epsilon_{xNL} + \bar{N}_y \epsilon_{yNL} + \bar{N}_{xy} \gamma_{xyNL}) dA \tag{15}$$

where the nonlinear strain components are

$$\begin{aligned}
(\epsilon_x)_{NL} &= \frac{1}{2} (v_{0,x}^2 + w_{,x}^2) \\
(\epsilon_y)_{NL} &= \frac{1}{2} (u_{0,y}^2 + (w_{,y} - \frac{v_0}{R})^2) \\
(\gamma_{xy})_{NL} &= -u_{0,y} (v_{0,y} + \frac{w}{R}) - v_{0,x} u_{0,x} + w_{,x} (w_{,y} - \frac{v_0}{R})
\end{aligned} \tag{16}$$

In the present analysis, the applied prebuckling loading is prescribed as a uniform in-plane stress state. The linear stiffness and geometric stiffness matrices are developed using analytical integration rather than numerical integration for computational efficiency. Finally, an eigenvalue problem is solved for determining the critical buckling load.

Chapter 3

USER INSTRUCTIONS

User instructions are provided for the FORTRAN code for the buckling analysis of variable curvature shell. The source code is found in directory “variable”. A make file is used to link all the subroutines. The input file to the code is “bez.inp” and the out put file is “b.out”. The executable for the code is “run” as specified in the makefile.

Results are presented for a composite cylindrical panel subjected to axial compression, a composite wing leading-edge panel subjected to combined axial compression and shear, and a composite and isotropic non-circular fuselage. Sanders-Koiter ([2, 3]) shell theory is used in these examples. Buckling loads from the present analysis are compared with those obtained from the STAGS ([6]) finite element code. The STAGS finite element model consists of the 410 element, curved surfaces are approximated as an assembly of flat surfaces, and the formulation of the 410 element is based on the classical laminated plate theory. The nominal ply mechanical properties for the composite material used are: $E_{11} = 13.75$ Msi; $E_{22} = 1.03$ Msi; $G_{12}=G_{13}=G_{23} = 0.420$ Msi and $\nu_{12} = 0.250$, The laminate ply stacking sequence is $[\pm 45/0/90/\pm 45]_s$, with equal ply thicknesses for each of the different laminate thicknesses. For the isotropic material, the mechanical properties are $E_{11} = E_{22} = 10.0$ Msi; $\nu_{12} = 0.3$, and $G_{12}=G_{13}=G_{23} = E_{11} / 2(1 + \nu_{12})$.

3.1 APPLICATION OF BOUNDARY CONDITIONS

Boundary conditions can be imposed along $\xi = 0, 1$, $\eta = 0, 1$ (Figure 2) and also at any control point by the subroutine “ibcs.f”. For example, if $u=0$ at $\xi = 1$ and $w = 0$ at $\eta = 0$ on segment 1, then these constraints are entered as

2 ! Number of line constraints
 1,1,1,1 ! coordinate No., coordinate value, segment No., Dof No.
 2,0,1,3

Characters after the “!” are only comments. Coordinate No. can be either 1 or 2, coordinate No. = 1 for x and coordinate No. = 2 for y . Coordinate value = 0 or 1, coordinate value = 0 for ξ or $\eta = 0$, and coordinate value = 1 for ξ or $\eta = 1$. Segment No. is the segment No. where the constraint is applied. Dof No. can be 1, 2, 3, 4, or 5 and $u=1$, $v=2$, $w=3$, $\phi_x=4$, and $\phi_y=5$.

Point constraints can be applied by specifying the control point associated with the degree of freedom of concern. For example if control point q_{rs} , where $r = 1, 2, 3, \dots, 11$, and $s = 1, 2, 3, \dots, 6$, (see Figure 2) of segment $(I + 1)$ is to have $w=0$ constraint, then the number of point constraint is one and the entry format to be entered for q_{rs} with $w = 0$ is

No. of point constraints
 segment No., control point No., Dof No

The segment No. is $(I + 1)$, the control point No. for q_{rs} is $[(r - 1) \times 6 + s]$, and Dof No. is as described above. If there is no point constraint then the number of point constraint is entered as zero.

3.2 CYLINDRICAL PANEL

The first structure analyzed is a semi-circular laminated composite ($\alpha = 180^\circ$) cylindrical panel 22.0-in. long, and with a radius of 40.0 inches as shown in Figure 3. The simply-support boundary conditions are also shown in Figure 3. The cylindrical panel is modeled with five curved segments in the present analysis while the STAGS finite element modeled consists of a mesh of 20×40 elements in the axial and transverse direction, respectively. Table 2 shows the results for the curved panel subjected to axial compression load for different thicknesses, List 1 shows the input data for the problem where characters after the “!” are only comments and need not be included

in the input file. The input file is "variable/bcpan5.inp" on the compact disk and the file has to be named "bez.inp" for execution.

The results in Table 2 suggest that for $t = 0.072$ in. the present analysis result is 4.3 percent greater than the STAGS result, while for $t = 0.144$ in. and 0.216 in. the STAGS analysis results is 1.4 percent above that of the present analysis. The STAGS results are above that of the present analysis for $t = 0.144$ in. and 0.216 in. since these two panels are thicker and hence transverse shear deformation effects have an influence on buckling load.

3.3 WING LEADING-EDGE PANEL

The wing leading-edge panel is shown in Figure 4. It consists of three curved segments of radii 50.0 in., 6.136 in., and 50.0 in., respectively, and is 26.0-inches long, and has a maximum width of 32.0 inches. The boundary conditions of the panel is shown in Figure 4 and correspond to classical simply support conditions. Each ply of the laminate is 0.006-in. thick. Using the present analysis, the wing leading-edge panel is modeled as a combination of two segments for the 50.0-in.-radius section and one segment for the 6.136-in.-radius section. The wing leading-edge panel is also modeled as a quarter symmetric model in the present analysis as shown in Figure 5 with symmetry boundary conditions on two edges and classical simply support conditions on the other two edges. A combination of two segments for the 50.0-in.-radius section and one segment for the 6.136-in.-radius section is used for the quarter symmetry model. The STAGS finite element model consists of the 410 shell element and 30×30 elements in each curved segment.

Table 3 shows the results obtained from the present analysis for the full model and the quarter symmetric model for some selected combined load cases. Results from STAGS for the same selected combined load cases are also shown in Table 3. Figure 6 shows the buckling load interaction curve between axial compression and positive shear loading. The results from the present analyses for the full model are about 4.0 to 5.0 percent above those of STAGS except for the case of negative shear loading where the result from the present analysis is 7.0 percent above that of STAGS.

Better agreement with STAGS is obtained from the present method by using a quarter symmetric model except for the case where the shear loading is dominant as is seen in Figure 6. For example, there is only a very small difference between the results of the present analysis for the full and quarter symmetric model for the pure shear case. For the case where the loading condition is $N_x = N_{xy} = 1$, the result for the quarter symmetric model is about 3 percent above that of STAGS, and for the case of compression only, the result for the quarter symmetric model is in very good agreement with that of STAGS.

The quarter symmetric model provides results in better agreement compared to those of STAGS for cases where the buckling mode shape is symmetric or close to being symmetric since fewer control points can be used to provide a more accurate model of the structure. The symmetric model is not recommended for loading cases where the shear load is predominant. The input files for this problem is given in List 2 and 3 for the full model and quarter symmetric model, respectively. Comments to the input data are provided after the “!” in List 2 and 3. The input file is “variable/bw5.inp” and “variable/bwss3.inp” for the full model and quarter symmetric model, respectively, on the compact disk and any file has to be named “bez.inp” for execution.

3.4 NON-CIRCULAR FUSELAGE

A non-circular fuselage section is shown in Figure 7 and is 24-inches long. It consists of 30.0-in.-radius curved segments and flat segments, and has simply support boundary conditions. In both the present analysis and the STAGS analysis, a quarter symmetric model of the non-circular fuselage section is considered, and the boundary conditions are shown in Figure 8. In the present analysis, the quarter symmetric model of the fuselage consists of a combination of four segments, one for each flat and curved segment. The STAGS model consists of 410 shell element and a mesh of 40×40 elements in each segment.

The results are shown in Table 4 for the isotropic and laminated non-circular fuselage with different wall thicknesses subjected to axial compression. The buckling

loads for the isotropic non-circular fuselage obtained from the present analysis are less than 2.5 percent above those of STAGS for the different wall thicknesses considered. For the laminated non-circular fuselage, the buckling loads are in very good agreement with the those of STAGS for the wall thicknesses considered. The input file for this problem is given in List 4 for the isotropic case. Comments to the input data are provided after the “!” in List 4 The input file is “variable/bfs4.inp” on the compact disk and the file has to be named “bez.inp” for execution.

LIST OF FILES

List 1: Input file for cylindrical panel.

```

0.216                ! skin thk
1                    ! # of material
1,0.1375e+8,1.030e6,0.25,0.42e6 ! mat #, e1,e2,nu,g12
12                   ! # of ply
1,1,0.018,45.0      ! layer #, material #, layer thk, theta
2,1,0.018,-45.0
3,1,0.018,0.0
4,1,0.018,90.0
5,1,0.018,45.0
6,1,0.018,-45.0
7,1,0.018,-45.0
8,1,0.018,45.0
9,1,0.018,90.0
10,1,0.018,0.0
11,1,0.018,-45.0
12,1,0.018, 45.0
5                    ! # of segment
22.0,25.132741,40.0 ! length, width,radius of segment i
22.0,25.132741,40.0
22.0,25.132741,40.0
22.0,25.132741,40.0
22.0,25.132741,40.0
24                  ! # of line constraints
1,0,1,2             ! Coord. #, Coord Val., segment #, DoF #
1,0,1,3 -----
1,0,2,2
1,0,2,3 -----
1,0,3,2
1,0,3,3 -----
1,0,4,2
1,0,4,3 -----
1,0,5,2
1,0,5,3 ----- x=0, v=w=0
1,1,1,2
1,1,1,3 -----
1,1,2,2
1,1,2,3 -----
1,1,3,2
1,1,3,3 -----
1,1,4,2

```

```

1,1,4,3 ----
1,1,5,2
1,1,5,3 ---- x=1, v=w=0
2,0,1,1
2,0,1,3 ---- y=0, u=w=0
2,1,5,1
2,1,5,3 ---- y=1, u=w=0
0          ! # of point constraints
4          ! # of joints
2,1 ! segment 2 join to segment 1
3,2 ! segment 3 join to segment 2
4,3 ! segment 4 join to segment 3
5,4 ! segment 5 join to segment 4
1.0,0.0,0.0      ! Nx, Ny, Nxy

```

List 2: Input file for wing leading-edge panel (full model).

```

0.072                ! skin thk
1                    ! # of material
1,0.1375e+8,1.030e6,0.25,0.42e6 ! mat #, e1,e2,nu,g12
12                   ! # of ply
1,1,0.006,45.0      ! layer #, material #, layer thk, theta
2,1,0.006,-45.0
3,1,0.006,0.0
4,1,0.006,90.0
5,1,0.006,45.0
6,1,0.006,-45.0
7,1,0.006,-45.0
8,1,0.006,45.0
9,1,0.006,90.0
10,1,0.006,0.0
11,1,0.006,-45.0
12,1,0.006, 45.0
5                    ! # of segment
26.0,12.606817,50.0 ! length, width,radius of segment i
26.0,12.606817,50.0
26.0,9.037922,6.1362094
26.0,12.606817,50.0
26.0,12.606817,50.0
24                   ! # of line constraints
1,0,1,3              ! Coord. #, Coord Val., segment #, DoF #
1,1,1,3
2,0,1,3 ---- seg. 1, w=0
1,1,2,3
1,0,2,3 ---- seg. 2, w=0
1,1,3,3
1,0,3,3 ---- seg. 3, w=0
1,1,4,3
1,0,4,3 ---- seg. 4, w=0
1,1,5,3
1,0,5,3
2,1,5,3 ---- seg. 5, w=0
2,0,1,1
1,0,1,2
1,1,1,2 ---- seg. 1, in-plane b.c
1,1,2,2
1,0,2,2 ---- seg. 2, in-plane b.c
1,1,3,2
1,0,3,2 ---- seg. 3, in-plane b.c
1,1,4,2
1,0,4,2 ---- seg. 4, in-plane b.c

```

```
1,1,5,2
1,0,5,2
2,1,5,1 ---- seg. 5, in-plane b.c
0          ! # of point constraints
4          ! # of joints
2,1
3,2
4,3
5,4
0.0,0.0,1.0      ! Nx, Ny, Nxy
```

List 3: Input file for wing leading-edge panel (quarter symmetric model).

```

0.072                ! skin thk
1                    ! # of material
1,0.1375e+8,1.030e6,0.25,0.42e6 ! mat #, e1,e2,nu,g12
12                   ! # of ply
1,1,0.006,45.0      ! layer #, material #, layer thk, theta
2,1,0.006,-45.0
3,1,0.006,0.0
4,1,0.006,90.0
5,1,0.006,45.0
6,1,0.006,-45.0
7,1,0.006,-45.0
8,1,0.006,45.0
9,1,0.006,90.0
10,1,0.006,0.0
11,1,0.006,-45.0
12,1,0.006, 45.0
3                    ! # of segment
13.0,12.606817,50.0 ! length, width,radius of segment i
13.0,12.606817,50.0
13.0,4.518961,6.1362094
16                  ! # of line constraints
1,0,1,1            ! Coord. #, Coord Val., segment #, DoF #
1,0,2,1
1,0,3,1 ----sym
1,0,1,4
1,0,2,4
1,0,3,4 ----sym
1,1,1,3
1,1,2,3
1,1,3,3 ----w=0
1,1,1,2
1,1,2,2
1,1,3,2 ----v=0
2,0,1,3
2,0,1,1 ----segment 1, u=w=0
2,1,3,2
2,1,3,5 ----sym
0                  ! # of point constraints
2                  ! # of joints
2,1
3,2
0.8,0.0,1.0        ! Nx, Ny, Nxy

```

List 4: Input file for non-circular fuselage (isotropic)

```

0.100          ! skin thk
1              ! # of material
1,0.10e+8,0.10e+8,0.30,3846153.8 ! mat #, e1,e2,nu,g12 -isotropic(A1)
2              ! # of ply
1,1,0.050,0.0 ! layer #, material #, layer thk, theta
1,1,0.050,0.0
4              ! # of segment
12.0,21.213203,1.0e8 ! length, width,radius of segment i
12.0,70.685835,30.0
12.0,30.0,1.0e8
12.0,23.561945,30.0
16             ! # of line constraints
1,0,1,3 ---- seg. 1, w=0 ! Coord. #, Coord Val., segment #, DoF #
1,0,2,3 ---- seg. 2, w=0
1,0,3,3 ---- seg. 3, w=0
1,0,4,3 ---- seg. 4, w=0 at x=0 or xi=0
1,1,1,4 ---- seg. 1
1,1,2,4 ---- seg. 2
1,1,3,4 ---- seg. 3
1,1,4,4 ---- seg. 4 phi_x =0 at x=12 or xi=1
1,1,1,1 ---- seg. 1, u=0
1,1,2,1 ---- seg. 2, u=0
1,1,3,1 ---- seg. 3, u=0
1,1,4,1 ---- seg. 4, u=0 at x=12 or xi=1
2,0,1,2 ---- seg. 1, v=0 at y=0 or eta=0
2,0,1,5 ---- seg. 1, phi_y=0 at y=0 or eta=0
2,1,4,2 ---- seg. 5, v=0 at y=23,561945 or eta=1
2,1,4,5 ---- seg. 5, phi_y=0 at y=23,561945 or eta=1
0             ! # of point constraints
3             ! # of joints
2,1
3,2
4,3
1.0,0.0,0.0    ! Nx, Ny, Nxy

```


References

- [1] Kumar, V., and Singh, A. V., "Vibration Analysis of Non-circular Cylindrical Shells Using Bezier Functions," *Journal of Sound and Vibration*, Vol. 161, No. 2, 1993, pp. 333-354.
- [2] Sanders, J. L. Jr., "An Improved First Approximation Theory for Thin Shells," NASA Report R-24, 1959.
- [3] Koiter, W. T., "A Consistent First Approximation in General Theory of Thin Elastic Shells," *The Theory of Thin Elastic Shells*, Proceedings IUTAM Symposium, Delft, 1959, Amsterdam, the Netherlands, North-Holland Publishing Company, 1960, pp. 12-33.
- [4] Love, A. E. H., A Treatise on the Mathematical Theory of Elasticity, 4th edition, New York, Dover Publication, 1927.
- [5] Loo, T. T., "An Extension of Donnell's Equation for Circular Cylindrical Shell," *Journal of Aeronautical Sciences*, Vol. 24, 1957, pp. 390-391.
- [6] Brogan, F. A., Rankin, C. C., Cabiness, H. D., and Loden, W. A., "STAGS User's Manual," Lockheed Martin Missiles & Space Company Inc., Report LMMSC P032594, Version 2.3, 1996.

Table 1 Size of stiffness matrices for panel and shell for increasing number of segments.

$NSEG$	$ISIZE$ (Panel)		$ISIZE$ (shell)
	$[C^0]$	$[C^0, C^1]$	$[C^0, C^1]$
1	330	330	-
2	605	550	440
3	880	770	660
4	1155	990	880
5	1430	1210	1100
6	1705	1430	1320

Table 2 Comparison of buckling loads results for composite curved panel.

Thickness t (in.)	STAGS (lbs/in.)	Present analysis (lbs/in.)
0.072	374.55	390.68
0.144	1481.08	1459.45
0.216	3328.25	3278.86

Table 3 Comparison of buckling loads results for wing leading-edge panel.

Loading condition		Full Model		Quarter Model
		STAGS	Present Analysis	Present Analysis
N_x	N_{xy}	(lbs/in.)	(lbs/in.)	(lbs/in.)
1.0	0.0	301.73	317.03	299.93
1.0	0.4	193.96	202.57	196.97
1.0	1.0	106.34	110.90	108.82
0.4	1.0	123.93	129.53	127.93
0.0	-1.0	-117.13	-125.37	-125.60
0.0	1.0	138.78	145.55	144.64

Table 4 Comparison of buckling loads results for non-circular fuselage.

Thickness t (in.)	STAGS (lbs/in.)	Present Analysis (lbs/in.)
Isotropic		
0.080	14.64	14.90
0.100	28.18	28.84
0.144	82.02	84.13
0.180	157.52	160.79
Laminated		
0.072	6.34	6.32
0.096	14.77	14.77
0.120	28.40	28.41
0.144	48.39	48.29

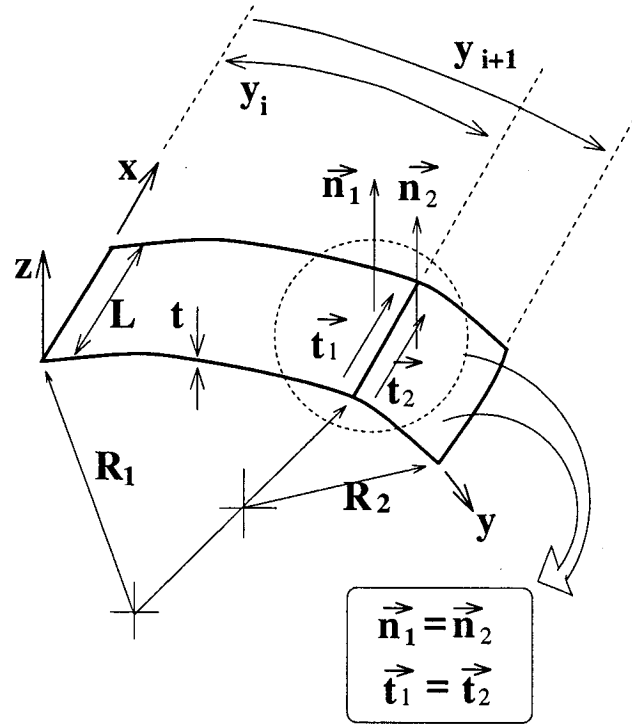


Figure 1: Coordinate system and geometry of shell with variable curvature.

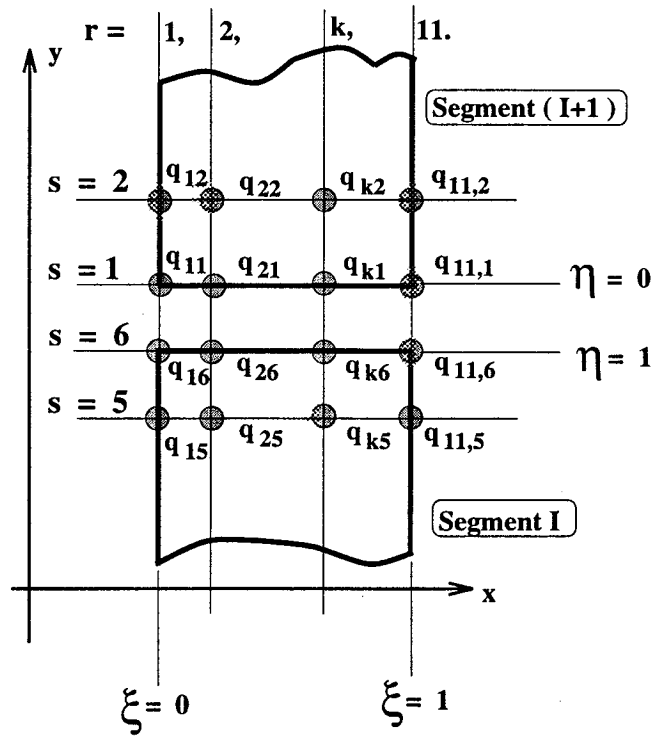


Figure 2: Control points for joining shell segments.

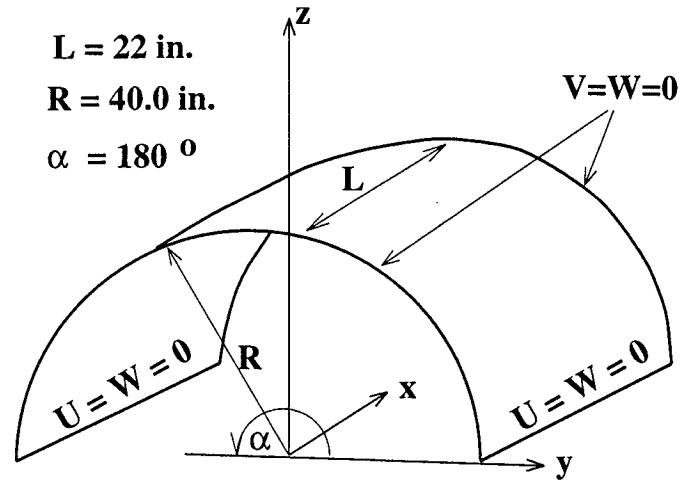


Figure 3: Geometry and boundary conditions of curved composite panel.

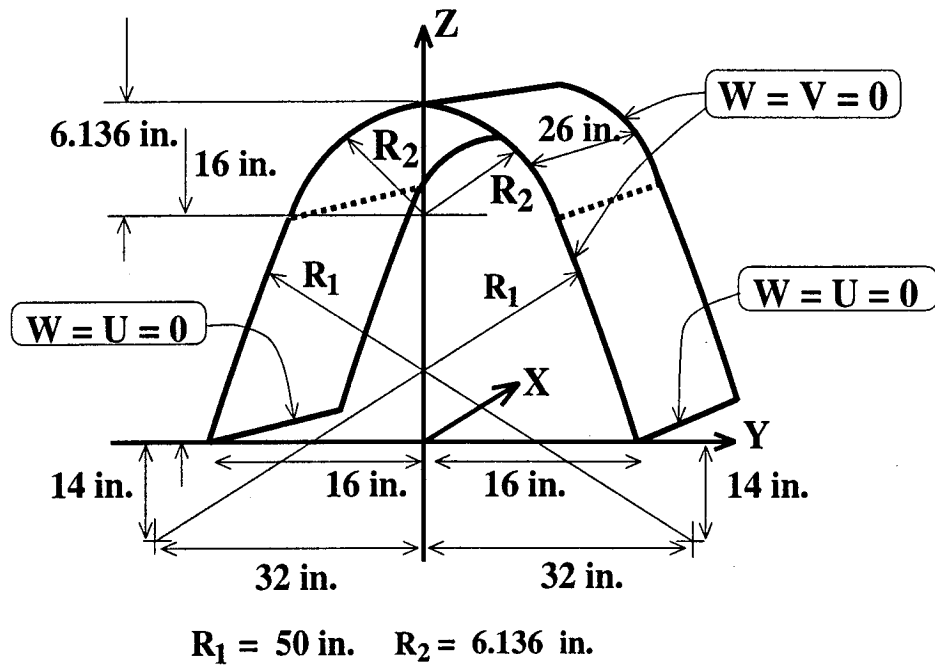


Figure 4: Geometry, dimensions and boundary conditions of composite wing leading-edge panel.

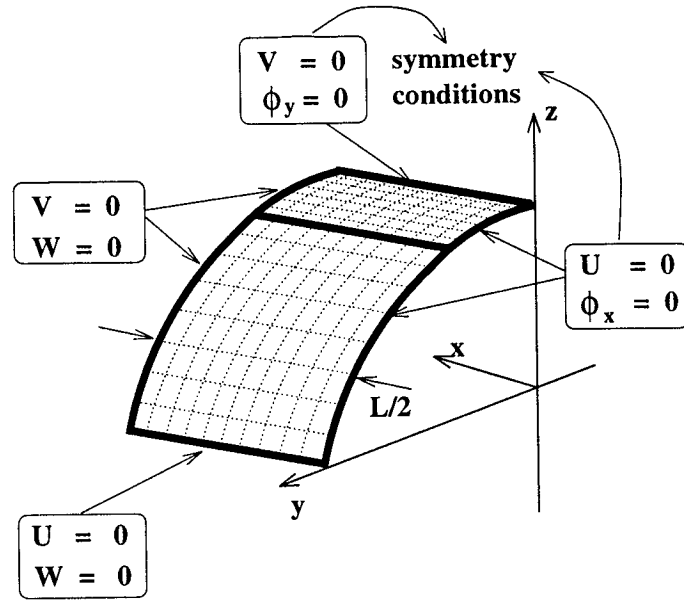


Figure 5: Boundary conditions for quarter symmetric model of composite wing leading-edge panel.

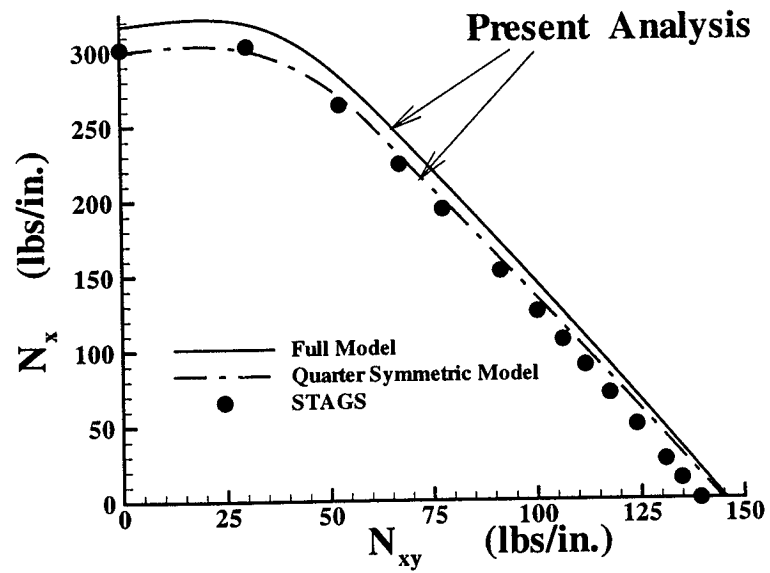


Figure 6: Buckling load interaction curve for the composite wing-leading edge panel.

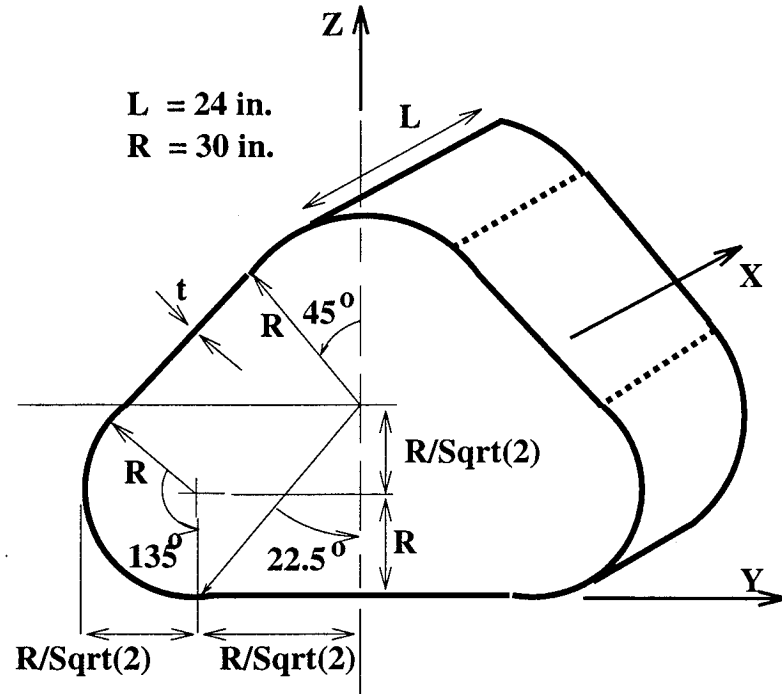


Figure 7: Geometry of non-circular fuselage.

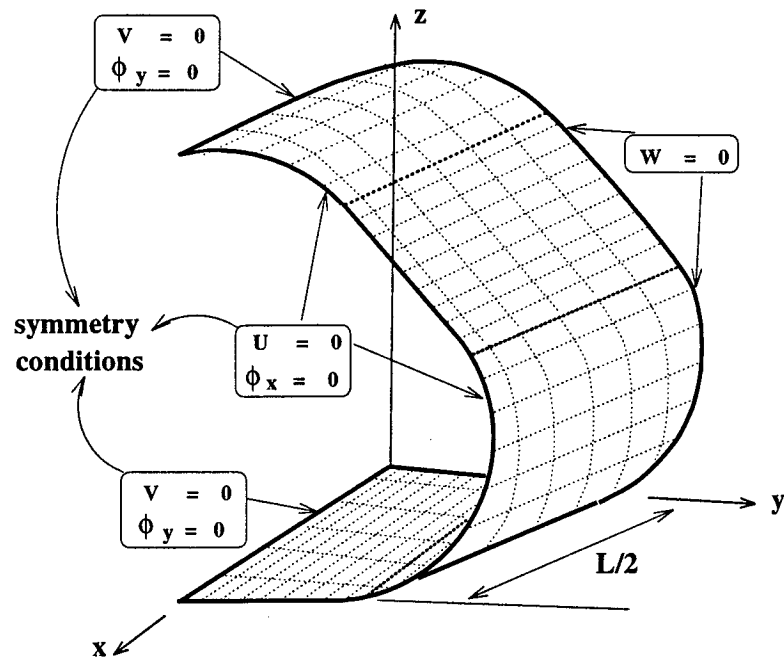


Figure 8: Boundary conditions for quarter symmetric model of non-circular fuselage.